A design methodology for low-cost, high-performance capacitive sensors

A design methodology for low-cost, high-performance capacitive sensors

PROEFSCHRIFT

ter verkrijging van de graad van doctor
aan de Technische Universiteit Delft,
op gezag van de Rector Magnificus Prof. dr. ir. J. Blaauwendraad,
in het openbaar te verdedigen ten overstaan van een commissie,
door het College van Dekanen aangewezen,
op dinsdag 28 januari 1997 te 13:30 uur

door

Ferencz Nandor TOTH

elektrotechnisch ingenieur
geboren te Sydney, Australië

Dit proefschrift is goedgekeurd door de promotor:

Prof. dr. ir. A.H.M. van Roermund

Samenstelling promotiecommissie:

Rector Magnificus,	voorzitter
Prof. dr. ir. A.H.M. van Roermund,	Technische Universiteit Delft, promotor
Dr. ir. G.C.M. Meijer,	Technische Universiteit Delft, toegevoegd promotor
Prof. dr. ir. S. Middelhoek,	Technische Universiteit Delft
Prof. dr. ir. H.F. van Beek,	Technische Universiteit Delft
Prof. dr. ir. J.H. Huijsing,	Technische Universiteit Delft
Prof. dr. ir. P.P.L. Regtien,	Technische Universiteit Twente
Ir. M. van de Lee,	Delft Instruments

Published and distributed by:

Delft University Press
Mekelweg 4
2628 CD Delft
The Netherlands
Telephone +31 15 2783254
Fax +31 15 2781661

CIP-DATA KONINKLIJKE BIBLIOTHEEK, DEN HAAG

Toth, F.N.

A design methodology for low-cost, high-performance capacitive sensors /
Ferry N. Toth. - Delft : Delft University Press. - Ill.
Thesis Delft University of Technology. - With ref. - With summary in Dutch.
ISBN 90-407-1407-X
NUGI 832
Subject headings: capacitive sensors / sensor systems

Printed in The Netherlands

TABLE OF CONTENTS

1 INTRODUCTION

1.1 Background and purpose of this research

Sensors can be considered the eyes and ears of any system that requires information about its environment. In many cases human beings take part in such a system. They can act as a sensor to provide a machine with data (entering visually observed date into a computer) or even control the response of a machine (driving a car). In other cases sensors are required to provide human beings with information they can not directly observe, like radiation.
With the recent growth of the capabilities of automatic information processing systems, there is a demand for more information, at higher speeds and from more different sources, at much lower costs then ever before. It is this growing demand for information that presently drives the development of low-cost, high-performance sensors. And it is believed by many that sensors based on the principle of capacitance can play an important role in this development.

Like all subjects that attract human interest, the field of capacitive sensors started with the discovery of a phenomenon. Generally, after the discovery scientists study the phenomena to try to understand and model it in the hope to bring the effect under their control so that it can be put to use.

In the case of capacitive sensors it was the discovery of one of the first electrical devices, the Leyden Jar, that started off research. The Leyden Jar was one of the earliest and simplest forms of an electric capacitor, discovered independently about 1745 by the Dutch physicist Pieter van Musschenbroek of the University of Leyden and Ewald Georg von Kleist of Pomerania [1]. The original Leyden Jar was a stoppered glass jar containing water, with a wire or nail extending through the stopper into the water. The jar was charged by holding it in one hand and bringing the exposed end of the wire into contact with a charge generator. After the contact was broken between the wire and the source of electricity, and the wire was touched with the other hand, a discharge took place that was experienced as a violent shock.
However, it took more then a century before Maxwell presented his treatise on the electromagnetic field [2] and gave a precise definition of capacitance.

With the invention of the vacuum tube, capacitors have been put into use for nearly a century. However, the precise measurement of small capacitances has always been perceived as a difficult task and their use has been limited mostly to areas where the precise value is not of great importance. Up to the 50's one of the most important applications where the stability of the capacitance value was of primary importance was the LC oscillator in radio transmitters and receivers, and many publications can be found on for instance the influence of humidity on the capacitance value.
Since then, things changed. A substantial improvement to the measurement of capacitance using a capacitive bridge was contributed by Thompson [3], [4] at the National Standards Laboratory in Sydney, Australia. He and his colleague Lampard [5], [6] also discovered an accurately calculable capacitance, giving capacitance a firm base in metrology.
After a while, the availability of precise capacitances and measurement instruments gave rise to a new interest for capacitance theory. This lead to the development of less costly and easier-to-use measurement equipment during the 70's and 80's. As a result of this, the development of capacitive sensors takes off during the 80's leading to a large amount of publications during recent years.

In Fig. 1-1 a selection of articles is shown that have been found during the course of this research and that are related to the fields of capacitance theory, capacitance measurement and capacitive sensors. Although the selection of publications is by no means complete or even random, it clearly illustrates the effect of the developments in the 1950's on the interest for capacitive sensors in the 1990's.

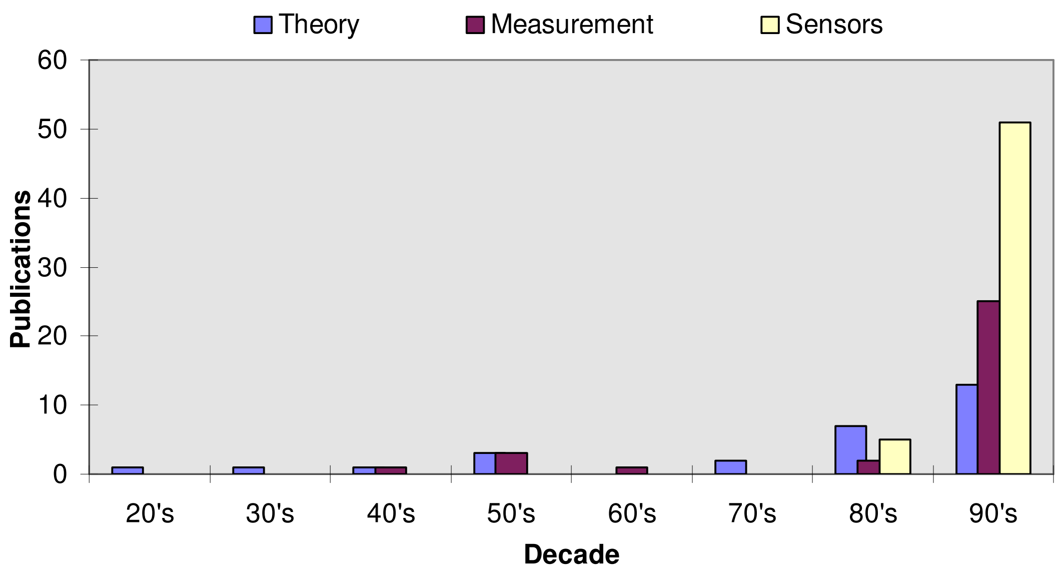

Fig. 1-1 Selection of publications related to capacitance over the last nine decades

Also at the Delft University of Technology, since 1992 the subject receives large attention from the side of different faculties, as can be seen from the number of Ph.D. theses on the subject of capacitive position measurement (Zhu [7] and Bonse [8], Faculty of Mechanical Engineering, de Jong [9], Faculty of Electrical Engineering), capacitive tactile imaging (Wolffenbuttel [10], Faculty of Electrical Engineering), smart sensor interfacing (van der Goes [11], Faculty of Electrical Engineering) and in scanning tunneling microscopy (Holman [12], Faculty of Physical Engineering).
The purpose of the work presented in this thesis is to continue the development of new capacitive sensors while simultaneously generalizing theories presented in

earlier work on the subject, in the hope to facilitate future capacitive sensor development.
The high-performance sensors are targeted at the low-cost, medium-volume, industrial sensor market and partially the high-end consumer market. However, it can be expected that by applying lower cost materials, the sensors can also be optimized for the low-cost consumer market.

1.2 Statement of the problem and objectives

Generally, the time required to develop a new sensor is very long, typically more then 5 years. This explains the relatively slow development in sensor technology and also the relatively high costs of sensors.
The main problem that is dealt with in this thesis is: "Can the development time and the cost of sensors in general and capacitive sensors in particular be reduced and the performance increased by adding intelligence to the sensor".

The main objectives are:

1. Finding a design strategy for capacitive sensors that reuses existing knowledge, parts *and* designs as much as possible, to simultaneously reduce manufacturing and development costs.
2. Finding flexible basic capacitive sensor designs that lend themselves for reusability
3. Implementing and evaluating capacitive sensor designs to demonstrate the feasibility of the approach.
4. Explore the area where capacitive sensors may be successfully applied.

To find an appropriate design strategy, some current design methods will be compared. Then existing knowledge about capacitance as well as the parts that make up a capacitive sensor are categorized for easy reusability. Following the proposed design approach, the design of three different types of capacitive sensors demonstrated.

1.3 Organization of this thesis

In the first chapters we will discuss the aspects of capacitive sensors and sensor systems that are common to all sensors of this type.
In Chapter 2 we will define the problem area that is covered in this thesis. According to the title of this book, the area concerns low-cost high-performance capacitive sensors and sensor systems. We will try to narrow the problem area further without defining these entities at this point.
In Chapter 3, some problems that are particular to the design of sensors are discussed as well as strategies to solve them. In this chapter, a new paradigm from the information sciences called Object Oriented analysis and design is proposed to develop sensors and sensor systems.
In Chapter 4 we finally define the entities sensor and sensor system. It appears that what is called a sensor system by one person is considered a sensor by another. Using the object model presented in Chapter 3, general definitions for sensing elements, sensors and sensors systems will be given, as well as for intelligent sensors.

After having defined what we will consider a sensor and a sensor system we will look more specifically at the class of capacitive sensors. Evidently, all capacitive sensors utilize a capacitance change to measure the physical quantity the sensors are

meant for. A capacitive sensor will therefore at least consist of a capacitive sensing element (electrode structure) and a device to measure the capacitance (modifier). Therefore in Chapter 5 we will start by discussing the physical aspects of capacitances. This is followed by an analysis of electrode configurations that are suitable for capacitive sensing elements. Then possible error sources such as the finite guard-ring and electrode-gap dimensions as well as contamination effects are discussed. Finally an object model of capacitive sensing elements is presented.
Chapter 6 is concerned with the measurement of capacitance. First, techniques that are incorporated into most precision capacitance meters are described, followed by a discussion of the basic capacitance measurement methods. Then we arrive at the measurement methods that are suitable for low-cost, intelligent capacitive sensors. Finally an object model of modifiers for capacitive sensors is presented.

In the last chapters, applications of capacitive sensors are presented. The designs are based on the generic model for an intelligent capacitive sensor presented in Chapter 4. In Chapter 7 the design of an intelligent force sensor is described. A leaf spring is used to convert the applied force to an electrode distance change. The sensor is suitable to measure force accurately over a large temperature range.
In Chapter 8 a capacitive liquid level gauge is presented. The liquid changes the capacitances of a multi-electrode, from which the level can easily be calculated. The sensor is suitable for measuring the level of either conducting or non-conducting liquids accurately over a large range.
Finally the design of a capacitive persons detector is described in Chapter 9. The sensor can be used to count the number of persons passing in or out a gate. An second persons detector is presented that can even estimate the position of a person standing between the electrode structure using fuzzy logic. This type of sensor might find an application in the safeguarding of automatically working machines like robots.
And last but not least the conclusions are presented in Chapter 10.

1 *"Leyden Jar"*, Microsoft ® Encarta'95, Interactive Multimedia Encyclopedia
2 Maxwell, J.C., *"A treatise on electricity and magnetism"*, Clarendon, Oxford, 1873
3 Thompson, A.M., *"A bridge for the measurement of permittivity"*, Proc. IEE, Vol. 103, Pt. B., pp. 704 - 707, November 1956
4 Thompson, A.M., *"The precise measurement of small capacitances"*, IRE transactions on instrumentation, Vol. I-7, pp. 243-253, 1958
5 Thompson, A.M. and D.G. Lampard, *"A new theorem in electrostatics and its application to calculable standards of capacitance"*, Nature, Vol. 177, pp. 888, May 1956
6 Lampard, D.G., *"A new theorem in electrostatics with application to calculable standards of capacitance"*, Proc. IEE, Vol. 104, pt. C, pp. 271-280, September 1957,
7 Zhu, F., *"Development of capacitive position transducers through a mechatronic approach"*, Ph.D. Thesis, Delft University of Technology, April 1992
8 Bonse, M.H.W., *"Capacitive position transducers - Theoretical aspects and practical applications"*, Ph.D. Thesis, Delft University of Technology, December 1995
9 Jong, G.W. de, *"Smart capacitive sensors"*, Ph.D. Thesis, Delft University Press, Delft, April 1994
10 Wolffenbuttel, M.R., *"Surface micromachined capacitive tactile image sensor"*, Ph.D. Thesis, Delft University Press, Delft, April 1994
11 Goes, F.M.L. van der, *"Low-cost smart sensor interfacing"*, Ph.D. Thesis, Delft University Press, Delft, April 1996
12 Holman, A.E., *"A novel scanning tunneling microscope with inherent scan linearization"*, Ph.D. Thesis, PK Publishers, Delft, May 1996

2 BOUNDARIES OF THIS WORK

The whole area of sensors and sensor systems may be described as a multi-dimensional space, in the dimensions: physical principle, measurand and application field, as suggested by Middelhoek and Audet [13]. Specific sensors and sensor systems are represented by a point in that space. Similar classifications are also used by for instance Sze [14]. Here we will outline the boundaries of the area of the sensors and systems that are covered in this work.

2.1 Physical principle

As the title suggests, this thesis limits itself to capacitive sensors and sensor systems. Without strictly defining the terms at this point, it will be clear that these sensors and systems will at least have a sensing element that consists of a capacitance. The magnitude of this capacitance is influenced by the physical signal that is to be measured.

Sensors can have output signals in any domain. In fact many sensors with a mechanical or pressure output can be found on the market. Instead we will focus on sensors that can be used to provide information processing systems with data (i.e. computers). As a result we will focus on electronic sensors (preferably with a digital output) that measure the change in capacitance electronically.

2.2 Measurand type

Here we focus on the type of physical signal we actually want to measure. Generally the capacitance of two electrodes depends only on their size, shape, distance, the permittivity of the isolator and the presence of other electrodes. When these parameters are accurately known the capacitance between the electrodes may be calculated. However, analytical calculations are only possible when the structures have very simple shapes, while numerical calculations are either not very accurate or extremely computer time and memory consuming.

Fortunately we are not interested in the absolute capacitance but in the way the measurand modifies the capacitance. We may choose our electrode structures shape so that the way the measurand influences the capacitance is well known. This often leads to electrode structures that have a high degree of symmetry like flat electrodes, which are often parallel or in the same plane, or cylindrical electrodes. For

calculations, the length in one dimension is often assumed to be infinite so that the problem becomes a two-dimensional one, which greatly simplifies the problem.
Also simple dielectrics with a predictable behavior may be used, for instance air, which has a relative permittivity ε_{air} that is relatively independent of temperature, humidity and pressure.

The parallel plate capacitor serves very well to demonstrate the different kinds of capacitive sensor elements. These elements are based on changes in the:

1. permittivity (ε-type)
2. effective electrode area (A-type)
3. electrode distance (D-type)

The D-type electrodes have the advantage that ε and A can be relatively constant during the sensors life time (when for instance air is used as a dielectric), while the absolute values are calibrated during an overall system calibration. A disadvantage is the small measuring range due to the decreasing sensitivity at increasing distances. This type of electrodes is very well suited for application in low-cost displacement, force and pressure sensors.

The A-type electrodes have been researched extensively by for instance de Jong [15], Zhu [16] and Li [17]. Advantages are:

- Suitable as position sensor
- Very large measuring ranges possible
- High accuracy
- Easily extendible

These advantages can be attributed to the use of a capacitance array as suggested by Zhu, which consists of several small electrodes next to each other in the same plane.
Disadvantages are:

- Capacitance still depends on the electrode distance
- Mechanical accuracy of the electrode positions determines the final accuracy of the sensor system

The ε-type electrodes are dependent on material properties. They may be used to discriminate materials or to determine the position of interfaces between materials. Since the relative permittivity is not a very fundamental quantity (and can be temperature dependent, inhomogeneous or anisotropic for certain materials) the accuracy of the sensor will vary from material to material. However, for materials with relatively homogeneous permittivity reference measurements can be performed to reduce the effect of the inaccurately known value.

Considering the amount of work done already on A-type sensors, in this thesis we will describe the design of permittivity (ε-type) and electrode distance change (D-type) based capacitive sensor systems with respect to their costs and performance. Design examples that will be dealt with in the course of these thesis are:

- A capacitive force sensor (D-type).

A leaf spring with low temperature coefficient is used to convert the load to a displacement. The electronics are auto-calibrating while the mechanical part requires a minimal system calibration.

- A capacitive liquid-level gauge (ε-type).

The liquid level induces a permittivity change that is used to calculate the interface position. The level of both conducting and non-conducting liquids can be measured, while the accuracy is sufficient to detect leaks in underground storage tanks.

- A capacitive persons detector.

Based on permittivity change conversion, this detector uses large electrodes; for which electromagnetic-interference suppression is the main challenge.

2.3 Application field

Other boundaries are more difficult to specify. The term "high-performance" in the title of this thesis, suggests that the sensors that are discussed should be able to meet or surpass the specifications of sensors that are used for similar purposes, while "low-cost" suggests that the cost of manufacturing should be substantially lower. The costs and performance of a sensor are therefore relative to the costs and performance of all sensors in existence.

A much simpler approach would be to find a similar sensor on the market and consider its cost and performance. The new sensor should outperform available sensors on this market in one aspect while (at least) matching the others. However, it is generally recognized that the sensor market (like other markets) is divided into different segments such as consumer, industrial, military, automotive etc. The specifications that are demanded by these markets, with respect to the specifications and costs differ greatly as does the volume of the market.

For instance sensors for the consumer market often replace very simple and extremely low-cost detectors. Bimetal switches that are used in all sorts of temperature control systems (coffee machines, central heating) may be replaced by low-cost temperature sensors. The performance of the temperature sensor should (and can easily) be better than that of the temperature detector, but the cost of such a detector is extremely low, mainly due to its simplicity and high volume production.

In a limited number of cases the sensor competes with a sensor for the same measurand type but which is based on another physical principle. For instance mechanical kitchen scales are replaced by electronic (capacitive or resistive bridge) versions. It can be noted, however, that the electronic scales have substantially higher costs.

In our case the field of application is the low-cost, medium volume, industrial sensor market and partially the high-end consumer market. Although here the performance and costs of existing sensors are known, when deciding to design a new sensor one needs at least an estimate of the expected performance and costs of the sensor that will be developed.

Estimating costs beforehand is complicated because the numbers that are sold of a particular type of sensor is usually small (possibly tens of thousands) and of sensor systems even smaller (several hundreds to several thousands). It can easily be seen that the share of the costs of developing a sensor or sensor system are not negligible. Therefore, to optimize the sensor for low-costs, while maintaining performance, not only influences the design itself, but also the design process.

Another complication related to costs is that manufacturers are expected to support an industrial sensor for many years after selling the last one of a series. When there are no second sources for replacement parts, this may require keeping large stocks of parts that may never be needed, or risking that some parts may not be available in the future. In the latter case a redesign of the old sensor may be necessary. These costs need to be considered beforehand when developing a new sensor.

Estimating the pure performance of a sensor beforehand might be possible in some cases, but for the customer other specifications are equally important. On the industrial market, customers often agree to buy a certain sensor on the condition that a certain aspect is adapted to their specifications. For instance an analog output signal might need to be adapted to a different level or a digital signal protocol might need to be changed. Even worse, the interface at the input of the sensors might need to be slightly changed, to adapt it to a specific application.
The result of all this is, that the specifications of a particular sensor change in time, depending on customer demands, availability of components and changing technology. This is summarized in Table 2-1.

Table 2-1 Requirements for sensors for the target application field

Property	Requirement
Accuracy	high
Resolution	high
Speed	medium
Costs	low
Temperature range	large
Production quantities	small - medium
Flexibility	high
Second sources	important

2.4 Conclusion

The sensors and sensor systems that will be considered in this thesis are based on capacitance changes caused by changes in the electrode distance (D-type) or by changes in the dielectric (ε-type) and are targeted at a cost-driven, medium-volume, industrial market or the high-end consumer market.
As an example of the design of a D-type sensor, a capacitive force sensor will be described. Two examples of ε-type sensors will be presented, a capacitive level gauge for underground fuel storage tanks and a capacitive persons detector.

---

13 Middelhoek and S., S.A. Audet, *"Physics of silicon sensors"*, Academic Press, London, 1989
14 Sze, S.M., *"Semiconductor sensors"*, John Wiley & Sons, Inc., New York, 1994
15 Jong, G.W. de, *"Smart capacitive sensors"*, Ph.D. Thesis, Delft University Press, Delft, April, 1994
16 Zhu, F., *"Development of capacitive position transducers through a mechatronic approach"*, Ph.D. Thesis, Delft University of Technology, April 1992
17 Li, X.J., G.W. de Jong and G.C.M. Meijer, *"An accurate smart capacitive angular-position sensor with a full circle range"*, Proceedings IMTC'95, pp. 80 - 83, April 24 - 25, 1995

3
DESIGN CONSIDERATIONS FOR LOW-COST SENSORS AND SENSOR SYSTEMS

As has been discussed in the previous chapter, the design of industrial sensors and sensor systems differs somewhat from the design of many other products, especially from for instance high-volume low-end consumer electronics. In this chapter we will try to define the specific differences and how these differences affect the design of the whole system.
Several structured design strategies exist, based on the general systems theory, that attempt to solve the problems related to complexity, of which top down and bottom up system design are the most well known. However, these methods will appear to have some limitations that have a negative effect on the design time and flexibility of the design in the case of sensors and sensor systems.
Since these limitations have similar effects in software engineering, a new method from this field of science is introduced. This method which is generally known as Object Oriented Analysis and Design. It will be shown that an object oriented approach may help to overcome the limitations of structured design and to find a basis for designing sensors and sensor systems that should generally give good results, considering all aspects.

3.1 Specific problems in industrial sensor design

In the previous chapter we already mentioned some important properties of the industrial market like the limited volume of the market, the relatively long product life cycle and changing specifications. Other properties are more specific to sensors like environmental requirements and the interdisciplinary nature of sensors.

- Design time

As has been stated before, the cost of developing a certain sensor or sensor system cannot be neglected in many cases because the production quantities are in general not very large. Any design strategy trying to optimize the price/performance ratio of a sensor or sensor system will need to incorporate the costs of the design itself. In other words, reaching a technically slightly inferior result in a very short time might be preferable to a technically optimized result at the expense of an extra year of research.

Also the cost of developing a production line can not be ignored. As a result, the use of non-standard parts (for housing, physical connections etc.) that require custom-made machines or moulds might have a dramatic impact on the total costs.

- Interdisciplinary nature

By definition a sensor spans more than one physical domain. This means that several specialists on different fields need to work together or, in smaller projects, that one person needs to acquire knowledge on many different fields. In many cases the extra overhead in the form of communication between designers not speaking each others' (technical) language or extra learning time increases the design time and therefore the cost of the product.

The need for several specialists to work together leads to another complication. Solutions suggested by one specialist to a problem in one part of the system might cause problems in others parts and might therefore be unacceptable to other specialists. Even worse, the overall optimal solution might be overlooked.

- Environmental requirements

Sensors often have to operate under harsh environmental conditions. While with other systems environmental conditions can often assumed to be relatively constant or controlled, sensors often operate under conditions where humans can not survive. In many cases these conditions cannot even be assumed constant, since at least one parameter is changing - the one to be measured. It would be very fortunate if all other conditions remained constant.

As a result, sensors need a relatively long period for testing during all phases of the development. Consequently, the design often needs to be adapted in a very late stage, in many cases influencing the design of other parts of the system.

The most important parameters are generally the sensitivity to temperature, pressure and humidity. Other parameters may determine storage and operating conditions, like resistance to certain chemicals, temperature limits etc.

- Flexibility

It will be clear that a very important aspect of a sensor or sensor system is the flexibility of its design. This should allow the designers who are trying to solve a certain design problem to quickly select another solution after testing a prototype proved the proposed solution ineffective or revealed new problems. A flexible design can also be easily adapted to specific customers wishes, or to incorporate new components instead of older types that are not available anymore.

3.2 Design strategies

To solve the specific design problems a systematic approach is obviously required. Several well known systematic approaches exist, while other new approaches have recently emerged. In this paragraph we will try to find an approach that is most suitable in the field of sensor design.

3.2.1 General systems theory

Most systematic approaches are based on the general systems theory, the foundation of which was laid by Von Bertalanffy in 1932. Together with Boulding, Rapoport and Gerrard he founded the "Society of General Systems Research" in 1957. In the Netherlands a similar organization "Systeemgroep Nederland" was founded in 1970. The result is that, although the theory is relatively young and the application field is interdisciplinary, a significant degree of standardization has been achieved. In this section definitions will be given in accordance to those of the Systeemgroep

Nederland, presented by Umbach [18], which are similar to those in the English literature, see for instance Van Gigch [19].

<u>System</u>

A system is the set of elements that are distinguished from the environment, depending on the purpose of the researcher, having mutual interaction and that interacts with the environment.

<u>Element</u>

The smallest part that we can distinguish for our purpose carrying certain properties. This means we can look at an element as undividable.

The elements can be conceptual or physical entities.

<u>Property</u>

We can assign certain properties to an element, and certain values to each property. In this way we can distinguish one elements from another.

<u>Interaction</u>

The process of the changing of a property or value of a property of one element by another element.

As a result of the interaction, elements can enter the system (inputs) or leave it (outputs).

<u>Environment</u>

The set of elements in the universe that interact with the elements of the system but that are not part of the system.

<u>Universe</u>

All elements that exist.

The definition of element depends on our purpose, in other words on the level of consideration. From this it follows that on one level of consideration a set of elements will be considered as only one element that is part of a larger system. At a lower level of consideration it might be considered as a system while the larger system will be part of the environment. When the set of elements is temporarily considered as one element it is called a black box.

A <u>subsystem</u> is a subset of the system with a minimum of two elements that all interact with each other (Fig. 3-1). When there is at least one element in the subset that does not interact with the other elements in the subset it is called an <u>aggregate</u>.

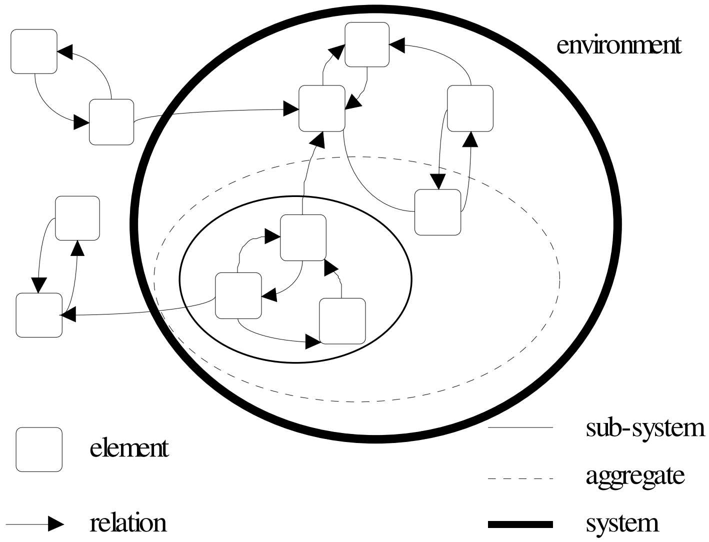

Fig. 3-1 System, aggregate and sub-system

3.2.2 Top down system design

This is probably the most applied design technique. It relies heavily on the use of black boxes of which the inputs, outputs and the transfer functions are the most important aspects. It is assumed that the (possibly complex) function of the system can be by decomposed resulting in subsystems, each performing a part of the total function. The result is a hierarchy of (sub)systems (Fig. 3-2).

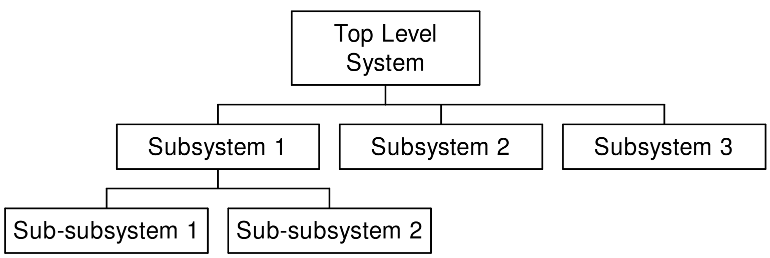

Fig. 3-2 Hierarchy of (sub)systems

A system is assumed to have a transfer function; the relationship between its inputs and its outputs. It is often assumed that the subsystems interact only through their respective inputs and outputs, in other words: they are closed systems. The outputs can somehow be described in terms of the inputs. The result is that information flows from one subsystem to the next (Fig. 3-3).

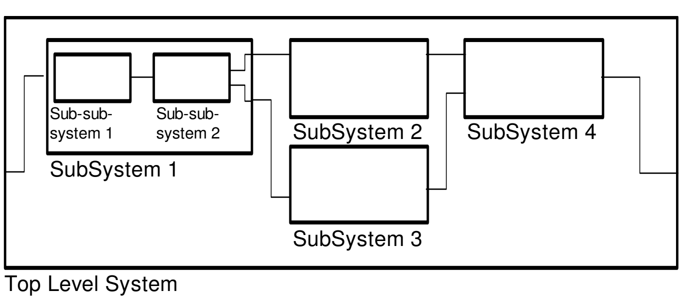

Fig. 3-3 Flow chart showing the information flow between (sub)systems

Top down system design is mostly used during the analysis of design problems and during the specification of the requirements. Starting from the requirements for the total system the problems is decomposed, from which new requirements for the subsystems result.

In reality, most subsystems cannot be assumed to be closed as they all interact with each other in numerous ways. This would lead to a description of the subsystems with an infinite number of inputs and outputs, which is rather impractical. Therefore only the most important interactions and functions are specified.
There is, however, in this phase of the design no systematic way to identify which interactions will be the most important, in other words to look ahead to the implementation of the system. To solve this problem a designer often relies on his own experience or on that of others, to predict the result of a certain decision. Sometimes legislation helps to prevent certain undesired interactions, like in the case of EMC.
There is also no systematic way to divide the system into smaller subsystems. Usually the division comes to ones mind automatically, for instance the thought “there must be a power supply”. So there will be a part in the system called the power supply. The division might also be based on experience, but often another designer would have made a different division. In fact, there probably is no “correct” division, since the subsystems are in reality not closed, so a border between them cannot be drawn.
Another problem is that, although information flows from one subsystem to another and these subsystems perform a transformation on this information, the way the information is represented is not described. The information is normally contained in an object, like a piece of paper or modulated on a physical quantity, which is called a signal. According to the definition, the signal itself (an element) entering the system is the input. It is the interface of the system that must be able to accept the signal.
The result is that although many transformations are commutative (the order in which they are performed should mathematically lead to the same result), the respective subsystems cannot exchange places because the input and output don’t modulate the same physical quantity, i.e. they are not compatible.

In the case of sensor design these drawbacks of the top down approach have severe implications. It is well known that although a sensor should be sensitive only to the measurand, in reality it will be sensitive to many other external influences. In this respect a sensor system might be considered less “closed” than many other (technical) systems. Moreover, since experience and insight are important to make effective decisions about how to divide the sensor system into subsystems, the multidisciplinary character of sensor systems complicates this approach even further. Chances are high that certain parts of a system need to be redivided or merged when the implementation of the design appears to be impossible or economically ineffective.
Another problem is that the flexibility of the design is not very high, because of the different physical quantities that carry the information. It is often not possible to insert or remove a subsystem between two existing subsystems because the inputs and outputs will not be compatible.

As a result of this, requirement specifications of sensor systems and subsystems often include specifications of interactions with other subsystems and external signals as well as specifications of the physical input and output quantities, modulation type and ranges. This severely limits the flexibility of the designer to optimize the overall sensor system design or to adapt the sensor system to specific customer demands, while it increases the design time.

3.2.3 Bottom up system design

This method assumes that the elements of the systems are already existing or well known. The subsystems can then be constructed from these elements. However, it is virtually impossible to compose a system from existing building blocks without knowing what to build.
Therefore this method is mostly used in conjunction with a top down design. Several iterations of top down decomposition and bottom up composition are often required until the designers arrive at a stable requirement specification and prototype sensor system.

This design technique is probably the most popular approach in sensor system design. It tries to solve the limitations of both design techniques by applying the both in an iterative process, explaining why the design of a sensor system generally takes many years.

3.2.4 Object oriented analysis and design

In software design recently a new design approach has become popular (Nelson [20]) and is slowly migrating into fields of system design (Pei and Cutone [21], Garceau *et. al*. [22]), modeling (Ninois *et. al*. [23]) and even into manufacturing (Wu [24]). Although the approach clearly needs some maturing, at present it is gaining a large momentum, considering the large number of publications concerning the subject in recent years. It can be expected, that the general ideas will migrate to other fields of science in the near future.
The basis of the object oriented approach is that the world does not consist of functions but of objects. Objects can be compared to black boxes, they are element and system simultaneously. However, they do consist of other interacting objects.
Compared to the general system theory, objects nicely fit in. An object is an element. But where the general systems theory merely places a circle around a group of interacting elements and calls it a (sub)system, in object oriented analysis and design such a group of elements is also called an object. Because of this, the definition of an object does not depend on the level of consideration, as does the definition of a system.

However, the most important addition to the systems theory is the recognition that objects can be categorized into classes. Each object that is a member of a certain class has at least the same attributes (or properties) as the other members of the class. This results to hierarchies in which each object inherits properties and functions from its class ancestors.
Partridge [25] shows that real (physical) world objects are related to specific concepts in the mental world and that classes in the physical world relate to general concepts. He also shows that classes of objects are objects themselves (class objects), and can be grouped into classes of classes of objects, etc. It must be noted that most object-oriented programming (OOP) languages differ slightly from this model. In OOP, objects model physical objects and classes model physical classes of physical objects. There are no classes of classes in most OOP languages.

A class object is a somewhat abstract type. As it relates to a general concept, which exists in the “mental world”, the class object is assumed to exist in the “physical world”, like the object “car”. There also exist implementations of specific brands and types of cars. However all cars share specific properties and functions. They have wheels, a stirring mechanism, an engine and many other things in common. Note that these things are in many cases class objects too. As a result of this we can speak in general terms of a “queue of cars in a traffic-jam” although a “car” is a class and in our minds exists as a general concept.

Important aspect of objects are:

- Encapsulation and data abstraction. In software engineering this means the packing of information (properties and values) and functions together, so the information internal to the object can not be accessed other than through the interface functions. The result is that the implementation of an object can be changed without affecting the object that interfaces with it. This is a result of modeling the software as close to reality as possible.

However, a sensor (system) is not a model of reality but part of it. Still the concept of encapsulation is useful when deciding where to store which kind of information. According to this concept, calibration values for a sensor should be stored in the sensor (encapsulated) instead of at a higher level in the system.

- Inheritance. Common properties and functions of different objects are thought to be properties and functions of their class (which is also an object). All the members of the class automatically inherit these properties and functions. This mechanism allows us to reuse parts of a design.
- Polymorphism. This is related to inheritance and encapsulation. Completely different objects of the same class may be exchanged, without other objects in the system knowing it but still changing the overall behavior of the system.

There are several similarities between objects and systems.
Firstly, a system consists of elements, or more accurately, a certain set of elements forms the system. An object is an element that consists of other objects. Obviously, top down and bottom up approaches should also apply to objects.
Secondly, when a system is seen as a black box, it is temporarily seen as an element, that has properties (including its input and output interfaces) and functions (the transfer functions between the input and output interfaces). This is similar to the definition of an object. Interaction between objects takes place through their interface functions to change their internal properties or to pass information.

This means that all systems can be considered objects. However, not all objects can be considered systems. For example, a class object is an object but not a system, because a class object exists in the real world and is related to a general concept in the mental world, while a system relates to a specific concept.

Aside from the philosophical implications, the most important properties of objects are that they inherit many of their functions and properties of their class ancestors, add a few new ones or modify the implementation of some the existing ones.
This gives us the foundation for a modular design, allowing us to start designing by using an existing class object (when there is one available) for the design. When necessary we can replace parts (class objects) by new ones that belong to the same (higher level) class. Only during the implementation phase do we start to replace the

class objects by specific implementations. When during testing (and maybe even after production has started) we need to add, remove or replace certain modules, we can do so while maintaining the structure and the functionality of the design. We can derive a subclass of objects from an older (existing) class object, adding functionality (methods or properties) while leaving the structure basically the same.

This method promotes the design of reusable objects and at the same times encourages the reuse of existing ones. It is in fact an answer to the question how to divide a system into subsystems:

1. Assuming that a similar system exists, the new system should be partitioned in such a way that parts of the existing system can be reused.
2. When a similar system does not exist, the new system should be partitioned in such a way that existing components, or modules or parts (which belong to a certain class, for instance op amps) can be used.
3. When an applicable class of components, modules or parts exists, but an applicable type of component is not available, it must be derived from the existing class.

For example, lets assume the system has been divided in such a way that an opamp can be applied. Note that an opamp is an existing class of electronic components. If we can not find an appropriate opamp (with for instance sufficient bandwidth), we should create a new type of the class opamp (instead of another type of amplifier). This way the newly created opamp may find use in future designs.

4. When an applicable class of components does not exist (which is seldom the case), a new class must be created. The class must be defined as general as possible, so that the family of components that will be derived from it are also reusable in future systems.

An example could be the Universal Transducer Interface by van der Goes [26]. It is a component that belongs to the class of Transducer Interfaces, that previously did not exist (at least not as a single IC). The UTI has been defined general enough to support a large range of sensors. New versions of the UTI supporting additional sensors can be created with minor modifications.

It can be argued that inheriting many properties from a parent object might substantially increase the overhead in the design, since many properties implemented in the parent object might be redundant in the child objects. Still, the costs of the total system might be less then when a new optimized design would have been made for the specific purpose.

Examples:

1. A microcontroller implements a lot of functionality that is not needed, but remains the solution with the lowest cost simply because it is already available on the market and is produced in very large quantities. This is only possible because it is a general purpose device that contains a lot of redundant functionality.
2. A software package like a word processor that doubles its size with every release. Although large parts of previous versions that are incorporated to the newer version might not be used, the parts that are used can be assumed to be relatively reliable. This way the functionality and (more important) the reliability of the package can be increased in shorter

development times. Because memory prices (both RAM and hard disk) keep dropping, this redundancy doesn't lead to an overall increase of costs.

In other cases the overhead can be reduced by not implementing certain functionality or by disabling it.

Examples:

1. Not implementing functionality can often be found in consumer electronics. On the printed circuit board in an amplifier often spaces can be found where components have not been placed. Apparently the same printed circuit board (and design) is applied in more advanced versions of the same amplifier. The empty spaces only increase the cost of the simpler version slightly, while the costs of manufacturing are lower since only one production line is necessary for the two versions.
2. Disabling functionality can again be found in the Universal Transducer Interface. This interface is capable of measuring various types of sensor signals like capacitances in several ranges, resistive bridges and thermistors by selecting a mode. Instead of designing an interface for a specific sensor element, a general purpose interface has been created. Although parts of the integrated circuit will be disabled in certain application they still take up chip area. Also, additional design time has been spent to find a sufficiently broad area of sensor element types. However, being more versatile, larger quantities can be produced, reducing the costs. At the same time, the output signal of the chip remains the same for many applications, reducing the need for a new interface between microcontroller and UTI and thereby total costs. In this case, the software required in a microcontroller to interface with the UTI remains the same per microcontroller type and varies only slightly between different types of microcontroller.

It will be clear that the object oriented approach will suffer partly from the same limitations as the top down system design. The compatibility between interfaces remains a problem unless it is defined at the top parent object for each class and not allowed to change between different implementations of an object (or at least to modulate the same physical quantity). This means a certain degree of standardization of interfaces, which also limits the designer to choose the most optimal configuration.

However, the notion that the world consists of objects encourages a flexible and modular design. The reusability and extensibility of components, system designs and requirement specifications can lead to a tremendous reduction of design time and therefore costs.

It is for these reasons that many aspects of object oriented analysis and design are already implicitly applied in many cases by all kinds of designers. The "art of designing" is in fact the library of solutions in the heads of experienced designers.

3.3 Conclusion

In this chapter it has been shown that the complexity of sensors and sensor systems required a systematic design approach. Unfortunately traditional top-down and bottom-up approaches appear to have serious limitations in small and medium-volume low-cost sensors and sensor systems due to the interdisciplinary and

relatively open character of the (sub-)systems. Often many iterations are required, resulting in long design times and relatively inflexible designs.
To help overcome these limitations, a new systematic design approach from software engineering called object-oriented analysis and design is introduced. This approach focuses on the reuse of components, designs and specifications as much as possible, using the concept of inheritance. If not eliminating much work (by merely composing existing objects) this can help decomposing the problem to smaller existing abstract objects using a top-down approach.
The object-oriented approach appears to be in closer agreement to the intuition of the more experienced designer, who already considers the parts of the design to be objects instead of subsystems. When these objects have standardized interfaces they can be truly reusable in new designs or in variations of older designs.
Although the resulting design might not be optimized in every (technical) aspect, it is likely that the overall price performance ratio will be improved.

---

18 Umbach, F.W., *"Organisatie van instrumentatie - Onder auspiciën van de Systeemgroep Nederland"*, H.E. Stenfert Kroese B.V., Leiden/Amsterdam, 1981

19 Gigch, J.P. van, *"Applied general systems theory"*, Harper & Row, New York, Evanston, San Francisco, London, 1974

20 Nelson, M.L., *"An Object-Oriented Tower of Babel"*, OOPS Messenger, Vol. 2, No. 3, pp. 3 - 11, 1991

21 Pei, D. and C. Cutone, *"Object-oriented analysis and design"*, Information systems management, Vol. 12, No. 1, pp. 54 - 60, 1995

22 Garceau, L., E. Jancura and J. Kneiss, *"Object-oriented analysis and design: A new approach to systems development"*, J. of Systems Management, Vol. 44, No. 1, pp. 25 - 32, January 1993

23 Ninois, P., D.W. Bunn and K. Vlahos, *"Industry simulation: System modeling with an object oriented/DEVS technology"*, European journal of Operational Research, Vol. 81, No. 3, pp. 521 - 534, March 1996

24 Wu, B., *"Object-oriented systems analysis and definition of manufacturing operations"*, Int. J. Prod. Res., Vol. 33, No. 4, pp. 955 - 974, 1995

25 Partridge, C., *"Modeling the real world: Are classes abstractions or objects"*, J. of Object-Oriented Programming, Vol. 7, No. 7, pp. 39 - 45, November 1994

26 Goes, F.M.L. van der, *"Low-cost smart sensor interfacing"*, Ph.D. Thesis, Delft University of Technology, Delft University Press, Delft, April 1996

4
DEFINING SENSORS AND SENSOR SYSTEMS

Middelhoek [27] and Sze [28] define a transducer as *a device that inputs a physical quantity (the measurand) and converts it into a physical quantity of another kind that is output* (Fig. 4-1). On the other hand, a modifier is a device that *converts it into a physical quantity of the same kind that is output.* Generally six signal domains are distinguished:
1. Radiant signal domain
2. Mechanical signal domain
3. Thermal signal domain
4. Electrical signal domain
5. Magnetic signal domain
6. Chemical signal domain

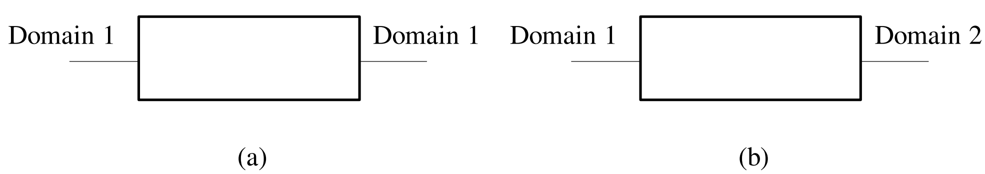

Fig. 4-1 A modifier (a) and a transducer (b)

The transducer at the beginning of the cascade of transducers and modifiers in an instrumentation system, is generally referred to as the input transducer or sensor, while the transducer at the end of the chain is called the output transducer or actuator (Fig. 4-2).

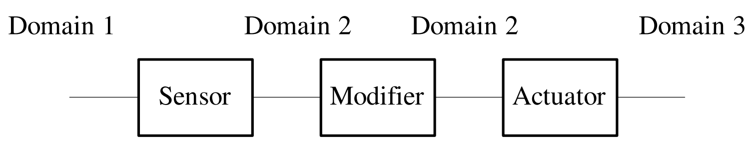

Fig. 4-2 General block diagram of an instrumentation system

In most cases the sensor output signal will be in the electrical domain so the input signal can lie in any other domain, for instance the mechanical or thermal domain. By this definition a Pt100 resistor will be considered a sensor.
A sensor system can then be defined as *a system that consists of one or more sensors and of a modifier (signal processor) that combines or moderates the output signals of the sensors into one or more output signals of the sensor system*. By this definition a

Pt100 combined with an electronic circuit that measures the resistance and converts it into a 4 - 20 mA current can be considered a sensor system. At the same time however, if this system would be put into a sealed package and therefore could be considered a *black box*, it would be sensor according to the first definition, since it converts a temperature into a current.
Apparently the difference between a sensor and a sensor system is relative to the system that it is part off. On the scale of an oil refinery it is considered a sensor and on the scale of the manufacturer it is considered a sensor system.

Instead we will follow an object oriented approach. We will define the smallest part in the sensor that interacts with the physical world and outputs an electrical signal to other objects the *sensing element.* An example would be a Pt100 resistor.
A sensor can then be defined as *consisting of a sensing element or another sensor and some form of modifier*. An example would be a system containing a Pt100 resistor and an electronic circuit that measures the resistance and converts it to a 4 - 20 mA current output.
This recursive definition does justice to the fact that it depends on the perspective what is called a sensor, but recognizes that a sensor consists of a sensing element (which may be contained in a part that is also a sensor) and one or more modifiers.
The modifier inputs an electrical signal and uses it to modify another electrical signal of another type (modulator) or of the same type (amplifier) after which the latter is output.
A sensor system can then be defined as *consisting of two or more sensors or sensing elements and some form of modifiers*. An example could be a pressure sensor with temperature compensation.
The output of a sensor or a sensor system is an electrical signal, that contains information about the measurand(s) (Fig. 4-3). This information is passed on to the system that it makes part of.
This is in contrast with instrumentation systems (also called measurement systems) and control systems. Both contain an output transducer (actuator) to output the information in another signal domain. An instrumentation system usually contains a display, while a control system contains an actuator that can influence its measurand.

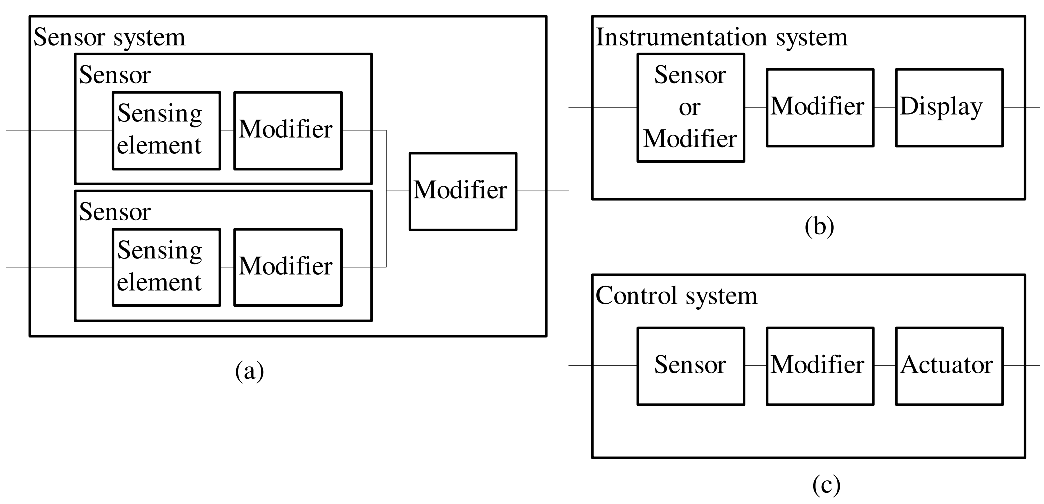

Fig. 4-3 (a) Sensor system (b) Instrumentation system (c) Control system

4.1 Object models for sensors and sensing elements

Using these definitions we can use the object model to create descriptions of sensing elements and sensors. A standard representation for such a model has not yet been developed, mainly because we want to describe additional relations of certain objects, the lineage, at the same time as the interactions between them, which is difficult to realize in a single diagram. Instead we will use the class diagram, following Booch [29]. In this diagram the ordinary arrow denotes inheritance, while the dashed arrow indicates that one object uses the other.

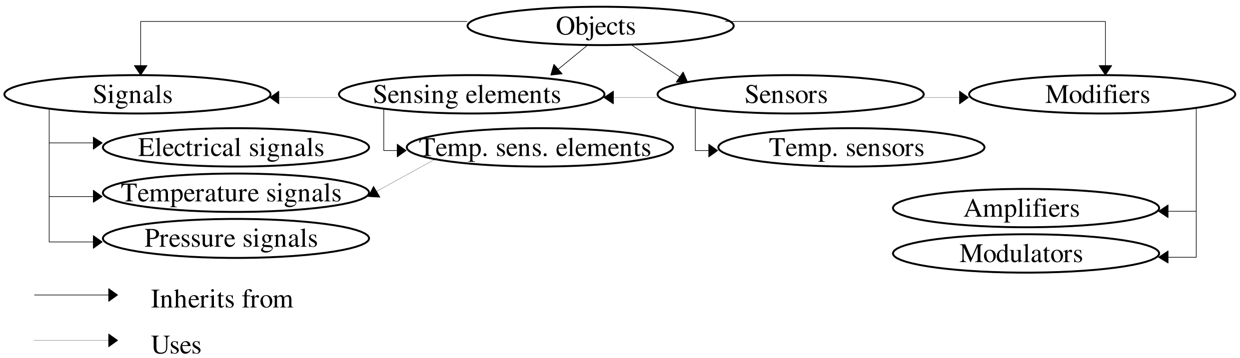

Fig. 4-4 Class diagram for signals, modifiers, sensing elements and sensors

From Fig. 4-4 we can see that the classes signals, sensing elements, modifiers and sensors belong to the class of objects. Several sub-classes of signals exist, including the ones shown here. We can also see that a temperature sensing element is derived from a sensing element and uses a temperature signal, which is derived from signals.

We can also note from Fig. 4-4 that there are relationships that limit the reusability of the objects. For instance, although a sensing element inputs a signal, we must explicitly indicate that a temperature sensing element inputs a temperature signal. This shows that we can not create another type of sensing element by merely replacing the type of input signal.

At higher levels in our hierarchy of objects, these relationships are not necessarily required. A high level object can *ask* an object at a lower level what kind of information it supplies and in what format. A signal can not supply this information. You can not ask a signal what kind of information it represents or how it is coded. It is the interface in the sensing element that needs to know what kind of signal is at its input.

The result of this is that interfaces must be implemented high in the hierarchy and can not be allowed to change in subsequent derivations of the high level object. This is also known as *standardization*.

4.2 Smart and intelligent sensors

On the other hand, the sensor itself might be intelligent enough to identify itself to the higher level object (process computer etc.).

A class of sensor exists that is generally referred to as smart sensors. This term is used by Middelhoek and Audet [27] for integrated sensors, where the sensing element and modifier are integrated on the same substrate, usually silicon (integrated silicon sensors) and hybrid sensors, where the sensing element and modifier are placed in the same housing. It is debatable whether this type of sensors deserves the label “smart”, for instance simply adding a pre-amplifier does not really make the sensor any smarter (although it might require a smart designer to actually implement it). Other authors (Huijsing *et. al.* [30]) define an integrated smart sensor as a single chip, that includes sensing element, interfacing (signal conditioning, conversion, bus output), calibration and intelligence (self-test, identification). An example of this type has been given by Hogenbirk *et. al.* [31].

Instead we will use the term intelligent sensors to refer to the class of sensors that have an intelligent behavior, regardless of the implementation. Meijer [32] recognizes that such an intelligent behavior should include Adaptability, Reliability, Interchangeability and Identification, Data reduction and Standardized bi-directional communication.

- Adaptability

An intelligent sensor system should adapt itself to the circumstances that it operates in. We can distinguish controlled adaptability and self adaptability. With controlled adaptability, a higher level object (for instance a process computer) tells the sensor to adapt one or more of its processing parameters. This obviously requires a bi-directional communication. On the other hand, self adaptability requires a higher level of intelligence in the sensor itself to decide which parameters need to be adapted.

Examples of adaptability include:

1. Increasing biasing currents of input amplifiers in the case of small sensor signals or strong interference at the sensor input.
2. Increasing the rate of the data acquisition for fast changing input signals to prevent aliasing. Slowly changing input signals need not be measured often. This way it might be possible to reduce the power consumption of the sensor or to increase the resolution by averaging intermediate results.
3. To limit power consumption, parts of the sensor can be brought into an idle mode or can be switched off.

- Reliability

A smart sensor might improve its reliability by performing self-tests regularly or at system start-up.

Examples are:

1. The proper connection of sensor wires is checked by the Analog Devices transducer interface [33].
2. Acceleration sensors for application in air bags exert an electrostatic field at startup, to simulate an acceleration.

Other possibilities to increase the reliability include:

1. The sensor might check if its inputs (or changes of the inputs) are out of range in which case an alarm function is activated.
2. Several inputs can be combined leading to the conclusion that the combination of inputs is impossible and therefore the system must be malfunctioning.

- Interchangeability and Identification

A (defect) intelligent sensor should be easily replaced. The sensor should be able to identify itself, so the sensor system it is part of can adapt to the properties of the new sensor. Alternatively the sensor should be able to send its properties to the higher level system.
An even better approach is to have the intelligent sensor hide all its properties from higher levels. One example could be calibration values. The interchangeability would be greatly improved if the sensor outputs only calibrated values. To achieve this the sensor might perform (continues) auto-calibration or store all its calibration values internally in a look-up table (Schlichting *et. al*. [34]).
Meijer [32] distinguishes between two-signal and three-signal auto-calibration. With a two-signal calibration, apart from the measurand S_x, a reference signal S_{ref} is measured in exactly the same way. The measurement result is then either the ratio $M = S_x / S_{ref}$ or the difference $M = S_x - S_{ref}$, eliminating multiplicative or additive errors respectively.
The more advanced three-signal auto-calibration requires an additional measurement, preferably the offset S_{off}. The measurement result is then

$$M = \frac{S_x - S_{off}}{S_{ref} - S_{off}} \tag{4-1}$$

which eliminates additive and multiplicative errors simultaneously.

- Data reduction

The desire for data reduction results from the wish to use bandwidths of communication channels as effectively as possible or to save power.

Examples are:
1. In many cases a sensor system measures several physical quantities, but may combine these values to one result.
2. Slow changing values need not be output continuously. The sensor may adapt it's output rate to the rate of change of the input signal. Alternatively it may output only the changes in the input signal..

- Standardized bi-directional communication

Every sensor (system) communicates data to higher level systems, but an intelligent sensor should be able to accept data, like new calibration data, or commands, like mode changes. Additionally, instead of "polling" the sensor, the sensor may request servicing by the higher level system. This may aid the higher level system to efficiently use its processing capabilities.
The communication needs to be standardized at least at the physical layer (signal type) to eliminate the need for a different hardware interface for each type of sensor. When the protocols are also standardized, different types of intelligent sensors will be truly interchangeable.

An attempt to achieve such a standardized output interface for smart sensors is presented by Riedijk [35], [36]. The presented IS^2 (Integrated Smart Sensor) bus, which is derived from the I^2C bus, allows for the addressing of both analog and digital sensors.

4.3 Intelligent sensor object model

The object 'Intelligent sensor' may now be derived from the object 'Sensor' (Fig. 4-5). Most of the additional functionality can be implemented by a programmable device like a microcontroller. The microcontroller can be used to control the power supply of the sensors, the speed at which they measure, combine the data and the calibration table to one output value, apply data reduction techniques and can have a bi-directional digital communication to the sensor system.

Haskard [37] attempted to integrate the microcontroller along with the sensing element and signal conditioning onto one chip, to obtain a true smart sensor, but concluded that this approach leads to a significant increase in silicon area and hence unacceptable increase of costs. Instead, Wouters *et. al*. [38] applied a finite state machine, which still occupied more then two-thirds of the 33.4 mm^2 chip area. However, in this application (implantable transponder) dominant requirements are the small size and low power consumption of the system, which justifies the large chip area.

Apparently, the most flexible and low-cost solution is to have a separate microcontroller. The large production volumes guarantee an optimal price per chip area, while the type of controller can be chosen to suite the specific application (clock speed, 4, 8 or 16 bit core) or available development tools (compiler, debugger, real-time kernel, in-circuit emulator).

Such an intelligent sensor can only be constructed at low costs when the sensing element's input and output signals are modified so that they are compatible with the microcontroller. In general, microcontrollers input and output only digital signals. These signals are time dependent voltages that are allowed to have two different levels (0 and 5 V) and to change at discrete time intervals only (the clock). Some specific types of microcontrollers do include an A/D converter, usually with 0 to 5 V input range and a relatively slow sampling rate.

Since the microcontroller clock is usually an accurate and stable reference and all microcontrollers are therefore able to measure periods or duty-cycles of digital signals over a very large range, the most convenient output format of the sensors seems to be period or duty-cycle modulation of square waves. Period modulation has the advantage that only one edge of the signal needs to be monitored, so the designer can take advantage of interrupt inputs of the microcontroller (when available) that are often either positive or negative edge triggered.

In some cases it might be necessary to use an analog voltage as the modifier output signal. The range of this format is however limited to the power supply (usually 0 V to 5 V), the resolution varies from type to type and the stability depends on the stability of the voltage reference, which is usually not very high.

The digital outputs of the microcontroller can be used to control switches in the modifier or in the power control.

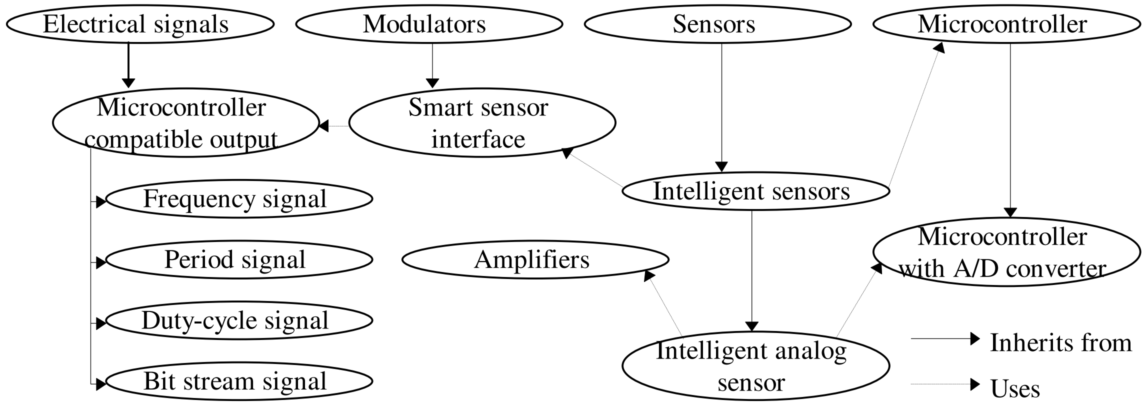

Fig. 4-5 Class diagram for intelligent sensors

In Fig. 4-6 the generic data flow diagram for an intelligent sensor that results from the object model is shown. The modifier in the sensor is preferably a modulator which gives us maximum flexibility in the choice of microcontroller.
The modulator can be either a free-running oscillator of which frequency, period or duty-cycle depends on the output signal of the measurand, or a synchronized (clocked) oscillator, like a Sigma-Delta oscillator where the information is contained in the average of a bit stream.
Although such a modulator can be specifically designed for a certain sensing element, also generic types are available like the Universal Transducer Interface. This interface is suitable to measure capacitances, resistors, thermistors and bridges with one and the same low-cost device.

On the other hand, the modifier can also be an amplifier. From Fig. 4-5 we can see that we then require a specific type of microcontroller that includes an A/D converter or add an external one. The resulting intelligent analog sensor will not be investigated further in this work, since it leads to a sub-optimal solution (less flexible, higher costs) in our field of interest.

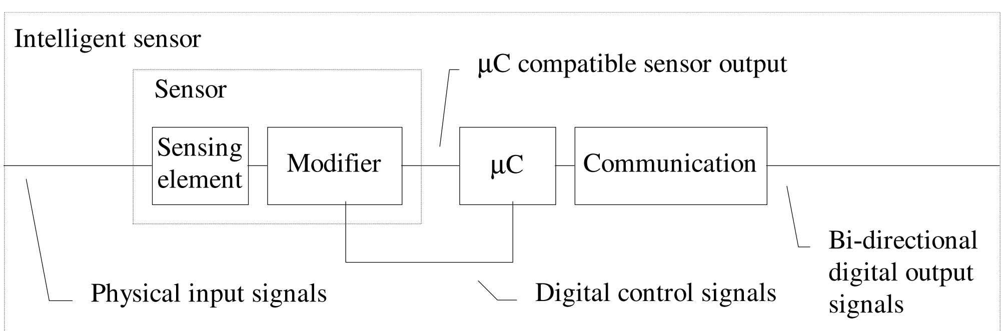

Fig. 4-6 Generic data flow diagram for an intelligent sensor

In some cases the sensing element and oscillator have even been integrated on one integrated circuit, resulting to a smart integrated sensor, like the Smartec temperature sensor (Fig. 4-7). Here the term "smart" is used to stress that the sensor has a calibrated, standardized output (microcontroller compatible duty-cycle) and that the sensing element and modifier are integrated on the same IC. By combining this sensor with a microcontroller we arrive at an intelligent temperature sensor.

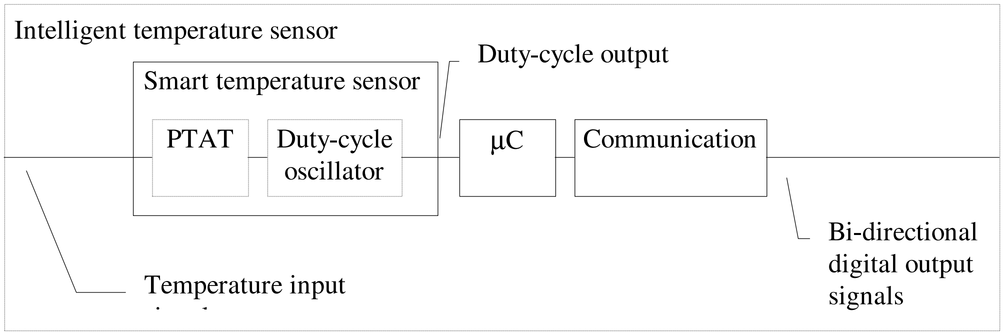

Fig. 4-7 Data flow diagram for an intelligent temperature sensor

Riedijk [36] presents another class of smart integrated sensors. These sensors have an Integrated Smart Sensor (IS^2) bus output (Fig. 4-8). IS^2 (a variation on the I^2C bus) has the capability to allow also analog (0 to 5 V) and time modulated signals on the bus. The (integrated) bus driver also takes care of the addressing of the sensor. Using this concept the microcontroller is not duplicated for each sensor and the wiring between sensors and microcontroller can be simplified. The disadvantage is that the specific behavior of each sensor is not encapsulated in the smart sensor, but at a higher level, resulting in a less flexible system. This solution seems most practical in high-volume (consumer) products where many sensors are to be applied.

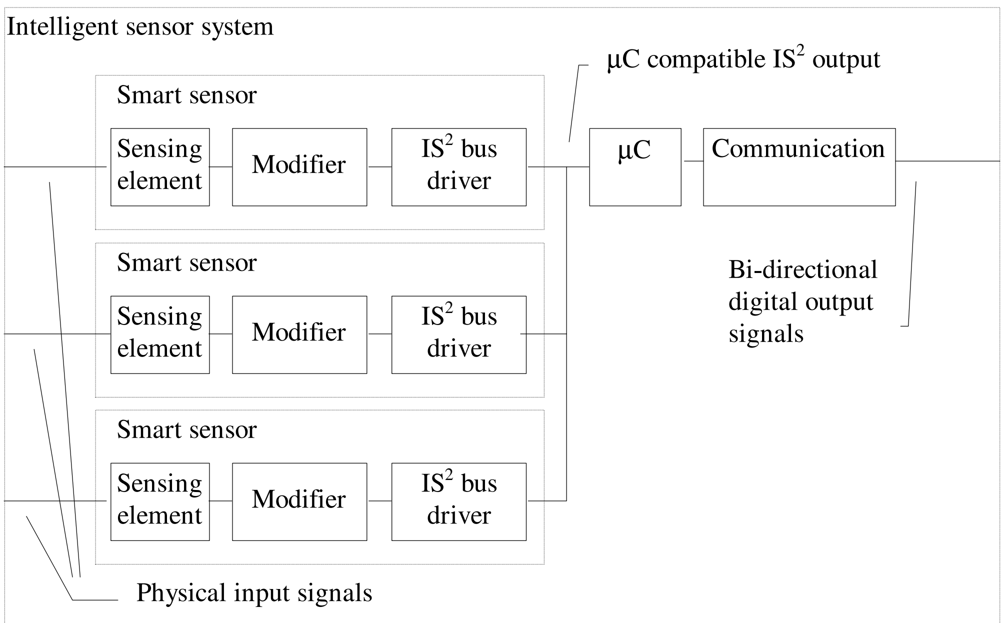

Fig. 4-8 Generic data flow diagram for an intelligent sensor system with IS^2 bus

The modularity of the design in Fig. 4-6 and availability of different components and types for each of the modules, assures a flexible design that can easily be adapted during the design process and later on. This design will be used as the basis of the designs throughout this thesis.

4.4 Conclusion

In this chapter object definitions for sensors and sensor systems have been given, as well as for the objects they consist of like sensing elements, signals and modifiers (like amplifiers and modulators). The relationships "uses" and "inherits from" between these objects have been presented using class diagrams.

Using these definitions, the class objects called Smart Sensor and Intelligent Sensor have been defined. The former name is usually used for silicon sensors (also called integrated silicon sensors) and hybrid sensors, where the sensing element and modifier are placed in the same housing. Since these properties of the sensor have mainly to do with the implementation, we elaborate further on properties that are generally recognized to qualify a sensor intelligent, like adaptability, reliability, interchangeability and identification, data reduction and standardized bi-directional communication.

Finally a generic data flow diagram for an intelligent sensor is presented as well as examples of an intelligent temperature sensor and an intelligent sensor system using a sensor bus (IS^2).

The intelligent sensor object model and its generic data flow diagram will be used as the basis of the designs throughout this thesis.

---

27 Middelhoek, S. and S.A. Audet, *"Physics of silicon sensors"*, Academic Press, London, 1989

28 Sze, S.M., "Semiconductor sensors", John Wiley & Sons, Inc., New York, 1994

29 Booch, G., *"Object oriented design: With applications"*, Benjamin/Cummings, 1991

30 Huijsing, J.H., G. van der Horn and F.R. Riedijk, *"Developments in integrated smart sensors"*, The 7th Int. Conf. on Solid-State Sensors and Actuators, pp. 320-326, June 1993

31 Hogenbirk, E.J., J.H. Huijsing and H.J. Verhoeven, *"An integrated smart sensor for flow and temperature with bus interface based on thermal sigma-delta modulation"*, The 7th Int. Conf. on Solid-State Sensors and Actuators, pp. 792-795, June 1993

32 Meijer, G.C.M., *"Concepts and focus points for intelligent sensor systems"*, Sensors and Actuators A, 41-42 (1994) 183-191

33 Analog Devices, *"Signal conditioners AD771X family"*, Data sheet, Norwood, USA, 1992

34 Schlichting, V., D. Hammerschmidt, B.J. Hosticka, E. Obermeier, G. Pollak-Diener and F.V. Schnatz, *"Digital programmable pressure sensor with on-chip signal processing and data storage"*, The 7th Int. Conf. on Solid-State Sensors and Actuators, pp. 988-991, June 1993

35 Riedijk, F.R., M. Bredius, J.H. Huijsing and R.F. Tuk, *"A bus controlled interface environment for an accurate read-out and flexible interconnection of integrated smart sensors in local systems"*, The 7th Int. Conf. on Solid-State Sensors and Actuators, pp. 327-330, June 1993

36 Riedijk, F.R., *"Integrated smart sensors with digital bus interface"*, Ph.D. Thesis, Delft University Press, Delft, November 1993

37 Haskard, M.R., *"An experiment in smart sensor design"*, Sensors and Actuators A, 24 (1990) 163-169

38 Wouters, P., M. de Cooman and R. Puers, *"A multi-purpose CMOS sensor interface for low-power applications"*, IEEE J. Solid-State Circuits, Vol. 29, No. 8, pp. 952 - 956, August 1994

5
CAPACITIVE SENSING ELEMENTS

A capacitive sensing element is an object that belongs to the class of modulating sensing elements. This means that this kind of sensing element only yields an output signal when external energy is supplied. This is in contrast with the class of self-generating sensing elements, like for instance a thermocouple, that generates a voltage from a temperature difference.
At the end of this chapter we will try to define an object model for capacitive sensing elements, in other words find the properties and internal and external relationships. Although the basic properties can be deduced by looking at the class ancestors, some properties in the class are new because they are required to make the sensing element useful.

Although a capacitive sensing element belongs to the class of modulating sensing elements, it at the same time belongs to the class of capacitors. Therefore it inherits properties from both classes at once.
From the class of capacitors the properties: electrode structure (which consists of electrodes), dielectric (nonconductor), connecting leads, capacitance, parasitic capacitances and the physical relations that determine the capacitances are inherited.
The class of modulating sensing elements adds the non-electrical input, the electrical quantity that is modulated and the electrical quantity that is output.

The electrode structure in a capacitor consists of at least two electrodes. However, a useful capacitive sensing element needs a well-defined transfer function which leads in many cases to electrode structures that consist of more than two electrodes (often called three or multi-terminal capacitors, Heerens [39]). A well-defined transfer function means the function is well understood, stable and selective. This leads to the following requirements:

- A well understood transfer function is determined by known, universal physical laws.
- A stable and selective transfer function does not change in time, or alternatively is not influenced by other parameters like temperature, material changes etc.
- The transfer function is also not influenced by the electrical quantities that are modulated and output.

First we will discuss the physical laws that govern the behavior of capacitance. Then some often used electrode configurations are presented and their (ideal) behavior is described, followed by a description of the non-ideal properties like electrode bending effects, finite gap sizes, parasitic capacitances and contamination influences as well as methods to reduce these influences.
Finally we arrive at the object model of the capacitive sensing element.

5.1 Physical aspects

In this section we first look at the fundamental physical laws describing the electric field. Using this law we can define the properties of dielectrics and conductors. Then the definition of capacitance is given, followed by a method to measure the capacitance in a practical situation. Although this automatically leads to a time-dependent electromagnetic field, using a quasi-static approximation the capacitance can still be determined. Finally, the non-idealities of capacitive sensing elements are determined.

5.1.1 The electric field

From a physical point of view a capacitive sensing element is very attractive compared to other types of sensing elements (for instance resistive or inductive) because the physical laws that characterize its behavior are so fundamental. These laws are known as Maxwell's equations for the electromagnetic field (in differential form)

$$\begin{aligned} &\operatorname{div} \vec{E} = \frac{\rho}{\varepsilon_0} \\ &\operatorname{div} \vec{B} = 0 \\ &\operatorname{curl} \vec{E} = -\frac{\partial \vec{B}}{\partial t} \\ &\operatorname{curl} \vec{B} = \mu_0 J + \varepsilon_0 \mu_0 \frac{\partial \vec{E}}{\partial t} \end{aligned} \quad . \tag{5-1}$$

The first two equations are also known as Gauss's law for the electric and the magnetic field, while the third and fourth equation are also known as the Faraday-Henry and Ampère-Maxwell law respectively.
In most cases we can assume the electric field to be static (in which case there is no magnetic field) and also that there are no currents (which implies infinite resistance between electrodes). In this case Maxwell's equations simplify to Gauss's law for the electric field:

$$\operatorname{div} \vec{E} = \frac{\rho}{\varepsilon_0} \tag{5-2}$$

with ε_0 the permittivity in vacuum (which has a value of 8.854 pF/m) and ρ the total charge density.

The electric potential is defined as:

$$\vec{E} = -\operatorname{grad} V \tag{5-3}$$

5.1.2 Dielectrics

When an external electric field is applied to a non-conducting piece of matter it generally becomes polarized. Such a material is called a dielectric. The polarization P is in many cases proportional to the applied field

$$\vec{P} = \chi_e \varepsilon_0 \vec{E} \tag{5-4}$$

where χ_e is called the electric susceptibility. As a result the charge per unit area σ_P on the surface of polarized matter is equal to the component of polarization normal to the surface of the body.

As we will see further on, instead of the total charge often only the free charge (the charge on the conductors) is considered, while the effect of the polarization is taken into account by replacing the electric field by the displacement

$$\vec{D} = \left(1 + \chi_e\right) \varepsilon_0 \vec{E} \,. \tag{5-5}$$

In this case Gauss's law for the electric field change to

$$\operatorname{div} \varepsilon_0 \vec{E} = \rho_{free} \tag{5-6}$$

in vacuum, and to

$$\operatorname{div} \varepsilon_0 \left(1 + \chi_e\right) \vec{E} = \rho_{free} \tag{5-7}$$

in the case of a dielectric.

5.1.3 Conductors

On the other hand, when an external electric field is applied to a conductor it also becomes polarized, but since the charges in a conductor can move around freely, they will be distributed in such a way that the resulting electric field inside the conductor is zero. Consequently all points of the conductor are at the same potential. From Gauss's law it follows that all the electric charge of a conductor resides on the surface of the conductor.

5.1.4 Capacitance

A capacitor consists of electrodes (conductors) separated by dielectrics (non-conductors). When then are two electrodes that are kept at different potentials V_1 and V_2, an electric field will result between them. Then the electrical capacitance is defined as

$$C = \frac{q_{free}}{V_1 - V_2} \tag{5-8}$$

where q_{free} is

$$q_{free} = \oint_S \sigma_{free} \, dS \tag{5-9}$$

the total free charge on the electrode surface S.

When we replace the vacuum with a homogenous dielectric material (Fig. 5-1) the free charges on the conductor must increase (when the potentials are kept constant) to compensate the polarization charge (from Eq. (5-3) the electric field must remain constant).

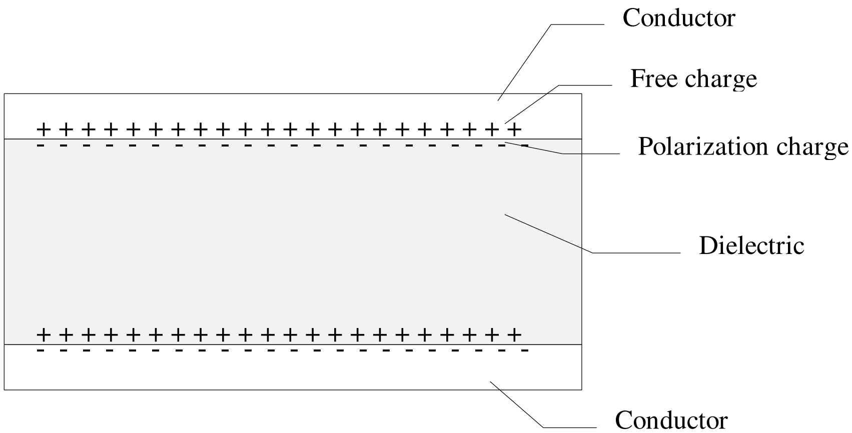

Fig. 5-1 Dielectric placed between two conductors kept at a constant potential difference

In other words, in Eq. (5-2) the total charge can be replaced by the free charge minus the polarization charge.

$$\operatorname{div} \vec{E} = \rho_{free} - \vec{P} \tag{5-10}$$

substituting Eq. (5-4)

$$\operatorname{div} \varepsilon_0 \left(1 + \chi_e\right) E = \rho_{free} \tag{5-11}$$

normally $1 + \chi_e$ is replaced by ε_r, the relative permittivity of the material.

From these equations it can be shown that the capacitance between two electrodes depends only on their geometry, their distance and the permittivity of the material between them.

5.1.5 Measurement of capacitance

Note that the capacitance does not depend on the electrodes potential (i.e. if the electrode is grounded or not) and charge. However, Eq. (5-8) does suggest that we can measure the total charge induced on an electrode that is kept at a constant voltage, by a voltage change on a second electrode. As long as all the electrodes that are not of interest are also connected to a constant potential, from Eq. (5-8) it follows that their contribution to the total induced charge is zero. In other words, all electrodes that are not of interest are connected to the same voltage and can then be considered as one electrode. An electrical model with multiple conducting elements (electrodes E_1, E_2 and E_3) is shown in Fig. 5-2. This model can be considered as the general electrical model of a multi-electrode sensing element during the measurement of the capacitance of interest.

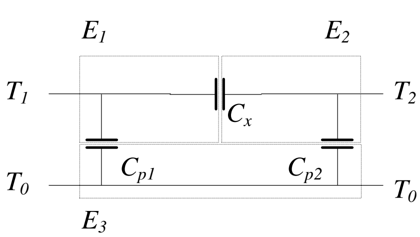

Fig. 5-2 Static electrical model for a multi-electrode capacitor

5.1.6 Time-dependent electromagnetic field

In a practical capacitor (and therefore also capacitive sensing element), the charge on the electrode can not easily be measured at a constant voltage. However, a voltage that changes in time means that the electric field is not static. Also, the isolation resistance of the dielectric is not infinite, so a current will flow from one electrode to another. As a consequence, Maxwell's equations for the electromagnetic field will need to be used.

However, when the wave length of the voltages is much larger then the dimensions of the structure, the electric and magnetic fields are almost independent of space. The electrical model then consists of a network of capacitances, resistances and inductances. This is called the quasi-static approximation. An example is shown in Fig. 5-3.

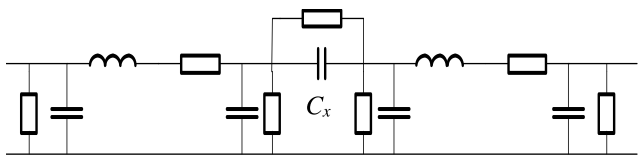

Fig. 5-3 An example of the electrical model of a multi-electrode structure at higher frequencies using the quasi-static approximation

In this model, the connecting leads of C_x have series inductances and resistances and capacitances with parallel resistances to ground. Also, C_x itself has a parallel resistance. It is clear that in such a complicated model (which is by no means complete) it will be very difficult to measure C_x externally while eliminating the influence of the other network elements.

On the other hand, the lumped model concentrates the electric and magnetic fields in certain points. According to Maxwell's laws they are linked, so that the values of the network elements will also be linked. In other words, when used as a sensor the measurand can not be assumed to influence only C_x and the information about the measurand will be distributed over all the network components. In fact, the value of C_x might not be the best representation of the measurand.

> Example:
> This situation arises for instance when measuring the water content in corn, as presented by Kandala *et. al.* [40]. A lumped model representing the parallel plate capacitor that holds the single kernels of corn would be very complicated and quite useless. Instead, the authors measured the transfer function (in terms of capacitance and loss factor) of the network as a function of the frequency. It appears that in this case the moisture content can be predicted by a combination of the change in capacitance, loss factor and phase angle when the frequency changes from 1 MHz to 4.5 MHz.

At low frequencies the model in Fig. 5-3 can be reduced to Fig. 5-4.

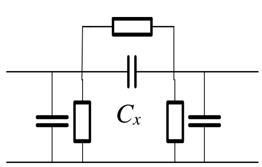

Fig. 5-4 Reduced electrical model at low frequencies

The series inductances of the leads can be ignored at low frequencies since their impedance becomes insignificant compared to the impedance of series resistors. The series resistors itself are usually insignificant compared to the high isolation resistors of the dielectric and the high impedances of the capacitors at low frequencies. The resulting model is now similar to the model in Fig. 5-2 with the addition of a resistance parallel to each capacitance.

5.1.7 Non-idealities

In the introduction to this chapter we required the transfer function to be determined by known, universal physical laws. This appears to be the case for the time-dependent electromagnetic field. When the electric field is static or when the quasi-static approximation is valid (at low frequencies) calculations on the electric fields are much simplified which can help to create a "well understood" transfer function.

It was also required that the transfer function is stable and selective, i.e. does not change in time and is not influenced by other parameters like temperature, material changes, etc. This appears to be the case only in part, as the capacitance is determined by the geometrical factors of the electrodes and by the permittivity of the dielectric. A special case of the latter, the influence of humidity on the permittivity of air will be discussed in the next subsection.
The geometrical factors may be unstable or influenced by other parameters themselves. When these effects are known, their influence on the capacitance may be calculated. Often this is not the case, but by applying multi-electrode structures, the influence of these effects can be reduced.

> Example:
> For instance, geometrical factors are normally affected by temperature. This effect can be approximated by introducing a linear expansion coefficient. When two identical capacitances are created, in a multi-electrode structure, the ratio of the capacitances will remain independent of the temperature.

The permittivity of the dielectric, being a material constant, strongly depends on the (purity of the) material. Also some materials behave different at different orientations. The permittivity might even be influenced by the strength of the electrical field, violating the third requirement. However, in many cases it can be assumed that the permittivity is homogeneous and independent of the orientation, again allowing us to apply multi-electrode structures to reduce the effect of unknown parameters on the permittivity.

The final requirement is that the capacitance is not influenced by the potential or charge on the electrodes. It will be clear from Gauss's law that, when the dimensions of the electrode structure are known and with an ideal dielectric material, such a dependence does not exist. However, the dimensions of the structure themselves might be influenced by the potential or the charge, while many dielectrics exhibit a voltage dependency.
For instance, since the electric field exerts a force F on the surface charges on the electrodes, the distance d between the electrodes may vary as a function of the voltage V. With

$$F = \frac{V^2 C}{d} \tag{5-12}$$

and V = 1 Volt, C = 1 pF and d = 1 mm this results to F = 10^{-9} N.
In many applications this effect may be neglected. However, in integrated accelerometers (for use in air bags) where the electrode distance is much smaller, this effect is used for self-testing the sensor. At power-up a known voltage is applied to the electrodes. The resulting force is then measured by the sensor and compared to the expected value.

Here an important advantage of capacitive sensing elements arises compared to for instance strain gauges. Since a capacitor does not dissipate power, no heat is produced in the sensor. Not only does this prevent the change of dimensions of the electrode structure as a function of the voltage, also no heat is transferred to the environment. This proves to be an important feature in cryogenic measurements, where the absolute temperature can be below 1 mK.

5.1.8 The effect of humidity on the permittivity of air

In most sensor applications a reference electrode will be used to measure a capacitance ratio. The capacitance ratio is then a measure for the quantity to be measured. If both capacitors (sensing capacitor and reference capacitor) are air capacitors filled with air with equal permittivity, the ratio will be independent of the humidity. However, when one of the capacitors is not an air capacitor, the ratio will depend on the permittivity of air, and the influence of the humidity on the capacitance will need to be taken into account. Lea [41] estimated the relative dielectric constant by

$$\varepsilon_{moist\,air} = 1 + \frac{a_1}{T}\left[P_d + \frac{a_2 P_w}{T} H\right] \tag{5-13}$$

in which

$$a_1 = 1.58 \times 10^{-6}\ \mathrm{K/Pa}$$
$$a_2 = 48\mathrm{K}$$

where T is the absolute temperature in K, P_d is the pressure of the moist air, P_w is the pressure of saturated water vapor at temperature T, and H is the relative humidity.
Bonse [42] reviewed later work of Bell and Bell [43], Froome and Essen [44] and Bean and Dutton [45]. A comparison is given in Table 5-2.

Table 5-2 Sensitivities of ε_r for temperature, air, water and CO_2 vapor pressures and humidity according to various authors for standard air (T = 293.15 K, P_d = 100 kPa, P_w = 117.5 Pa, P_c = 30 Pa).

		Lea	Bell	Froome	Bean
$\varepsilon_r - 1$	[ppm]	645	610	602	603
$\partial\varepsilon_r/\partial T$	[ppm / K]	-2.56	-2.32	-2.29	-2.29
$\partial\varepsilon_r/\partial P_d$	[ppm / kPa]	5.40	5.39	5.30	5.30
$\partial\varepsilon_r/\partial P_w$	[ppm / kPa]	88.42	87.78	91.08	91.08
$\partial\varepsilon_r/\partial P_c$	[ppm / kPa]	-	-	9.09	-
$\partial\varepsilon_r/\partial H$	[ppm / %]	2.06	-	-	-

Values partly taken from Bonse [42] and converted to SI units

The sensitivity for CO_2 can normally be neglected since the CO_2 content of the atmosphere is small and so are the absolute changes in the partial vapor pressure. Although the values calculated by Lea differ slightly from those in more recent work, his paper does present a graph showing the relation between relative humidity, temperature and permittivity at a single glance.

> Example:
> At $T = 348$ K and $P_d = 100$ kPa, when H rises from 20% to 60% the maximum change in permittivity can be estimated to be 1000 ppm, while at $T = 293$ K an increase of H from 0% to 100% causes a change of only 200 ppm.

5.2 Capacitive sensing element electrode configurations

Although in theory any electrode configuration can be used as a capacitive sensing element, in practice some limitations exist.

- Even when the quasi-static approach is valid and Laplace's law for the electric field can be used instead of Maxwell's laws, solving Laplace's law analytically proofs to be difficult if not impossible in most cases. The use of numerical packages (that utilize finite element or finite difference techniques) appears to be time consuming and inaccurate, while the results remain difficult to interpret.
- Mechanical tolerances are not infinitely small. Symmetrical structures generally benefit from some form of compensation for some of the tolerances, relaxing the requirements for manufacturing.
- In geometries where one of the dimensions can be assumed infinite compared with the other two, Laplace's law reduces to a two-dimensional one. For several of these electrode geometries these equations have been solved in general by Heerens [46, 47]. Heerens defined a set of 5 archetypes of toroidal capacitor geometries and calculated the capacitance by solving Laplace's equation in cylindrical coordinates. All other types of capacitors in the torus can be found by summation.

The resulting equations are very complex while the construction of toroidal structures is costly. However, by applying a set of transformations, solutions to cylindrical as well as uniplanar and biplanar shapes have been derived.

Although especially the uniplanar structures can be manufactured at low costs, biplanar structures are in general more easily calculated. First we will look at a special class of biplanar structures that are called cross-capacitors. The capacitance of these structures appear to depend only on one geometrical parameter (length). After this, the properties of ordinary biplanar and uniplanar structures will be discussed.

5.2.1 Thompson and Lampard cross-capacitors

This is a family of capacitors of which the capacitance depends only on a length multiplied by a dimensionless factor. Thompson and Lampard [48], [49] first presented a general theorem on cylindrical capacitors having this property and which are now generally known as (Thompson-Lampard) cross-capacitors.

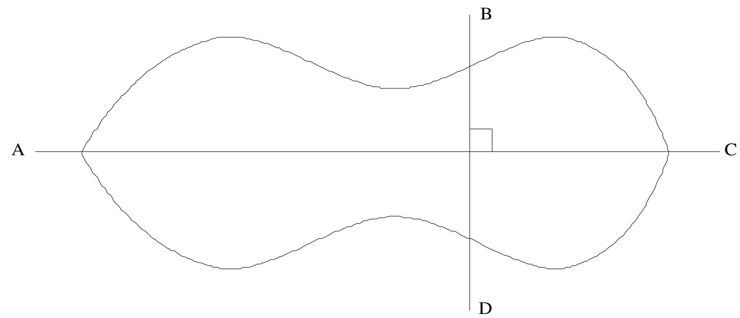

Fig. 5-5 Cross-section of cylindrical shell

The theorem states that if we have a cross-section of a conducting line-symmetric cylindrical shell (Fig. 5-5), that is divided into four parts by its axis of symmetry *AC* and another line *BD*, perpendicular to the axis of symmetry, the cross-capacitance (between two opposing parts of the shell) will be (after rewriting to SI units)

$$C_{cross} = \frac{\varepsilon_0 \, \varepsilon_r \, l}{\pi} \ln 2 \tag{5-14}$$

with *l* the length of the shell.
Capacitances based on this principle are used at the National Bureau of Standards as the primary standard of capacitance [50] (Fig. 5-6).

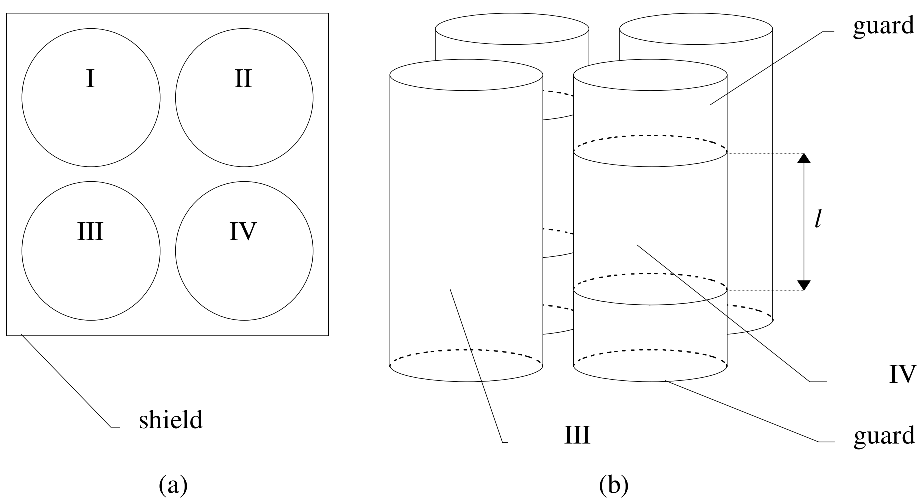

Fig. 5-6 Thompson and Lampard standard capacitors (a) top view (b) perspective

The capacitances between electrode I and IV and II and III are successively measured and averaged. The capacitance now depends only on the length *l* of rod IV and is given by Eq. (5-14).
The main advantage of this structure is that the capacitance can be made extremely stable and is very accurately calculable. However, in capacitive sensors the requirements for the reference capacitor are often just good stability (and low cost) since the sensor needs to be calibrated to the physical parameter to be measured. The overall system calibration eliminates the need for a reference capacitor with an accurately known value. In this case, other structures based on the Thompson and Lampard cross-capacitor might be better suited.
Heerens [47] presented a circular version of the cross-capacitor (Fig. 5-7a) that is better suited to low-cost implementation. By applying a transformation he also derives a linear, biplanar version.

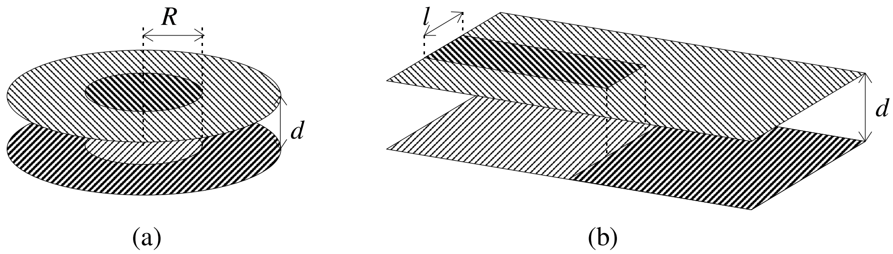

Fig. 5-7 (a) Circular and (b) linear biplanar cross-capacitor

Assuming an equal radius R for the top and bottom inner electrode and an infinite outer electrode radius, the cross-capacitance of the circular cross-capacitor can be shown to be

$$C = \varepsilon_0 \varepsilon_r \frac{\ln 2}{\pi} 2\pi R \left[1 + 0.000043507 (d/R) - 0.050631437 (d/R)^2 + \ldots \right] \quad (5\text{-}15)$$

Toth *et. al*. [51] presented a variation to the circular structure, suited well to low-cost sensor applications. The structure was implemented using low-cost printed circuit board material and displays a stability of 0.1% over a temperature range from -25°C to +75°C and humidities ranging from 0% to 100% (non-condensing).

Similar structures can be created with the linear biplanar cross-capacitor (Fig. 5-7b). The cross-capacitance of the linear biplanar cross-capacitor is then equal to Eq. (5-14). With such a structure it is possible to connect more electrodes in parallel, resulting in an adjustable reference capacitor.

5.2.2 Biplanar electrodes

The most simple electrode structure is the parallel plate capacitor. However, the electric field bending near the fringes make the capacitance fairly unpredictable. By adding a so-called Kelvin guard ring, the field bending is moved out of the area of interest (Fig. 5-8a) and the capacitance can be calculated to be simply

$$C = \varepsilon_0 \varepsilon_r \frac{A}{d} \quad (5\text{-}16)$$

with A the area of the smaller electrode and d the distance between the electrodes. This electrode can also be implemented using PCB at a very low cost, especially since the capacitance does not depend on the lateral position or rotation of the electrodes.

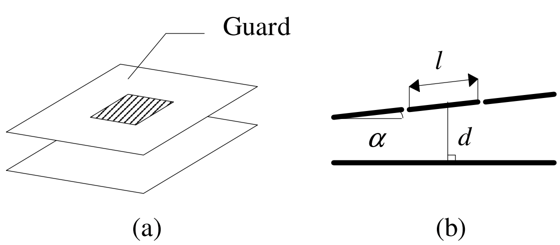

Fig. 5-8 Parallel plate capacitor (a) perspective (b) cross-section

Toth [52] and de Jong [53] calculated the capacitance of the structure when the electrodes are oblique (Fig. 5-8b) with angle α in radians

$$C = \varepsilon_0 \varepsilon_r \frac{w}{\alpha} \ln\left(\frac{2d\cos\alpha + l\sin\alpha}{2d\cos\alpha - l\sin\alpha} \right) \tag{5-17}$$

with $w = A / l$. Applying a second order Taylor expansion and assuming $d < l$, then (5-17) can be simplified to

$$C = \varepsilon_0 \varepsilon_r \frac{A}{d} \left[1 + \frac{1}{12} \left(\frac{l}{d} \alpha \right)^2 \right]. \tag{5-18}$$

Although the error term can be made small by properly dimensioning the electrode area and distance, the effect of the obliqueness is a virtually increased electrode area. The electrode area A is usually unknown and will calibrated during an overall system calibration. Therefore only small changes in the angle need to be considered.
We can calculate the sensitivity to changes in the angle

$$S_\alpha = \frac{\dfrac{\partial C}{\partial \alpha}}{\dfrac{C}{\alpha}} \tag{5-19}$$

substituting Eq. (5-17) and using a third order Taylor expansion we arrive at

$$S_\alpha = \frac{4d^2 + l^2}{6d^2} \alpha^2 \tag{5-20}$$

We can compare this to the sensitivity to distance changes

$$S_d = -\frac{6d^2 + l^2 \alpha^2}{6d^2} \tag{5-21}$$

which results to $S_d \approx -1$ in most practical situations, where $\alpha l < d < l$.
From this we can see that the larger the electrode compared to the electrode distance, the stronger the influence of the obliqueness.
This type of electrode structure can be used when small displacements (compared to the initial electrode distance) need to be measured at very low-costs.

Other types of biplanar structures include:

- A differential parallel plate capacitor (Fig. 5-9) presented by Heerens [47] and Zhu [54]. Bonse [42] applied the principle in a two-dimensional array. When w is sufficiently large (as we will discuss in section 5.3), the capacitance can be approximated by

$$C_1 - C_2 = \varepsilon_0 \varepsilon_r \frac{l\,x}{d} \tag{5-22}$$

where x is the displacement from the center of the structure. From Eq. (5-22) it can be seen that the capacitance also depends on the size of the electrodes and the distance between them. The resulting requirements for the accuracy of the manufacturing of the electrodes prohibit the use of materials like PCB when a high sensor accuracy is desired. Also the accurate positioning of the electrode distance can be problematic.

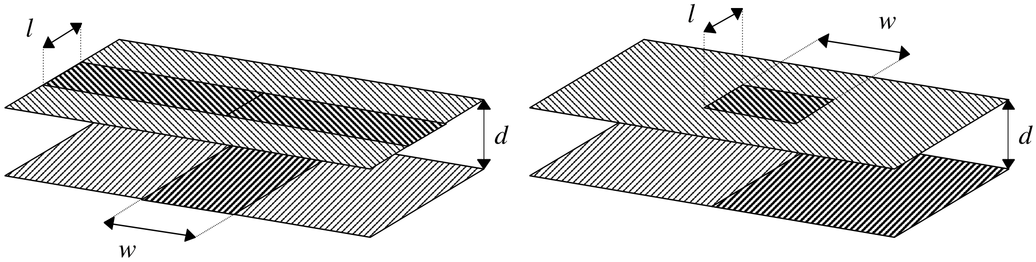

Fig. 5-9 Differential biplanar electrode structures

- A multi-electrode structure of this type is presented by De Jong [53] as well as a similar type where a grounded screen electrode is used (Fig. 5-10). Assuming equal electrode areas, the electrode distance changes are eliminated. The structure has been applied in an angular encoder with a 90°C range. Li *et. al*. [55] presented a modified structure that resulted to an angular encoder with a full-circle range. In both structures electric field bending effects appear to limit the accuracy. Still a high accuracy has been obtained at low cost.

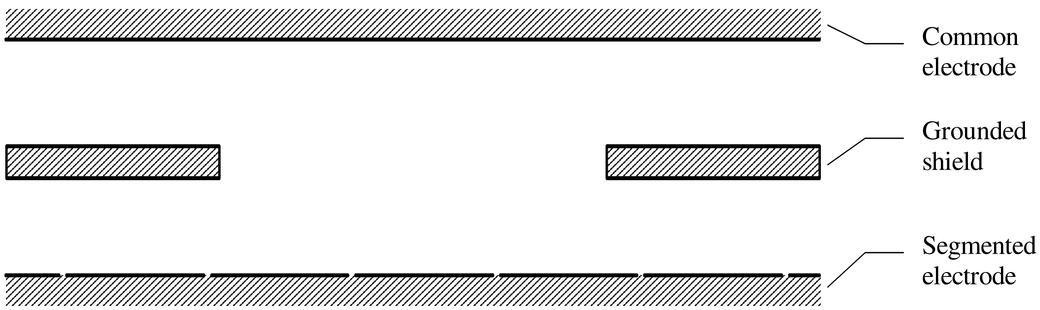

Fig. 5-10 Cross-section of multi-electrode biplanar structure with grounded shield

These structures are based on electrode-area changes. They are very suitable to measure position over large ranges (compared to the electrode sizes and distances) when used in multi-electrode configurations, but can also be used to measure changes in the dielectric over a large range.

5.2.3 Uniplanar structures

The class of uniplanar electrode structures is very interesting for application in low-cost capacitive sensors. Since all electrodes can be created on a single substrate the accuracy of the capacitances depend on the accuracy lithographic process, which is generally better than the positioning accuracy for biplanar electrodes (at comparable costs). Using archetypes presented by Heerens [47], [56] these structures can be transformed from a toroidal structure to a cylindrical (Fig. 5-11a) and from a cylindrical to an uniplanar structure (Fig. 5-11b). The uniplanar structure includes a grounded second electrode, which is necessary to define a bounded problem area. However, the influence of this electrode on the capacitance decreases quickly with distance between them. Therefore tolerances in the position accuracy of this electrode will have an insignificant influence on capacitance at larger distances.

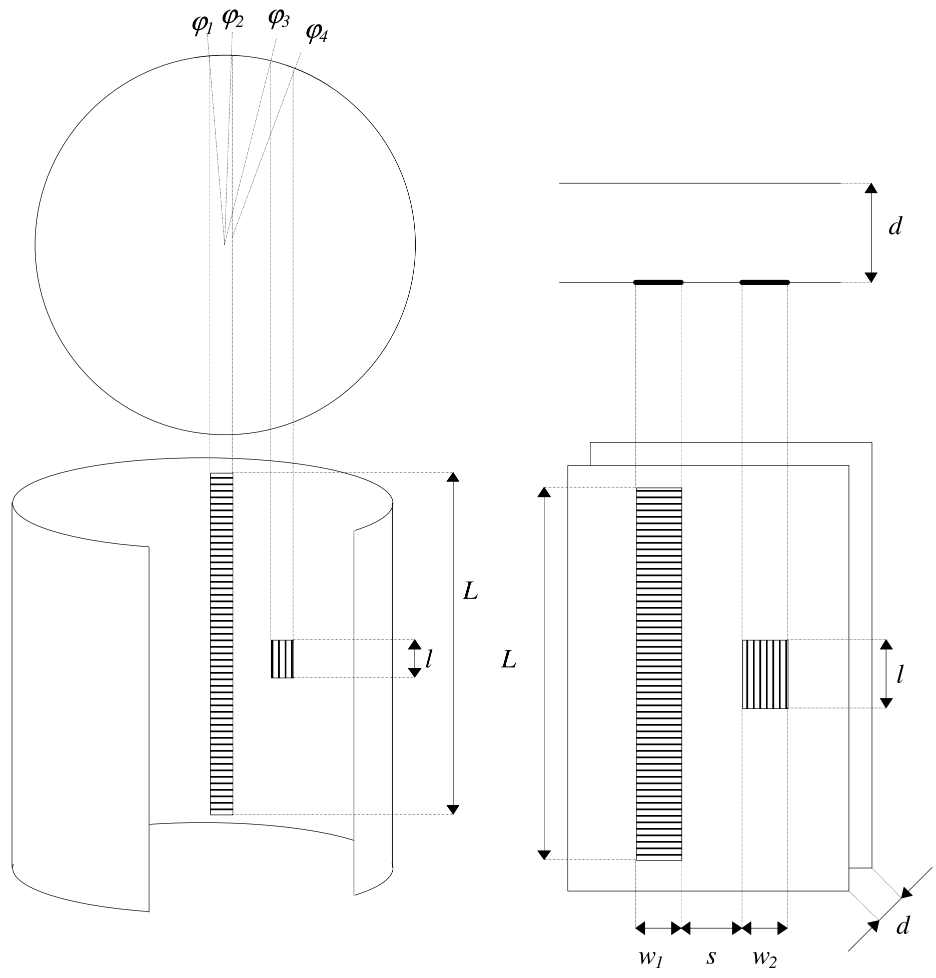

Fig. 5-11 Cylindrical (a) and uniplanar (b) square-strip electrode structures

In the uniplanar structure the internal capacitance between the square with length l and width w_2 and the strip with infinite length L and width w_1 is given by

$$C = \frac{\varepsilon_0 \varepsilon_r l}{\pi} \ln\left(\frac{\sinh\left(\frac{\pi}{2}\frac{w_2+s}{d}\right)\sinh\left(\frac{\pi}{2}\frac{w_1+s}{d}\right)}{\sinh\left(\frac{\pi}{2}\frac{s}{d}\right)\sinh\left(\frac{\pi}{2}\frac{w_1+w_2+s}{d}\right)} \right). \tag{5-23}$$

When $d > 5\ s$, Eq. (5-23) can be simplified to

$$C = \frac{\varepsilon_0\ \varepsilon_r\ l}{\pi} \ln\left(\frac{(w_1+s)(w_2+s)}{s(w_1+w_2+s)} \right) \tag{5-24}$$

The cylindrical structure, although more difficult to construct, has an additional interesting feature: the capacitance does not depend on the radius R of the tube. The capacitance of both the internal and the external geometry is described by

$$C = \frac{\varepsilon_0 \varepsilon_r l}{\pi} \ln\left(\frac{\sin\left(\frac{1}{2}(\varphi_1-\varphi_3)\right)\sin\left(\frac{1}{2}(\varphi_2-\varphi_4)\right)}{\sin\left(\frac{1}{2}(\varphi_2-\varphi_3)\right)\sin\left(\frac{1}{2}(\varphi_1-\varphi_4)\right)} \right), \tag{5-25}$$

although in any real application for the capacitance of the external geometry the influence of packaging etc. will have to be taken into account.

These structures seem especially suitable as level gauges based on the change of permittivity.

> Example:
> Heerens [56] presented a level gauge for liquids and powders based on the cylindrical structure. Electrodes are created on the outside of a glass tube and the internal capacitance between them is measured. The level can be determined by interpolating between the capacitance of a completely filled and a completely empty electrode structure.

This design has the advantage that the electrodes can be protected from the product by a (thin) glass layer, which is especially important in the case of aggressive products that otherwise might permanently damage the electrodes. The glass layer can be modeled as a (relatively large) series capacitance in the case of non-conducting liquids (Fig. 5-12a), that will cause only a small error on the measured level. In the case of liquids with a high conductance that are connected to ground, the capacitance of a completely covered electrode will be nearly zero since the conducting fluid with act as a grounded shield (Fig. 5-12b). Still this structure can be used to measure the level of the liquids, interpolating between zero and the capacitance of a completely empty electrode structure.

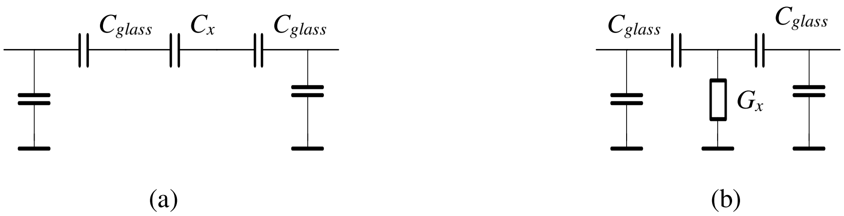

Fig. 5-12 Electrical model with series capacitances in the case of (a) non-conducting and (b) conducting liquids

In the case of slightly conducting liquids like demineralized water, the influence of the series capacitances becomes more unpredictable. However, when the electrodes are in direct contact with the liquid the equivalent circuit becomes simply as in Fig. 5-13.

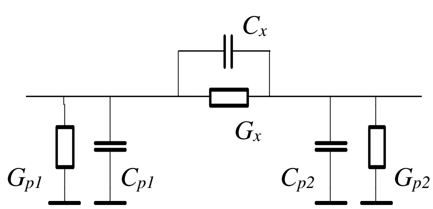

Fig. 5-13 Electrical model in the case of slightly conducting fluids in direct contact with the electrodes

Using the basic electrodynamics equations

$$div\left(\vec{E}\right) = \frac{\rho}{\varepsilon_0 \varepsilon_r} \tag{5-26}$$

and

$$\vec{j} = \sigma \cdot \vec{E} \tag{5-27}$$

with σ the conductivity, ρ the charge density and $\vec{j}$ the current density, we can easily find the remarkable relationship between C_x and G_x (Brabetz *et. al.* [57])

$$\frac{C_x}{G_x} = \frac{\varepsilon_0 \varepsilon_r}{\sigma} . \tag{5-28}$$

It appears that the ratio of C_x and G_x depends only on the characteristics of the liquid and not on the geometrical factors of the electrodes. By measuring C_x and G_x in the liquid and C_x in vacuum (or air), the permittivity and the conductivity can be calculated.

The latter property makes these structures also suitable for sensors that measure the permittivity and conductivity of liquids or liquid mixtures. This can be used by for instance alcohol fuel sensors. Such a sensor measures the ratio of methanol and gasoline so the stoichometric air-fuel ratio can be adapted to the current mixture, enabling a so called flexible fuel vehicle (FFV) [57], [58], [59].

5.3 The influence of guard rings and gaps

Analytical (but also numerical) calculations on capacitors often depend on at least one of the following assumptions:

- The electrodes have an infinite size or are surrounded by another electrode of infinite size.
- The gap between two adjacent electrodes is infinitely small.

Instead, finite electrode and gap sizes have to be taken into account when precision capacitors are required, like in the case of capacitive sensing elements or capacitance standards.
First, we will look at the influence of the finite guard electrode size. After that, the influence of finite electrode gaps in various cases will be discussed.

5.3.1 Finite guard rings

The finite electrode sizes cause a deviation of the electric field near the fringes, which is called electric field bending. This deviation of the electric field can usually not be calculated analytically. However, when the environment of the electrodes is well known the field bending can be calculated numerically. Since we are dealing with sensing elements, the environment is in general not well known and it is better to reduce the effect of the field bending to an insignificant level. When such measures are not taken, placing a conductor near the fringes of the electrodes can have a large, unpredictable effect.

To prevent undesired influences of the environment on the capacitance (and to make the structure easier to model, so the electric field can be calculated analytically) the electrodes are often surrounded by another electrode: the Kelvin guard or guard electrode.
It is not always necessary to surround both electrodes by a guard electrode (Fig. 5-14). Here only the small electrode is surrounded by a guard electrode. The electric field is now homogeneous in the area of interest, so the capacitance can easily be calculated.

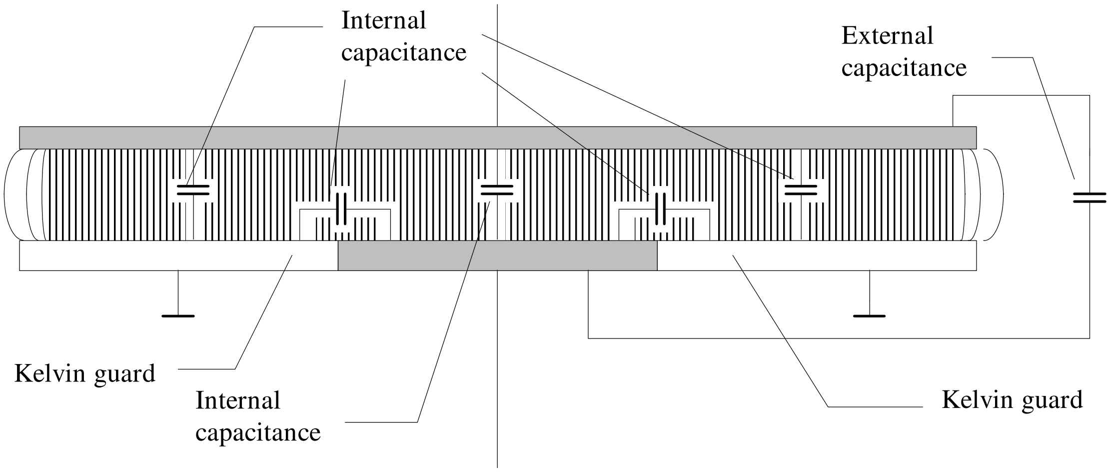

Fig. 5-14 Simple parallel plate capacitor with Kelvin guard electrode

The guard rings serve two purposes:
1. they function as a shield
2. they move electric field bending effects out of the area of interest.

As can be seen from Fig. 5-14, there are two capacitances of interest, one internal in the electrode structure, the other external. For many sensing elements, the external capacitance must be reduced to an insignificant level. Although in Fig. 5-14 this is also accomplished by the guard ring, in practice the surroundings of the sensing elements are often not well known. Then extra grounded shield electrodes at the outside are required.

Since the guard electrodes themselves are also not of finite size some field bending effects will remain. These effects have been studied in detail by Heerens [39], [47], [60], Zhu [54] and Bonse [42]. Heerens presents a rule of thumb to estimate the worst case error caused by the finite size of guard electrodes and gaps.

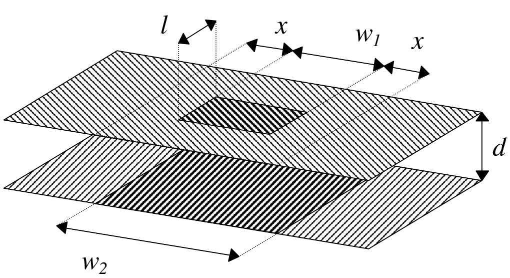

Fig. 5-15 Biplanar square-strip geometry

This can be calculated using the structure in Fig. 5-15. Assuming that the square (top electrode) lies in the middle of the strip (bottom electrode), so that $w_2 = w_1 + 2\,x$, Heerens [47] and de Jong [53] show that

$$C = \frac{\varepsilon_0\,\varepsilon_r\,l}{\pi}\ln\left(\frac{\cosh\left(\frac{\pi(w_1+x)}{2d}\right)\cosh\left(\frac{-\pi(w_1+x)}{2d}\right)}{\cosh\left(\frac{\pi\,x}{2d}\right)\cosh\left(\frac{-\pi\,x}{2d}\right)}\right). \qquad (5\text{-}29)$$

Assuming $x \gg d$ this can be approximated by

$$C \approx \frac{\varepsilon_0 \, \varepsilon_r \, l \, w_1}{d} \tag{5-30}$$

as can be expected. We can also calculate the difference between (5-29) and (5-30), which is the error caused by the finite guard electrode

$$\delta_{guard} < -\frac{2\,d}{\pi\, w_1} e^{-\frac{\pi\, x}{d}} \,. \tag{5-31}$$

This leads to Heerens rule of thumb [47] that with $d > 5\,x$, the worst case error caused by finite guard widths is less then 1 ppm.

5.3.2 Finite gap width in linear biplanar cross-capacitors

Heerens *et. al.* [61] calculated the influence of finite gaps on the cross-capacitance, in the case of thick and thin electrodes. This was done by using an approximation of the electric field in the gap and assuming the permittivity in the gap equal to the permittivity between the electrodes. In the case of thick electrodes ($h > 5\,s$), the relative error is

$$\delta_{gap} < e^{-\frac{\pi h}{s}} \tag{5-32}$$

where h represents the depth of the gap and s the gap width.

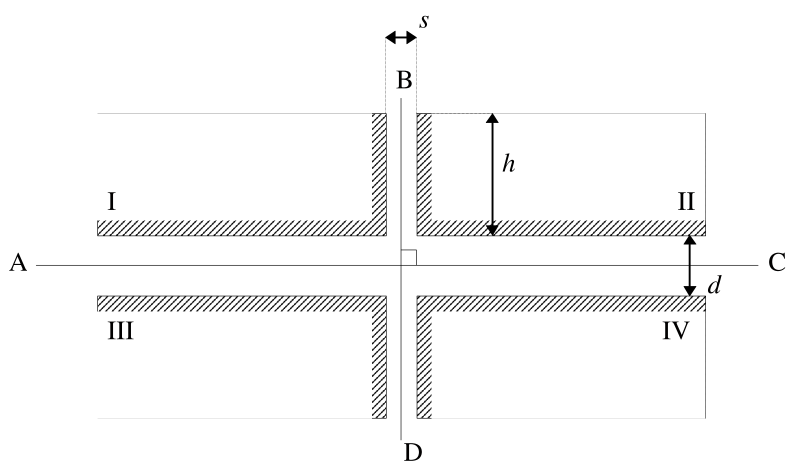

Fig. 5-16 Cross-section of a cross-capacitor with infinite deep gaps

In Fig. 5-16 a cross-section of four electrodes (I to IV) with infinite length is shown. Between electrode I and II (and similarly between III and IV) are infinite deep gaps ($h \to \infty$).

It can be seen that the cross-capacitance (between electrodes I and IV) has a line of symmetry AC and that the line of intersection BD can lie anywhere in the gap (see also Fig. 5-5). This means that Thompson and Lampard's general theorem for cross-capacitances holds and the capacitance is given by Eq. (5-14).
It can also be shown (using the equation for guard widths or with numerical methods) that the charge on the electrodes in the gaps decreases exponentially with the distance from the beginning of the gap. So with finite gap depths, the error caused by the ignored charge at the bottom of the gap will also decrease exponentially with the gap depth. This explains Eq. (5-32).

In the case of thin electrodes ($h << $ s), the relative effect is

$$\delta_{gap} < e^{-\frac{\pi s}{d}} \tag{5-33}$$

with d the electrode distance.
These effects can be understood using a similar method as with deep gaps.

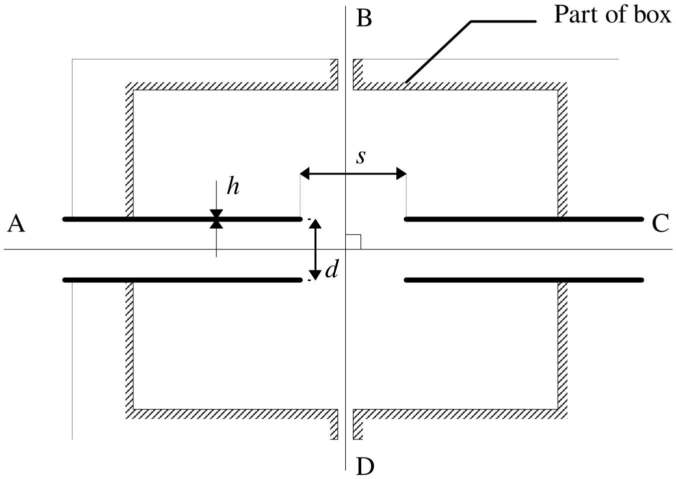

Fig. 5-17 Cross-section of a cross-capacitor with infinitely thin electrodes

For this purpose we imagine a conducting box around the electrodes that is also divided into four parts (Fig. 5-17). The four parts are connected to the respective electrodes, so there is again a line of symmetry AC and an intersecting line BD. When the size of the box is infinite Thompson and Lampard's theorem again holds, resulting to a cross-capacitance given by Eq. (5-14), independent of the width of the gap.
However, when the size of the box is not infinite, the charge on the part of the box will decrease exponentially with the distance from the gap. Heerens assumed the distance from the gap to the box to be equal to the distance d between the electrode, which resulted to Eq. (5-33).

For low-cost sensing elements the electrodes are usually mounted on a substrate (for instance printed circuit board) which has a significantly different permittivity from air. In combination with thin electrodes this can lead to considerable errors, as can be seen from Fig. 5-18.

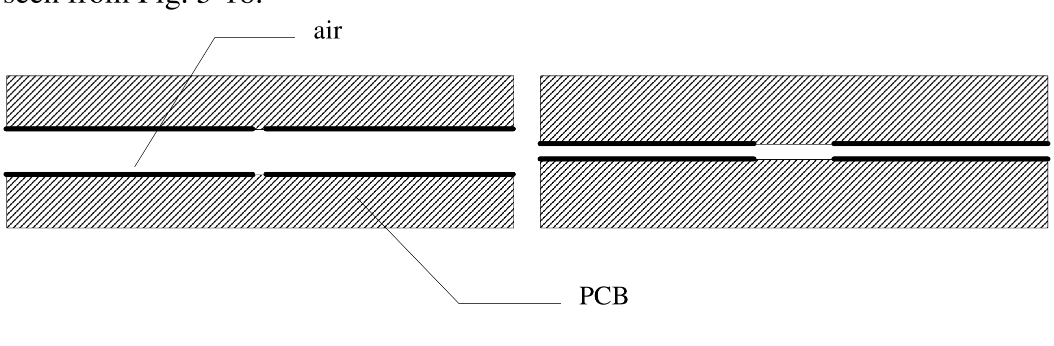

Fig. 5-18 Cross-capacitors with thin electrodes on printed circuit board, (a) with thin gaps and (b) with wide gaps

The cross-capacitor in Fig. 5-18a has a very small gap compared to the electrode distance, so the cross-capacitance will be approximately equal to the value calculated by Eq. (5-14), with ε_r equal to 1.

However, in Fig. 5-18b the gap width is large compared to the electrode distance, so the cross-capacitance (in this case the external cross-capacitance) will be determined by the permittivity of the substrate, so the value of the cross-capacitance will be approximately equal to the value calculated by Eq. (5-14), with ε_r equal to the permittivity of epoxy (≈ 4).

This effect will also be noticeable at smaller gap widths, as has been measured by Heerens *et. al*. [60]. As a result, for accurate reference capacitors cross-capacitors with thick electrodes are the best solution.

5.3.3 Finite gap width in biplanar strip-block capacitors

Another important case to calculate the influence of finite gaps is the guarded parallel plate capacitor and similar types like the biplanar strip-block and biplanar guarded strip capacitor (Fig. 5-19). Corrections for the finite gap have even been given in international standards, by the IEC [62] and the ASTM [63].

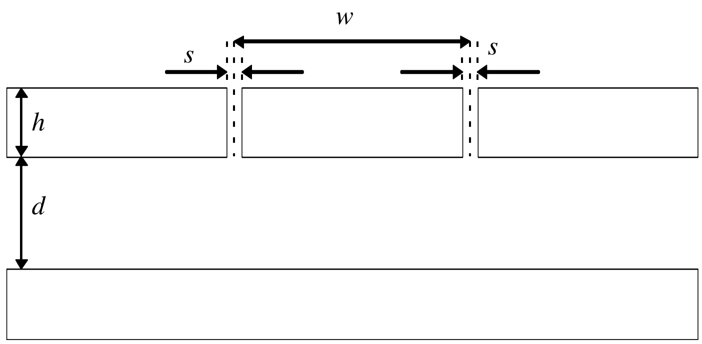

Fig. 5-19 Cross-section of a parallel plate capacitor with guard electrodes and finite gap widths

According to the IEC, the effective width of the electrodes extend to halfway the gap. In other words, although the actual width of the electrode is w - s, the effective width of the electrode is w, so the capacitance can be calculated from

$$C_{IEC} = \varepsilon_0 \varepsilon_r l \frac{w}{d} \tag{5-34}$$

The ASTM uses the actual width of the electrode, but calculates the extra capacitance due to the gap C_g using a first order approximation

$$C_g / l = \left(\varepsilon_0 B\, s/2d\right) \varepsilon_r \tag{5-35}$$

with

$$B = 1 - 2\,\varphi / s \tag{5-36}$$

where φ is called the fringing coefficient.
Since it seems natural to assume that the effective width of the electrodes extend halfway the gap (following the IEC and other publications) we rewrite Eq. (5-35) to

$$C_{ASTM} = \varepsilon_0 \varepsilon_r l \frac{w-s}{d} + \varepsilon_0 \varepsilon_r l \frac{s-2\varphi}{d} = \varepsilon_0 \varepsilon_r l \frac{w-2\varphi}{d} \tag{5-37}$$

Now we can calculate the relative deviation from Eq. (5-34) δ_{gap} caused by the gap

$$\delta_{gap} = \frac{-2\varphi}{w} \tag{5-38}$$

The problem is now to find the value of φ. Apparently it is not a constant, but depends on the gap width, the electrode distance, the permittivity of the electrode substrate etc. Goad and Wintle [64] present equations for $2\,\varphi\,/\,s$ for the electrode structure of Fig. 5-19 in case of thick and thin electrodes with equal permittivity inside and outside of the capacitor. They also present an equation in the case the permittivity inside the capacitor is much larger then the permittivity outside, which can be relevant when using this electrode structure to measure the permittivity of a sample between the electrodes.

- Thick electrodes

In the case of thick electrodes when we assume that $h/s \to \infty, \varepsilon_1 = \varepsilon_2 = 1$, according to Goad and Wintle

$$\frac{2\varphi}{s} = \frac{2}{\pi}\arctan\left(\frac{s}{2d}\right) - \frac{2d}{\pi s}\ln\left[1+\left(\frac{s}{2d}\right)^2\right] \tag{5-39}$$

The formula is exact and has been derived previously by Thomson [65], Endicott [66] and is quoted by the ASTM [63]. Substituting (5-39) into (5-38) yields

$$\delta_{gap} = -\frac{s}{w}\left(\frac{2}{\pi}\arctan\left(\frac{s}{2d}\right) - \frac{2d}{\pi s}\ln\left[1+\left(\frac{s}{2d}\right)^2\right]\right) \tag{5-40}$$

which is again exact. For small gap widths $|s/2d| \ll 1$, we can approximate this by

$$\delta_{gap} = -\frac{s}{\pi w}\left(\frac{s}{2d} - \frac{1}{6}\left(\frac{s}{2d}\right)^3 + \ldots\right) \tag{5-41}$$

Previously [51], [52], we have applied Heerens rule of thumb for cross-capacitors with deep gaps Eq. (5-32) for biplanar strip-block capacitors as well. This apparently has been incorrect.

In Fig. 5-20 we show the gap error according Eq. (5-40) together with Heerens rule of thumb and numerical results according to a simulation using Ansoft's Finite Element simulator (FEM) Maxwell. The values we used for this simulation are shown in Table 5-3. The modern version of Maxwell automatically refines the mesh until a preset accuracy has been reached. This calculated accuracy (the relative total energy error) has been set to 0.001% and resulted to about 6000 triangle meshes.

According to the simulations, equation (5-40) is indeed exact.

Table 5-3 Values for numerical verification of the gap influence

Variable	Value
d	1 mm
h	10 mm
w	5 mm
s	0, 0.2, 0.4, 0.6, 0.8, 1 mm

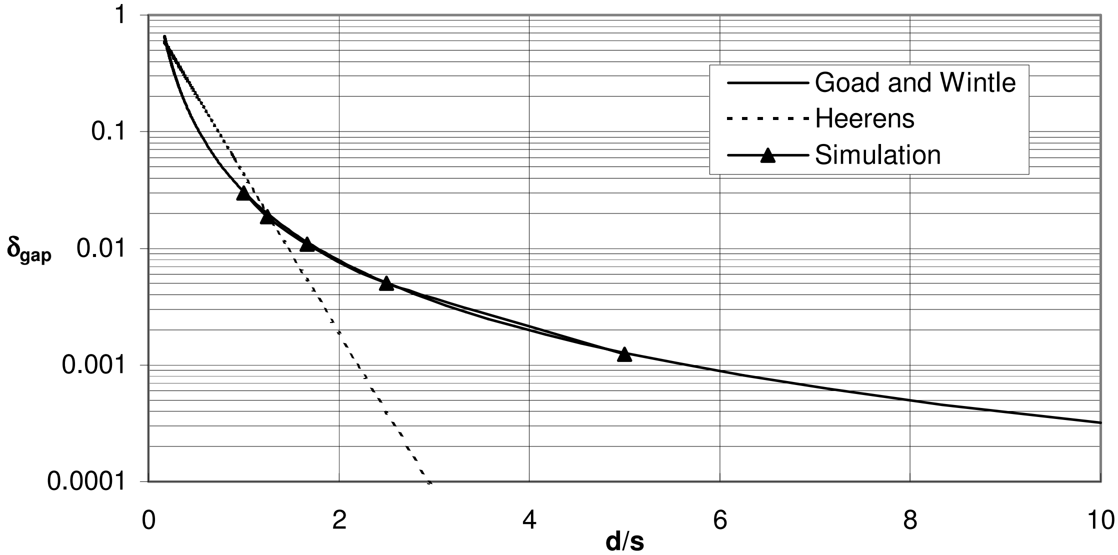

Fig. 5-20 Gap error according to Heerens, Goad and Wintle and simulations

Note that in Fig. 5-20 the error due to the gap has been plotted against *d*/*s*, so higher values of *d*/*s* indicate a smaller gap width.

- Thin electrodes

In the case of thin electrodes, when we assume that $h/s \to 0, \varepsilon_1 = \varepsilon_2 = 1$, again according to Goad and Wintle

$$\frac{2\varphi}{s} = \frac{2d}{\pi s}\frac{\left(\sqrt{p}-1\right)^2}{2\sqrt{p}}$$
$$\frac{\pi s}{2d} = \frac{1}{2}\ln p + \frac{p-1}{2\sqrt{p}} \tag{5-42}$$

This pair of parametric equations is again exact and presented before by Lauritzen [67], Endicott [66] and quoted by the ASTM [63]. When the gap is small, $\left|s/2d\right| \ll 1$, Eq. (5-42) can be replaced by the expansion

$$\frac{2\varphi}{s} = \frac{1}{8}\left(\frac{\pi s}{2d}\right) + \frac{1}{32}\left(\frac{\pi s}{2d}\right)^2 + \frac{1}{768}\left(\frac{\pi s}{2d}\right)^2 + \ldots \tag{5-43}$$

Substituting this into (5-38) we arrive at

$$\delta_{gap} = -\frac{s}{w}\left(\frac{1}{8}\left(\frac{\pi s}{2d}\right) + \frac{1}{32}\left(\frac{\pi s}{2d}\right)^2 + \frac{1}{768}\left(\frac{\pi s}{2d}\right)^2 + \ldots\right). \tag{5-44}$$

Comparing Eq. (5-44) with Eq. (5-41), the relative error in the case of thin electrodes appears to be similar to that in the case of thick electrodes (when the gap width is small), except for a factor $\pi^2/8$ (~ 1.23).

Apparently Heerens gap rules are only valid for cross-capacitors. In the case of biplanar strip-block capacitors Eq. (5-41) and Eq. (5-44) have to be used.

5.4 Parasitic capacitances

According to Fig. 5-14 the mere presence of one extra (guard) electrode results to two extra capacitances, called parasitic capacitances. These capacitances are modeled in Fig. 5-2 as C_{p1} and C_{p2}. As has been discussed in Section 5.1, the effect of these parasitic capacitances can be eliminated by applying a voltage change on terminal T_1 with respect to terminal T_0 and measuring the charge flowing out of T_2.

There are two other parasitic capacitances. One is the external capacitance, the other the capacitance between the connecting wires. Both are in parallel to the internal capacitance. In Fig. 5-2 they have been included in C_x, which means that the parallel capacitance can not be electronically distinguished from the internal capacitance. Although in many cases the parallel capacitances are only required to be constant, their value depends on factors external to the sensing elements. Therefore, it is generally necessary to reduce their values to an insignificant level compared to C_x.
As has been explained before, this can be achieved by using guard electrodes and by shielding the outside of the electrode structure. When we apply guards rings according to section 5.3.1 the influence of the external capacitance can be reduced to less than 1 ppm. of C_x. Toth and Meijer [52] have shown that by using shielded coaxial cables to connect the electrodes, the capacitance between the connecting wires can easily be reduced below a value of 20 aF (the resolution of their measurement setup).
As a result of this, C_{p1} and C_{p2} will increase dramatically (up to 1000 times the size of C_x), but the model of Fig. 5-2 is still valid, while C_x now includes only the desired capacitance. As has been explained in section 5.1.5, even large values of C_{p1} and C_{p2} do not necessarily influence the measurement of C_x.

5.5 Contamination of the electrodes

Contamination of the electrodes occurs when material is deposited on the electrodes, thereby influencing the capacitance. Typically, the deposited material will be dust, scale, sludge, dirt, moisture and so on. To prevent the contamination of the electrodes a thin sleeve of PTFE, FEP or other dirt and moisture repellents can be applied, as suggested in Section 5.2.3, Fig. 5-12. In some cases it is possible to add extra capacitors so the presence of contamination can be detected and the user of the sensor can be warned that the sensor needs to be cleaned.
Still the chances of contamination might be unacceptable in certain applications, although it must be noted that all sensors and even electronic circuits suffer from some kind of contamination.

In most cases however humidity proves to be the dominant source of contamination, sometimes in combination with other deposits. For instance, although PTFE is thought to repel water drops from its surface, a calcareous deposit (scale) might counteract this property.

Much work has been done in the past by Zahn [68], Stranathan [69], Ford [70] and Bertone *et. al.* [71] to understand the effect of humidity on capacitors, called the anomalous humidity effect. This work shows that at higher humidities, layers of water molecules can be expected to appear on the electrodes or to be absorbed by the insulators. It should be clear from the previous sections that neither of these should have a great impact on the capacitance, as these layers are rather thin and the effect of (parasitic) capacitance of the insulators is practically eliminated.

Conductive layers of water, on the other hand, will short-circuit the electrodes with the guards (when there is no PTFE sleeve) and make measurement impossible, or dramatically increase the measured capacitance (with PTFE sleeve). Although undesirable, this should be easy to detect in most cases.

The effect of humidity has been studied on a circular cross-capacitor by Toth *et. al.* [51]. The capacitor's electrodes were constructed of 1.5 mm thick printed circuit board (PCB) that were glued to a ceramic spacer of 1 mm (Fig. 5-21). To measure the cross-capacitance the electrodes are connected as shown in Fig. 5-22.
The sensing element was cycled over a large temperature range from -25°C to +75°C. During the heating phase from -25°C to +20°C a very rapid change in capacitance was observed. This can be attributed to the rapid change in the temperature of the air compared to that of the electrodes. As a result, water droplets are formed on the electrodes. These eventually short-circuit the inputs of the measurement system. The applied capacitance measuring system (a relaxation oscillator) measures a rapidly decreasing capacitance until finally the oscillator stops.

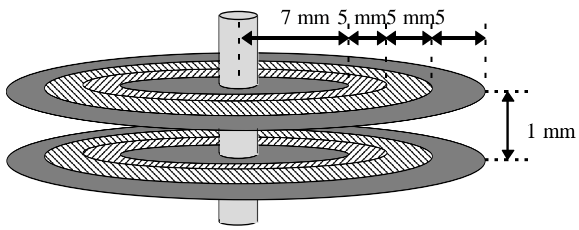

Fig. 5-21 Experimental circular cross-capacitor

To study the effect further, the cross-capacitance and trans-capacitance were measured using a capacitance controlled oscillator. In Fig. 5-22 the right-half cross-section of the circular cross-capacitor of Fig. 5-21 is shown. By connecting the respective electrodes to either the voltage source, the oscillator input or to ground the cross-capacitance (Fig. 5-22a) or the trans-capacitance (Fig. 5-22b) is measured.

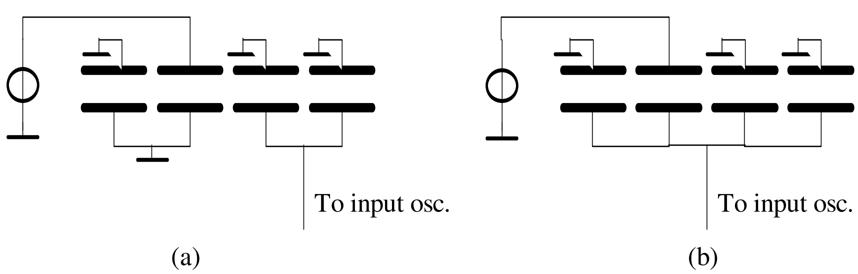

Fig. 5-22 Right-half cross-section of the electrode structure for measuring (a) cross-capacitance and (b) trans-capacitance

The experimental capacitor was placed in a climate chamber at a constant temperature of 80°C, while the humidity was slowly cycled (0.2 % RH/min.). In Fig. 5-23 the relative deviation of the capacitance is shown at 80°C and increasing humidity.

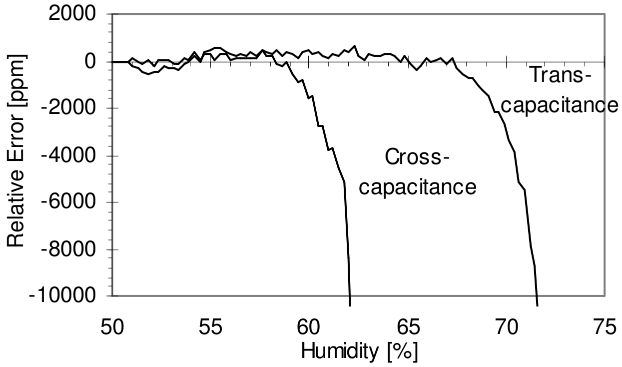

Fig. 5-23 Increasing humidity with 0.2%/min. at 80°C

At 80°C and 60% humidity the cross-capacitance suddenly drops due to short-circuiting between the electrodes at the oscillator input and the (grounded) guards. Shortly after the conductive layer is formed, the oscillator in the measuring circuit stops.
The trans-capacitance remains constant up 65% humidity. This is due to the large area (including the spacer) that must be covered to short circuit the electrodes at the input of the oscillator.
The same measurements where performed at 20°C. A similar capacitance break-down was then observed at 90% humidity.

Apparently the influence of non-condensing humidity is less then 1000 ppm, which is accordance to the calculations presented by Lea [41] as explained in Section 5.1.8. Condensing humidity can cause large errors, especially when using relaxation oscillators at low frequencies (10 kHz). The sensitivity of these oscillators to small conductances at the input does allow for the easy detection of condensing humidity.

5.6 Object model of a capacitive sensing element

From the previous sections it is clear that the physical relations that determine the capacitance of a capacitive sensing element are properties of the class Capacitors, since a capacitor has capacitance and capacitance is determined by physical relations. In the case of general capacitors these physical relations are Maxwell's equations for the electromagnetic field. Under certain conditions as explained in Section 5.1, Gauss law for the electric field can be used. However, in the case of certain descendants of the class capacitors, like uniplanar, biplanar and cross-capacitors, simplified solutions for Gauss law can be used.
In Fig. 5-24 is shown that the class Capacitors uses one or more objects of the classes Electrodes and Dielectrics. In other words Electrodes and Dielectrics are also properties of Capacitors.

Other properties of the class of Capacitive sensing elements are inherited from the more generic class Sensing elements. The attributes of this class have been derived in the previous chapter. The actual type of (non-electric) input signal is limited to attributes that a capacitor has, such as the dielectric or the electrode structure (i.e. electrode area and distance).
In some cases other properties of the electrode structure can be used, for instance elasticity, to create a pressure sensor. In other cases, a non-electrical sensing element will be used to form a cascade with the capacitive sensing element. An example of

the latter could be a capacitive force sensor, where the capacitive force sensing element consists of a spring (non-electrical sensing element) and a capacitive displacement sensor.

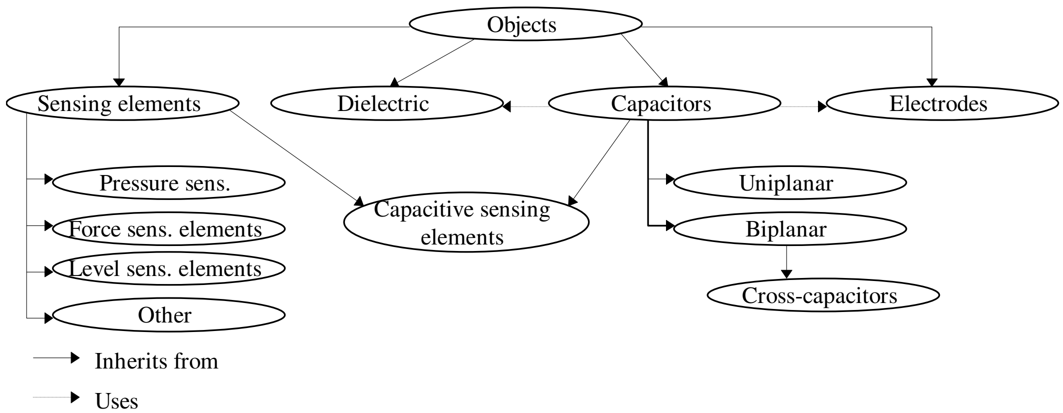

Fig. 5-24 Class diagram for capacitive sensing elements

Being a modulating sensing element, an electrical quantity must be supplied. From the theory derived in Sections 5.1 and 5.4, it follows that this quantity must be a voltage, in order to measure the desired capacitance instead of the parasitic capacitances. The information on the physical quantity that has been measured, is then stored in the charge. The capacitive sensing element therefore offers a charge as the output signal.

5.7 Conclusion

In this chapter we have derived an object model for the class of capacitive sensing elements, which is a fusion of the class of capacitors and the class of modulating sensing elements.

The behavior of the class of capacitors is completely determined by Maxwell's laws for the electromagnetic field and so is the behavior of the class of capacitive sensing elements. However, under the conditions that

1. the quasi-static approximation can be applied, meaning that the wavelength of the signals is not too high compared to the dimensions of the electrode structure,
1. the conductivity of the dielectric is infinite,

Maxwell's laws simplify to Gauss's law for the electric field.

The capacitance can be measured by applying a voltage change to the capacitor of interest, while keeping the voltage over all other capacitors constant and measuring the charge.

From the class of capacitors the class of uniplanar, biplanar and cross-capacitors have been inherited for which the solution to Gauss's law is known. These classes of capacitors are especially useful when used to create new classes of capacitive sensing elements since the influence of finite guard and gap widths can be easily predicted, when a suitable dielectric material has been chosen.

The class of cross-capacitors seems to be best suited as a standard or reference capacitor, since the capacitance depends only on the length. However for low-cost precision liquid level (ε-type) measurements multi-electrode uniplanar electrode structures are best suited, since the number of electrodes can easily be extended and the precision depends mainly on the precision of the manufacturing process (usually photolithography).

For position or displacement measurements multi-electrode biplanar electrode structures are more suitable (A-type), since here a moving electrode (or moving shield) is required. The dependence of the capacitance on the electrode distance can be eliminated by using unshielded electrodes as a reference. The resulting precision will then again depend on the manufacturing process of the electrodes.
A special case arises with the simple biplanar electrode structure. When used as a D-type sensor, it appears to be very suitable for low-cost measurements of small displacements (compared to the initial electrode distance). In this case, changes in angular position have only a small influence while changes in electrode area are in general very small.

---

39 Heerens, W. Chr., *"Basic principles in designing highly reliable multi-terminal capacitor sensors and performance of some laboratory test models"*, Sensors and Actuators A, 3 (1982/83) 137-148

40 Kandala, C.V.K., K.C. Lawrence and S.O. Nelson, *"Non-destructive electrical measurement of moisture content in single kernels of corn"*, J. Agric. Eng. Res., Vol. 44, pp. 125 - 132, 1989

41 Lea, N., *"Notes on the stability of LC oscillators"*, J. Inst. Elec. Eng., Vol. 92, Pt. II, pp. 261-267, 1945

42 Bonse, M.H.W., *"Capacitive position transducers - Theoretical aspects and practical applications"*, Ph.D. Thesis, Delft University of Technology, December 1995

43 Bell, D.A. and A.M. Bell, *"Temperature coefficient of capacitance and of inductance"*, Electronic Technology, Vol. 37, pp. 342 - 345, 1960

44 Froome, K.D. and L. Essen, *"The velocity of light and radio waves"*, Academic Press, London, 1969

45 Bean, B.R. and E.F. Dutton, *"Radio meteorology"*, Monograph 92, National Bureau of Standards, March 1966

46 Heerens, W. Chr., *"The solution of* Laplace's *equation in cylindrical and toroidal configurations with rectangular sectional shapes and rotation-symmetrical boundary conditions"*, J. of Appl. Phys., Vol. 47, No. 8, August 1976

47 Heerens, W. Chr., *"Application of capacitance techniques in sensor design"*, J. Phys. E: Sci. Instrum., 19 (1986), pp. 897-906

48 Thompson, A.M. and D.G. Lampard, *"A new theorem in electrostatics and its application to calculable standards of capacitance"*, Nature, Vol. 177, pp. 888, May 1956

49 Lampard, D.G., *"A new theorem in electrostatics with application to calculable standards of capacitance"*, Proc. IEE, Vol. 104, Ot. C, pp. 271-280, September 1957

50 McGregor, M.C., R.D. Cutkowsky, F.K. Harris, J.F. Hersch and F.R. Kotter, *"New apparatus at the national bureau of standards for absolute capacitance measurement"*, IRE transactions on instrumentation, Vol. I-7, pp. 253-261, 1958

51 Toth, F.N., A.J.M. Bertels and G.C.M. Meijer, *"A low-cost, stable reference capacitor for capacitive sensor systems"*, IEEE Trans. Instrum. Meas., Vol. 45, No. 2, pp. 526 - 530, April 1996

52 Toth, F.N. and G.C.M. Meijer, *"A low-cost, smart capacitive position sensor"*, IEEE Trans. Instrum. Meas., Vol. 41, No. 6, pp. 1041-1044, December 1992

53 Jong, G.W. de, *"Smart capacitive sensors"*, Ph.D. Thesis, Delft University Press, Delft, April 1994

54 Zhu, F., *"Development of capacitive position transducers through a mechatronic approach"*, Ph.D. Thesis, Delft University of Technology, April 1992

55 Li, X.J., G.W. de Jong, G.C.M. Meijer and J.W. Spronck, *"An accurate low-cost capacitive absolute angular-position sensor with a full circle range"*, IEEE Trans. Instrum. Meas., Vol. 45, No. 2, pp. 516 - 520, April 1996

56 Heerens, W. Chr., G. Keizer and F.W. Wedman, *"Theory and practice of multi-terminal bar and tube sensors for use in the chemical process industry and related branches"*, Sensor'83, Conf. Proc. Vol. 5, pp. 27 - 40, Basel, 17 - 19 May 1983

57 Brabetz, L., G. Schmitz and M. Siebert, *"The* Siemens *alcohol fuel sensor"*, IX Int. Symposium on alcohol fuels, ISAF - Firenze '91

58 Schmitz, G., R. Bartz, U. Hilger and M. Siedentop, *"Intelligent alcohol fuel sensor"*, SAE, 900231

59 Takeuchi, K. and T. Kita, *"Dielectric properties of methanol-blended gasoline as the bases of an alcohol sensor"*, Technical digest of the 9th sensor symposium, pp. 205 - 208, 1990
60 Heerens, W. Chr., E.M. Boogh and G. Keizer, *"Gap influences in guarded capacitors"*, Delft Prog. Rep., Vol. 8, pp. 149-160,1983
61 Heerens, W. Chr., B. Cuperus and R. Hommes, *"Analytical formulas for toroidal cross capacitances with rectangular sectional shapes, including gap correction formulas"*, Delft Prog. Rep., Vol. 4, pp. 67 - 87, 1979
62 IEC, Publication No 250, IEC Genova, 1969
63 ASTM, Publication D150, ASTM Philadelphia, 1986
64 Goad, D.G.W. and H.J. Wintle, *"Capacitance corrections for guard gaps"*, Meas. Sci. Technol., Vol. 1, No. 9, pp. 965 - 969, Sep. 1990
65 Thomson, J.J., *"Notes on recent researches in electricity and electromagnetism"*, pp. 227 - 235 (Oxford: Clarendon), 1893
66 Endicott, H.S., J. Test. Eval. 4, pp. 188 - 195, 1976
67 Lauritzen, J.I., 1963 Ann. Report, Conf. Electrical Insulation, Washington, NAS-NRC, pp. 67 - 70, 1964
68 Zahn, C.T., *"Association, adsorption and dielectric constant"*, Phys. Rev., Vol. 27, pp. 329-340, March 1926
69 Stranathan, J.D., *"Dielectric constant of vapor"*, Phys. Rev., Vol. 48, pp. 538-544, September 1935
70 Ford, L.H., *"The effect of humidity on the calibration of precision air capacitors"*, J. Inst. Elec. Eng., Vol. 95, Pt. II, pp. 709-712, 1948
71 Bertone, G.A., N.L. Carroll and Z.H. Meiksin, *"Elimination of the anomalous humidity effect in precision capacitance based transducers"*, IEEE Trans. Instrum. Meas., Vol. 40, No. 6, pp. 897-901, December 1991

6 CAPACITANCE MEASUREMENT

As has been discussed in Chapter 4, a capacitive sensor consists of a capacitive sensing element and a modifier. The prime task of the modifier is to accurately measure the capacitance that is output by the sensing element, without adding systematic errors like offset and gain errors or non-linearity, or random errors like noise. At the same time the effect of other parameters of the sensing element like parasitic capacitances and electromagnetic interference need to be eliminated.
It was also found that an intelligent sensor provides a more general design that might be reused in several applications. The most flexible way to make the sensor intelligent is to incorporate a programmable device like a microcontroller into the sensor and to make sure the signal that is output by the modifier is compatible with this device. A microcontroller does seem to be the most effective and low-cost programmable device, since generally additional interfacing circuitry is incorporated into the device, like timers, counters, digital output ports (that can control switches etc.), display drivers and digital communication facilities like UART's (asynchrone serial transmitter and receiver). When such a device is incorporated into the sensor, costs can be even further reduced by moving part of the modifier functionality into it, in other words to incorporate part of the microcontroller into the modifier.

In this chapter we will be examine available capacitance measurement methods, like capacitive bridges, resonance and charge-discharge methods, and various capacitance dependent oscillators. Then a family of methods will be selected that can be incorporated into intelligent capacitive sensors in such a way that minimal costs arise, while sufficient degrees of freedom are maintained. By choosing the appropriate member of the family, the requirements for the sensor can be optimally satisfied.
But first some basic techniques for the reduction of the effects of parasitic capacitances, offset and scale errors will be presented, followed by a discussion of the influence of electromagnetic interference.

6.1 Reduction of the effect of parasitic capacitances

In Section 5.4 we have already discussed the necessity to reduce the influence of the parasitic capacitance between the electrode wires and the external capacitance, by using guard electrodes and by shielding the outside of the electrode structure. Then

the electrical model of the sensing element is given by Fig. 5-2. This is considered to be an essential property of any good sensing electrode design and application.
It is then the task of the capacitance measurement system to reduce the influence of the remaining parasitic capacitances to an insignificant level.
We can achieve this by applying a 2-port measurement or by applying a 1-port measurement with active guards.

6.1.1 2-Port measurement

C_{p1} and C_{p2} represent the capacitances from the two electrodes to the guard electrode in parallel to the capacitance of the connecting wires to their shields. It should be noted that the capacitance of shielded cables is in the order of 50 to 100 pF/m. When shielded cable is applied, the capacitances C_{p1} and C_{p2} may be increased to several 100 pF.

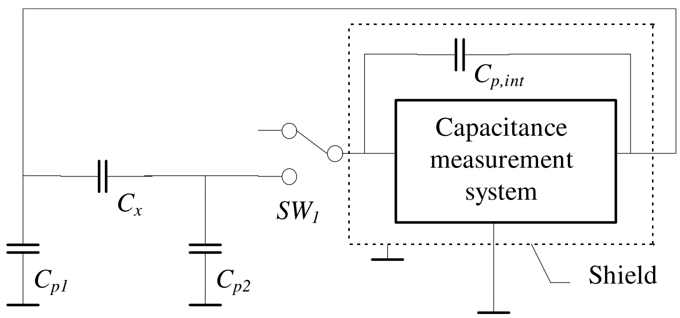

Fig. 6-1 Identification of parasitic capacitances

Fortunately the influence of C_{p1} and C_{p2} can be reduced by short-circuiting them. As has already been suggested in Section 5.1.5, this can be done by driving C_{p1} by a low-impedant voltage source V_{src} and by connecting C_{p2} to a current or charge amplifier (OA_1, C_f) with a low input impedance (Fig. 6-2). If we assume that the voltage V_{src} makes a step from 0 V to v V, the voltage on C_{p1} will after a certain time also reach v V, regardless of the value of C_{p1}. Similarly, when the DC gain of the op amp is large enough, after a certain time, the voltage on C_{p2} will return to 0 V, which means that the total charge that was transferred from C_x is stored on C_f. As a result the voltage at the output of the op amp V_{out} will be (assuming the initial charge on C_f zero)

$$V_{out} = -\frac{v\,C_x}{C_f}\,. \tag{6-1}$$

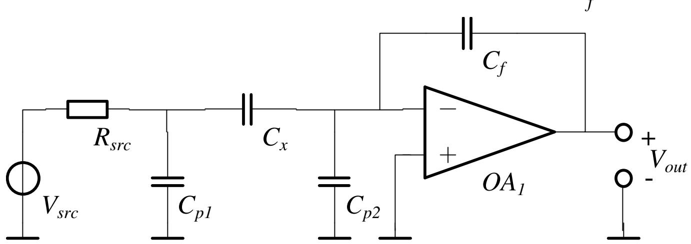

Fig. 6-2 Circuit to reduce the influence of C_{p2} and C_{p3}

Since we assumed the parallel resistances of the parasitic capacitances and the input resistance and gain of the opamp infinite, V_{out} depends only on the input voltage and the ratio between C_x and C_f.
In any practical circuit we have to consider the time constants that determine when all the charge has been transferred, as well as factors causing offset and scale errors

and non-linearity. However, as we will show later, offset and scale errors can be eliminated by performing additional measurements and will therefore not be considered here.
The first time constant we need to consider, involves charging C_{p1} to V_{src}. Assuming C_x much smaller then C_{p1} this time constant equals

$$\tau = R_{src}\, C_{p1} . \tag{6-2}$$

After a certain time T, the relative error of the voltage on C_{p1} decreases to

$$\delta = e^{-T/\tau} , \tag{6-3}$$

so with T = 10 τ, δ = 45 ppm.
The second time constant results from the limited bandwidth of the opamp. Assuming C_{p2} much larger then C_x and C_f this results to a time constant

$$\tau = \frac{C_f}{C_{p2}} \frac{1}{2\pi f_T} , \tag{6-4}$$

which also causes a relative error equal to Eq. (6-3).
In some cases the input resistance of the opamp R_{in} cannot be assumed infinite or an external input resistance is connected to ground. This causes a low frequency time constant. The effect is that the output voltage of the opamp will not remain constant over time (droop). The time constant is given by

$$\tau = C_f\, R_{in}\, A , \tag{6-5}$$

with A the open-loop gain of the opamp. The error will depend on the time the output voltage is sampled, for instance when this time is a constant the droop with cause a scale error. However, when the circuit is part of a capacitance controlled oscillator, the sample time will depend on C_x. The worst case non-linearity can then be calculated to be

$$NL = 4 \frac{C_{FS}}{C_f\, A} , \tag{6-6}$$

with C_{FS} the full scale value of the capacitance C_x (measurement range).

The above calculations assume that C_x is charged and discharged. As we will see later, other measuring principles apply a sine voltage to C_x and determine the amplitude of V_{out}. Then the influence of the above time constants on the gain in the frequency domain will need to be investigated. For now we will state that the influence of C_{p2} and C_{p3} can be easily reduced to insignificant levels when they are smaller then about 500 pF.

In Fig. 6-1 another parasitic capacitance $C_{p,int}$ is shown. This parasitic is the offset capacitor in the capacitance measuring system and might be caused by imperfect shielding between the output of the capacitance measuring system and its input. In other cases this capacitance might be deliberately added, for instance when the measurement system is a capacitance controlled oscillator. Then, when C_x is zero, the frequency of the oscillator would be infinite, which is clearly impossible. By adding an offset capacitance, the frequency of the oscillator can be limited to a range where the bandwidth limitation of the op amps etc. has a negligible influence.
By adding a switch SW_1 the system can choose to measure C_x + $C_{p,int}$ or $C_{p,int}$ alone, enabling auto-zero techniques, as will be explained in Section 6.2.

At this point we can conclude that the 2-port measurement method satisfies our requirements for the elimination of the parasitic capacitances of the sensing element. It does however allow for offset and scale errors of the modifier itself, so these errors need to be taken care of separately.

6.1.2 1-Port measurement with active guards

A 1-port measurement is often applied when one of the sensor electrodes is earthed and the other is floating (the active electrode). An attempt is made to reduce the influence of the parasitic capacitances by applying active guarding, i.e. by driving the guard electrodes at the same voltage as the active electrode. Then either a voltage is applied to the active electrode and the current measured (Fig. 6-3) or a current is applied and a voltage measured. Huang *et. al.* [72] notes that the major drawbacks of this method are that it does not eliminate the effect of the parasitic capacitance C_m of the measurement circuit itself and that it is difficult to obtain a voltage follower with suitable precision, especially at higher frequencies (1 MHz). Marioli *et. al.* [73] presents a method to compensate the residual capacitance with a negative capacitance, but being a parasitic capacitance, its value might not be stable and hence difficult to compensate over a large temperature range.

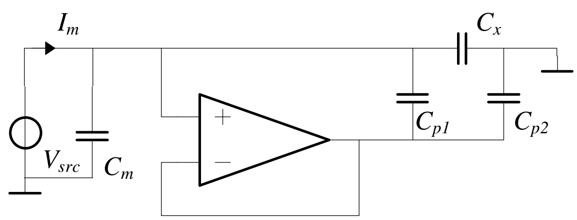

Fig. 6-3 1-port measurement with active guard

As a result of this, the 1-port measurement is not generally applicable and should be avoided when a 2-port measurement is possible.

6.2 Reduction of offset and scale errors: the 3-signal approach

In any measuring system the offset and scale error needs to be calibrated or reduced to an insignificant level. The offset might be caused by $C_{p,int}$ in Fig. 6-1. Because $C_{p,int}$ is internal in the measurement system it might be difficult to reduce it by applying shielding. Many capacitance measuring systems therefore offer a way to calibrate for this value.

The scale error might be caused by the transfer from one physical quantity (in our case capacitance) to another (voltage in Fig. 6-2). In our case

$$V_{out} = k\,C_x \tag{6-7}$$

with k equal to $v\,/\,C_f$. The value of k might not be exactly known, causing the scale error. A rather expensive solution would be to acquire a standard, or at least a stable and calibrated, voltage and capacitor. However, then we would not be taking advantage of the fact that there is only one scale factor, instead we would need two (or more) references.

This scale error does not necessarily appear when a relative measurement (with respect to one reference value) is performed. This is sometimes also called a two-signal approach. When the reference value is traceable to a standard, the system can still be used for absolute measurements. However, in many cases the capacitive sensor system will be used to measure another physical quantity, so only an overall system calibration is required.

A very simple and low-cost procedure to eliminate offset and scale errors at the same time is called the 3-signal approach, presented by van Drecht *et. al*. [74] and Meijer *et. al*. [75] and applied in a capacitive sensor system by Toth and Meijer [76]. It is basically an auto-calibration scheme that combines offset and scale calibration by measuring the offset, the capacitor C_x and a reference capacitor C_{ref} in *the same way*. This means that the same offset value is present during the measurement of C_x and C_{ref} and that the gain of the measuring system does not change between measurements. Assuming

$$\begin{aligned} M_{off} &= k_1 C_{off} \\ M_{ref} &= k_2 C_{ref} + k_1 C_{off} \\ M_x &= k_2 C_x + k_1 C_{off} \end{aligned} , \tag{6-8}$$

with M_x, M_{ref} and M_{off} the measured values when selecting respectively C_x, C_{ref} and C_{off}, the relative capacitance can be calculated by:

$$\frac{C_x}{C_{ref}} = \frac{M_x - M_{off}}{M_{ref} - M_{off}} . \tag{6-9}$$

Naturally a linear transfer function is assumed. When the non-linearity also needs to be measured, we can choose C_x and C_{ref} to have approximately the same value and perform an additional measurement by selecting both capacitances simultaneously (in the same way). Assuming a second order polynomial for the transfer function, the non-linearity relative to the full scale output (FSO) is then

$$NL = \frac{M_{x+ref} - M_{ref} - M_x + M_{off}}{M_{x+ref} - M_{off}} \tag{6-10}$$

with the FSO equal to $C_x + C_{ref}$.

This auto-calibration scheme combines very well with the 2-port measurement method. However, care must be taken that the measurements are performed in exactly the same way.
In practice it appears to be more difficult to achieve a low input impedance for the charge amplifier in Fig. 6-2 then to obtain a low output impedance for V_{src}. Especially when C_{p2} is very large, it's influence might not be eliminated completely, causing an additional scale error. However, when both C_x and C_{ref} are measured is such a way that C_{p2} remains constant, this scale error will also be eliminated. As a result of the finite input impedance, the setup shown in Fig. 6-1 would measure $C_{p,int}$ with a different scale error then when measuring C_x since the switch SW_1 also switches C_{p2}, resulting to a possibly large change of the total input capacitance between measurements. It is therefore necessary in most cases to place the switch (or multiplexer) at the side of V_{src}, i.e. at the output side of the measurement system (Fig. 6-4). In this situation, the total capacitance at the input of the system is independent of the position of switch SW_1.

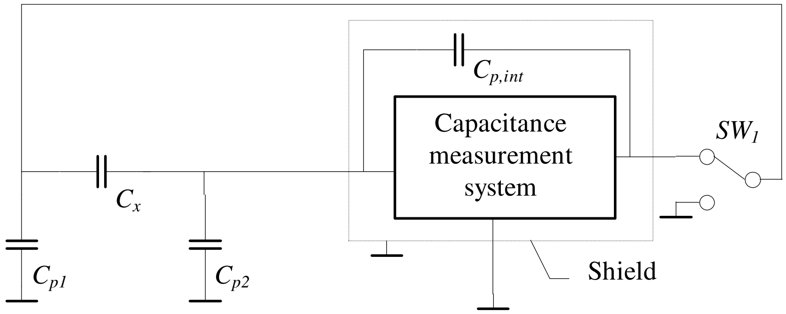

Fig. 6-4 Using an output multiplexer to keep in total input capacitance constant

This seems to limit the types of multi-terminal capacitors to the type with one common electrode. However, in some smart sensor systems multi-terminal capacitors are used without a common electrode. For instance when using a cross-capacitor it appears to be advantageous to add both (available) cross-capacitances to eliminate positioning errors in the construction. This requires multiplexing at both sides of the cross-capacitor.

Toth *et al*. [77] presented an autocalibration scheme that allows double-sided multiplexing for the sensing element, yet has an additional reference capacitor that is multiplexed at the output only. By selecting the desired sensing element capacitance using the input multiplexer and then performing the 3-signal auto-calibration all measurements are relative to the reference capacitor without changing the total input capacitance between the sub-measurements, required for the 3-signal auto-calibration. However, this auto-calibration scheme does increase the total measurement time even further.

At this point we can conclude that the 3-signal auto-calibration scheme satisfies our requirements for the elimination of the offset and scale errors of the modifier itself. The method does require several capacitances to be measured sequentially in the same way, but this does not necessarily reduce the general applicability of the method, since only the measurement time is increased.

6.3 Electromagnetic interference

Obviously the measurement of very small capacitances requires the use of very sensitive electronic circuits. Interfering electromagnetic signals can easily deteriorate the accuracy and the resolution of the measurement system or prevent the system from functioning at all, at higher levels of interference.

The prevention of electromagnetic interference (EMI) therefore plays an important role. All kinds of standard techniques can be applied such as the use of:

- shielded boxes around the measurement circuits
- shielded cables
- (shielded) twisted pair cables
- net filters

In some cases not all of these measures can be applied or are not effective enough. The remaining interference will have to be filtered out by the measurement system. The filtering is only possible when the frequency of the interference is substantially higher or lower than the frequency of operation of the measurement system. Since most low-cost capacitance measurement systems operate in the frequency range from 1 kHz to 1 MHz, we can divide the interference to low-frequency interference caused by the electric mains, with frequencies of 50 Hz (60 Hz in the US) and its harmonics, and high-frequency interference, with frequencies well above 1 MHz, caused by switching in digital circuits and by radio transmitters.

6.3.1 Low-frequency interference

In this region the most effective filtering occurs when some form of synchronous detection is applied. This means the measuring signal is mixed with its own frequency so a frequency of zero Hz results. Consequently, the interference is converted to higher frequencies and can be filtered out by applying a low-pass filter.
Without conversion, a high-pass filter can be applied, which is less effective, except when the operating frequency can be chosen much higher than the interference.
The remaining interference might by averaged, by increasing the measurement time or by choosing the measurement time a multiple of 20 ms in case of 50 Hz interference (16.66 ms in case of 60 Hz).

When high levels of interference are present, care must be taken that the input stage of the measurement system is not overloaded, since the resulting clipping of the signal plus interference will remove the signal completely or will cause distortion. A model for this situation is shown in Fig. 6-5. V_{net} is the sine shaped voltage of the electrical mains and generally has a voltage of 220 - 240 V and a frequency of 50 - 60 Hz (in airplanes 600 Hz is common). C_{net} can not easily be specified, since it depends solely on the position of the electrodes relative to the electrical mains cables. It does seem reasonable to assume that $C_{net} < C_x$, but this not always the case.

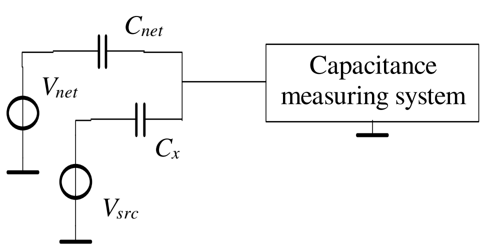

Fig. 6-5 Electrical model for LF interference

Since most capacitance measurement systems actually measure the charge changes using a charge amplifier it must be prevented that the slow but possibly large changes caused by the combination V_{net} and C_{net} cause the output of the charge amplifier to clip. One way of doing this, is to periodically reset the input of the measuring system, for instance by adding a switch at the input to ground. This way, only the charge changes during the relatively short integration time appear at the output.
Even more effective is to add a commutator at the input, so only the difference between two successive charge changes appears. This effectively results to synchronous detection directly at the input.

6.3.2 High-frequency interference

High-frequency interference can be folded back to the signal band by aliasing or can cause oscillators to lock. Generally, three techniques are applied to suppress the influence of high frequency interference: filtering, random sampling and balancing.

- Filtering

By choosing the bandwidth of all stages (but especially the input stage) not larger then necessary, the high frequency interference can be filtered out. Another form of filtering occurs when an inductance is inserted in series with the power supply.

- Random sampling

To prevent aliasing sometimes random sampling techniques can be applied. Similarly, to prevent lock in oscillators, dithering (pseudo-random noise) can be added (Mulder [78], van der Goes [79]).

- Balancing

Another method is to use balanced circuits. Using this method, the interference is converted to a common mode signal, which is effectively suppressed. A disadvantage is that the circuits generally double in size.

6.4 Basic capacitance measurement methods

Methods for accurately measuring capacitance exist for nearly a century. They can be divided into capacitive bridge methods, resonance methods and charge-discharge methods. In the following sections a review of these methods will be given in relation to their suitability for low-cost sensor applications.

6.4.1 Capacitive bridge method

The capacitive bridge is the oldest accurate measurement system for small capacitances. Bridge circuits rely heavily on the availability of an accurate divider in one of the two arms of the bridge. The ratio implemented by this divider is actually the reference of the measurement technique. Trowbridge [80] already reported the use of 3-winding transformers for capacitance and inductance comparisons in 1905. However the importance of these bridges for the precise measurement of small capacitors was not realized until Thompson [81] presented a bridge for the measurement of the complex permittivity of dielectrics and for the measurement of small capacitances [82]. The principle of a bridge with a 2-winding transformer is shown in Fig. 6-6.

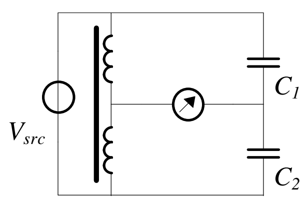

Fig. 6-6 Bridge circuit with 2-winding transformer

It appears that when the windings have the same resistance per turn and are wound symmetrical onto a high permeability core then the error on ratio can be smaller than 10 ppm. With close interleaving of the windings the error will even be less than 1 ppm.

When a 3-winding transformer is applied (Fig. 6-7), the resistances of the windings do not affect the open circuit ratios. When the primary winding is electromagnetically shielded from the secondary windings it is possible to obtain ratios with an error that is less than 0.1 ppm. This type of bridge was (and to the best of this authors knowledge still is) used at the National Bureau of Standards (McGregor *et. al.* [83]) and slightly modified, at the German PTB (Bachmair *et. al.* [84]).

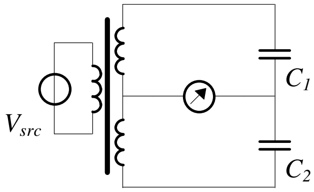

Fig. 6-7 Bridge circuit with 3-winding transformer

When the bridge is in balance, the ratio of the capacitors is equal to the ratio of the transformers. When the common arm of the transformer is connected to ground ,then the common node of the two capacitors is also at ground level. As a result, the influence of the parasitic capacitances will be negligible, provided all shields and guards are connected to ground.

The question is how to balance the bridge. Several basic methods are available:

- One of the capacitors can be made variable. This can be achieved by using a switched decade variable capacitor, which requires manual switching of the capacitance to obtain the required value.
- The ratio of the transformer can be made variable by tapping the windings of the transformer. Bertone *et. al.* [85] presents a capacitance-based displacement transducer using a tapped 3-winding transformer. In this article, the use of an opamp control system is mentioned to position the tap so, that the common electrode voltage is forced to zero. For use in studies of metal creep this solution appears to be acceptable.

Combinations of the both methods are used to save space and reduce costs. However, both methods do not seem appropriate for low-cost applications.

- The common node of the two capacitors can also be forced to ground by using a current meter (with low impedance) instead of a voltage meter.

Bonse et. al [86] presented such a system using a lock-in amplifier operating in current mode for application in two-dimensional capacitive position sensor. The measured current I_m will be

$$I_m = j\omega V_{src}\left(C_1 - C_2\right) \tag{6-11}$$

To determine the capacitance difference accurately, I_m, V_{src} and ω will need to be measured, which increases costs substantially. However, for the measurement of a very small capacitance difference compared to the absolute values of the capacitances, this method might prove to be the most appropriate.
In this mode, the bridge is not really used, which can easily be seen by making C_2 equal to zero. In this case Eq. (6-11) still holds. This method has been applied by Yang *et. al.* [87] for application in a multi-interface level measurement system for oil separators and for high frequency process tomography [88]. It is also interesting to note that this method has been commercially applied in a capacitive level gauge [89] since 1983.

- Finally, when the parasitic capacitances are negligible, the bridge imbalance can be measured using a voltage meter. However when the parasitic capacitances are not negligible, a large error will occur.

The equivalent circuit of Fig. 6-7 with a parasitic cable capacitance C_{p2} at the common electrode node is shown in Fig. 6-8.

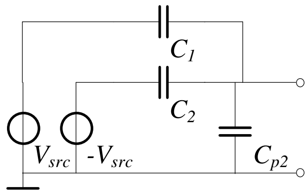

Fig. 6-8 Bridge imbalance measured with a voltage meter

The measured voltage V_m is

$$V_m = V_{src} \frac{C_1 - C_2}{C_1 + C_2 + C_{p2}} . \tag{6-12}$$

When $C_{p2} \gg C_1 + C_2$ we can simplify Eq. (6-12) to

$$V_m = V_{src} \frac{C_1 - C_2}{C_{p2}} . \tag{6-13}$$

Clearly the unknown and unstable value of C_{p2} has an unacceptable influence on the measurement result.

An application of the method has been presented by Peters [90], [91]. Here the method has been used for symmetric differential capacitive sensors where $C_1 = C + \Delta C$ and $C_2 = C - \Delta C$. In that case (and assuming negligible parasitic capacitances) Eq. (6-12) changes to

$$V_m = V_{src} \frac{\Delta C}{C} . \tag{6-14}$$

The resulting output voltage is proportional to the ratio of the sensor capacitance change and absolute value, and thus allows for the electrodes to be scaled down. However, in general this technique can not be applied because the parasitic capacitances can not be ignored.

6.4.2 Resonance method

This method adds an inductance L in parallel to the unknown capacitance C_x, so a resonance circuit is formed. The method then proceeds by tuning the frequency of the source voltage V_{src} to the resonance frequency f_r and measuring the current at resonance I_r (Fig. 6-9). C_x can then be calculated from

$$C_x = \frac{1}{(2\pi f_r)^2 L} \tag{6-15}$$

and R_x from

$$R_x = \frac{V_{src}}{I_r} \tag{6-16}$$

with I_r the measured current at resonance.

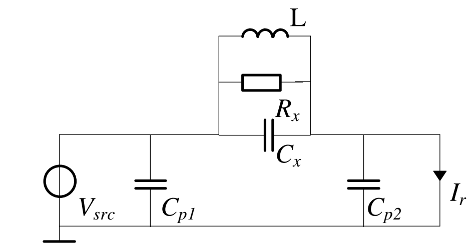

Fig. 6-9 Resonance method

The advantage of this method is that it can be used with relatively small parallel resistances (or dielectrics with high loss factors) and is therefore very suited for laboratory measurements of the dielectric properties of materials [72].
The tuning of the source voltage can be done applying feed-back between I_r and V_{src} so that a second order oscillator is formed. Some form of amplitude control will then be required, which slightly complicates the circuit.
Some authors (Moore et. al. [92], Tapson and Greene [93]) have successfully applied a phase locked loop (PLL) to find the frequency where the phase shift caused by the resonance circuit is zero. Still, the method does not seem to be very attractive for use in low-cost capacitive sensors.

6.4.3 Charge-discharge method

Huang *et. al.* [72], Bonse *et. al.* [94], Shi *et. al.* [95] and Wouters *et. al.* [96] report the use of a method called the charge/discharge method, patented by Endress and Hauser Ltd. [97]. The methods is based on charging the capacitance C_x to a voltage V_{src} and discharging it to a charge amplifier (Fig. 6-10). The discharging current pulse is averaged by the large capacitor C to a current that is then further amplified. By adding a similar stage with reference capacitor C_{ref}, the difference between the output voltages is

$$V_{dif} = f\, R_f\, V_{src}\left(C_x - C_{ref}\right). \tag{6-17}$$

Here the reference measurement does not eliminate the influence of the clock frequency, the integrator resistor and the voltage source.
Jordan *et. al.* [98, 99] add the reference capacitor to the input of the same charge amplifier but operates the switches of C_{ref} at a fixed frequency f_{fix}, while the switches of C_x are operated at the frequency of a VCO f_{VCO} that is connected to the output of the charge amplifier. The ratio of the frequencies is then

$$\frac{f_{VCO}}{f_{fix}} = \frac{C_{ref}}{C_x}. \tag{6-18}$$

In this system care must be taken to prevent the VCO from locking to the fixed frequency.

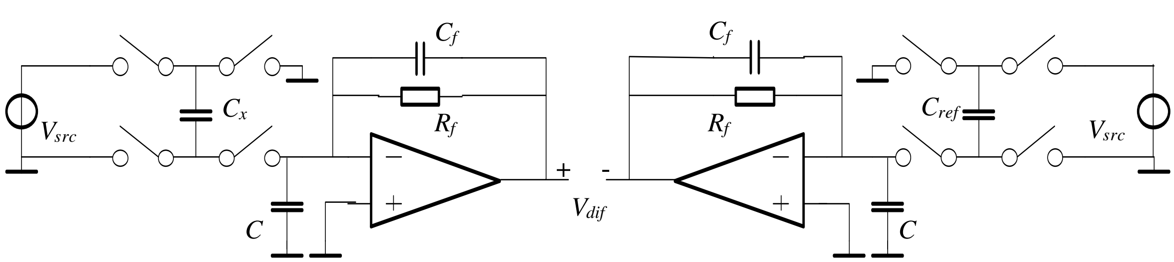

Fig. 6-10 Charge/discharge method

Other variations on this type include charge-balance and switched capacitor oscillators that balance the charge on the input of the charge amplifier by a current or alternatively by multiple charge packets from the switched capacitor [100].
These types of modulators suffer from charge injection from the CMOS switches. Although this causes an additive error that could be eliminated by an offset measurement, the presence of the switches that are connected to the input of the charge amplifier prevents the measurement of the offset capacitance in exactly the same way, as required for the 3-signal method (see Section 6.2). Especially when large parasitic capacitors are present, it will be difficult to eliminate the charge injection completely. Moreover, these types of modulators appear to be sensitive to $1/f$ noise (van der Goes, [79]) and have a relatively strong tendency to lock to high frequency interference.

To overcome these problems, Kung *et. al.* [101] presented a variation on the charge-discharge method called the charge-redistribution technique, which replaces the CMOS switches at the input of the integrator by a reset switch connected to ground. The most interesting feature of the circuit (Fig. 6-11) is however the charge amplifier, implemented using a comparator, followed by a successive approximation register (SAR) and a digital to analog converter (DAC). Using this combination, the (analog) voltage on C_f will quickly converge so that the input voltage of the comparator is minimized. The circuit works by starting at the most significant bit and successively adding less significant bits depending on the result of the comparator output. For a 10 bit DAC only 10 cycles are required.

Example:
Lets suppose the output voltage of the DAC must be 4 V to bring the input voltage difference of the comparator to zero. The SAR will find the correct value in 8 cycles starting at 2.5 V (Table 6-1).

Table 6-1 Operation of the SAR

Bit pattern	Voltage	Comparator output
1000 0000	2.5	1
1100 0000	3.75	1
1110 0000	4.38	0
1101 0000	4.06	0
1100 1000	3.91	1
1100 1100	3.98	1
1100 1110	4.02	0
1100 1101	4.00	0

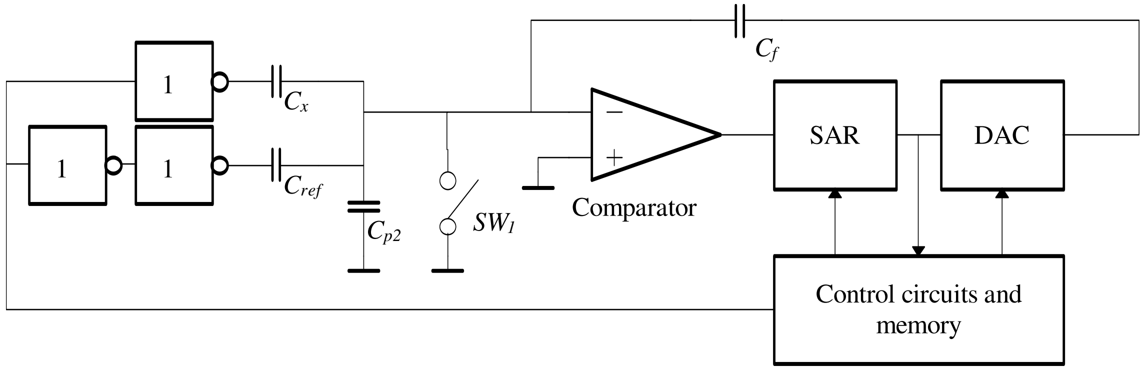

Fig. 6-11 Charge amplifier presented by Kung *et. al*.

After the loop has forced the input of the comparator to zero volts the digital value of the voltage is directly available at the output of the SAR. Kung shows that the input offset voltage of the comparator can be canceled as well as the charge injection of the switch by applying the correct switching sequence. At the beginning of the measurement sequence the output of the DAC is set to ground as is capacitance C_{ref}. Consequently C_x is set to the supply voltage of the inverter gates, V_{src}. Switch SW_1 is briefly closed and the opened again, long enough to discharge the total input capacitance C_T (in which C_{p2} is dominant). The opening of the switch will cause some charge injection Q_{S1} into the total input capacitance, which adds to the input offset voltage V_{io} of the comparator. Now a A/D conversion is performed by the SAR in combination with the D/A converter, resulting to output offset voltage V_{oo}

$$V_{oo} = V_{io}\frac{C_T}{C_f} - \frac{Q_{S1}}{C_f} \tag{6-19}$$

V_{oo} is available as a digital number and is temporarily stored. Now C_x is set to ground while C_{ref} is set to V_{src}. Kung shows that after performing a new A/D conversion V_x will be

$$V_x = V_{src}\left(\frac{C_x - C_{ref}}{C_f}\right) + V_{oo} \tag{6-20}$$

By subtracting V_x and V_{oo} digitally the desired result V_{xo} is obtained

$$V_{xo} = V_{src}\left(\frac{C_x - C_{ref}}{C_f}\right). \tag{6-21}$$

Note that V_{xo} still depends on V_{src} and C_f. A complete measurement takes about 90 µs with a 30 aF resolution using a 16b SAR/DAC. Using this method fast conversion times can be achieved with a reasonable resolution at the expense of an extra SAR/DAC.

The circuit can also be seen as a capacitive bridge using a voltage meter as the detector (the comparator). When the gain of the comparator stage is infinite, the limited resolution of the DAC causes a capacitance resolution C_{res} of the circuit of

$$C_{res} = 2^{-n} C_f \tag{6-22}$$

with n the number of bits of the DAC. To be able to detect a capacitance change of this size, the comparator gain should be larger then

$$A_{comp} >> \frac{C_{res}}{C_T}. \tag{6-23}$$

An effect that was not mentioned by Kung is the parasitic capacitance between the output and the input of the comparator. When the output of the comparator changes during the A/D conversion (which is necessary), charge will be injected. This causes hysteresis, which can severely limit the resolution of the circuit.

6.4.4 Conclusion

Although the capacitive bridge method is known as the most accurate capacitance measuring method, it appears to be also the most difficult to use. It can not easily by incorporated into an automatic measurement setup or into an intelligent sensor.
The resonance method seems to be unattractive because of the incorporation of an inductance. However, in some cases it might be possible to realize the inductance electronically, using a gyrator.
The most promising methods are based on the charge-discharge method. The components for this method (switches, capacitances) are available in discrete or in integrated form, so the method can be applied in both technologies.

6.5 Smart capacitance measurement methods

A smart capacitance measurement method combines the properties of the previous sections, i.e. it uses a 2-port measurement, measures the offset and a reference capacitor in the same way as the measurand, reduces electromagnetic interference and uses the available microcontroller to calculate the actual capacitance (relative to the reference), resulting in a low-cost high performance measurement system.

According to Section 4.3 the modulators with an output in the time domain are to be preferred over the ones with a voltage output, since the signal can be directly interpreted by the microcontroller. However it will be clear that by adding an A/D converter to for instance an unbalanced capacitive bridge with a current meter charge-discharge circuit, can also result to a smart capacitance measurement system. Because of the complexity of such a circuit (and the resulting higher costs) it will not be considered here.
In the following section we look at modulators that provide a microcontroller compatible output directly, without the need for explicit A/D converters or external signal generators, except for a variation of the charge redistribution technique.

6.5.1 Two-integrator oscillator

The two-integrator oscillator belongs to the class of Semi Ideal Sine Oscillators (SISO) presented by Doorenbosch [102]. A block diagram of the oscillator is shown in Fig. 6-12. The system consist of two integrators $-G_1 / s\ C_1$ and $-G_2 / s\ C_2$ and an amplitude control loop that consists of the amplitude detector and two amplifiers with variable gain G_3 and G_4. When $G_1 = G_2 = G$, $C_1 = C_2 = C$ and $G_3 = G_4$, the amplitudes of U_1 and U_2 will be equal. When the amplitude of U_1 and U_2 has the desired value, G_3 and G_4 will be set to zero and the system can be described by the following differential equation

$$\frac{d^2U_2}{dt^2} + \left(\frac{G}{C}\right)^2 U_2 = 0 \tag{6-24}$$

with the solution

$$U_2 = A\sin\left(\frac{G}{C}t + \psi\right). \tag{6-25}$$

Likewise the solution for U_1 is

$$U_1 = A\cos\left(\frac{G}{C}t + \psi\right). \tag{6-26}$$

where the amplitude A is determined by the amplitude control loop and ψ is the arbitrary phase. So the square of the frequency of the oscillator is

$$\omega^2 = \left(\frac{G}{C}\right)^2. \tag{6-27}$$

When U_1 and U_2 are of equal magnitude, the amplitude can be determined instantaneously by a so called phytagorator

$$A = \sqrt{\left(U\sin(\omega t + \psi)\right)^2 + \left(U\cos(\omega t + \psi)\right)^2}. \tag{6-28}$$

Doorenbosch has shown that when the gain of both integrators G / C change simultaneously, both amplitudes remain constant, while the frequency of the oscillator changes instantaneously according to Eq. (6-25) and (6-26). De Jong [100] has calculated the effect of the finite DC gain of the integrators, that results to a LF pole unequal to zero, and the finite bandwidth, that results to a HF pole. Toth [103] calculated the effect of additional poles and zeroes in the loop. Apparently the influence of the two LF poles compensate each other, while the remaining influence (a damped or underdamped sine-shaped signal) is eliminated by the amplitude-control loop. The HF poles (with time constants τ_{HF}) cause some non-linearity, resulting to

$$\left(\frac{G}{C}\right)^2 = \omega^2\left(1 + 2\,\tau_{HF}{}^2\,\omega^2\right). \tag{6-29}$$

In other words, the influence of the bandwidth decreases with the square of the ratio of the bandwidth and oscillator frequency.

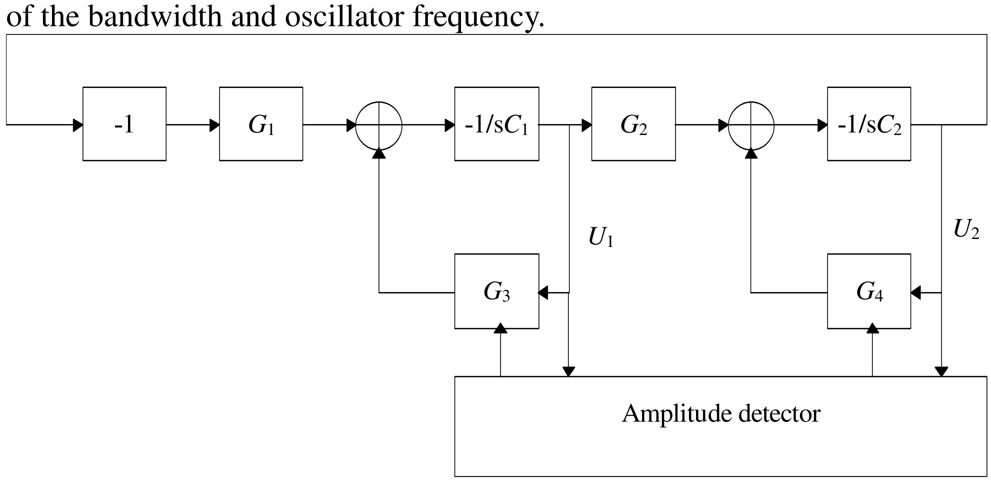

Fig. 6-12 Two-integrator oscillator

When we compare the two-integrator oscillator with an LC oscillator, it appears that the circuits are similar, with the inductance replaced by a capacitor and a gyrator. This means that it can be used to measure capacitance, following the resonance method (Section 6.4.2).

In a capacitive sensor it will be difficult to have two capacitors change simultaneously. As a result, amplitude variations of the signal will occur, which the amplitude control loop will try to adjust to the set point. Indirectly this will cause the

frequency changes not to occur instantaneously (as is the case in the ideal situation presented by Doorenbosch).
Another problem is that the continuous amplitude detector, the phytagorator, presented by Doorenbosch will not function properly. This circuit relies on the presence of two sine shaped signals with equal amplitudes that are 90° out of phase. The amplitude can then be detected by taking the sum of the squares. When the amplitudes are not equal, as is the case here, the resulting signal will contain an AC component that will cause distortion of the oscillator signal.

An alternative is to change only one capacitor at a specific zero-crossing of the signal. This is possible since the fastest capacitance changes occur when switching from one capacitor to another. By synchronizing the switches to the oscillator frequency, one of the signals can be kept constant. Still the phytagorator circuit can not be used as amplitude detector.
Instead, Messchendorp [104] and De Jong [100] investigated the application of a 2-integrator oscillator for use in a capacitance measurement system, using a weakly non-linear feedback. The period of this oscillator is proportional to the square root of the capacitance $C_x + C_1$. A microcontroller measures the period and takes the square of the value, after which the 3-signal approach is applied to eliminate the values of G_1, G_2, C_1 and C_2. The resulting modulator has on oscillating frequency of about 10 kHz, a measurement range of 2 pF, with a non-linearity of 5 ppm and a resolution of 8 aF at a measurement time of about 1 s.

The modulator circuit is rather complex and has been was implemented with discrete components. The values of C_1 and C_2 need to be relatively large (10 pF) compared to C_x, which limits the advantage of the relatively good stability of this oscillator. It is expected that an even better performance is obtained when the circuit is implemented as an IC.

6.5.2 Modified Martin oscillator

The modified Martin oscillator is based on a switched capacitor oscillator presented by Martin [105]. Van Drecht [106] modified the circuit by replacing the switched capacitor by a resistor. Toth and Meijer [76] used this circuit to realize the capacitance-controlled oscillator shown in Fig. 6-13. The method is somewhat similar to the charge-discharge method (Section 6.4.3), except that when the capacitor is charged, simultaneously an opposite charge is stored in the charge amplifier. The charge amplifier is then discharged by the resistor. This means no switches are required at the input of the charge amplifier, so no charge injection occurs.
An application of the circuit has been described by de Jong *et. al*. [100, 107].

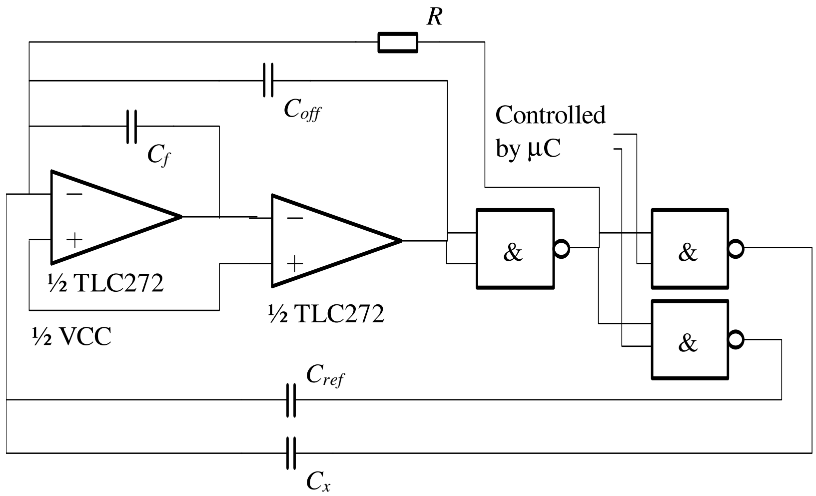

Fig. 6-13 Modified Martin oscillator

Depending on the control signals from the microcontroller, C_x and C_{ref} can be connected in parallel to C_{off} (Fig. 6-13). An important aspect is that in all cases the capacitance at the input of the oscillator remains constant, which is necessary when applying the 3-signal approach. The period of the oscillator is

$$T = 4RC_i + 4t_d\,, \tag{6-30}$$

with t_d the delay time caused by the comparator and C_i is (C_{off}, $C_{off} + C_x$, $C_{off} + C_{ref}$) for i is 0, 1 and 2. The (measured) output signal of the integrator is shown in Fig. 6-14.

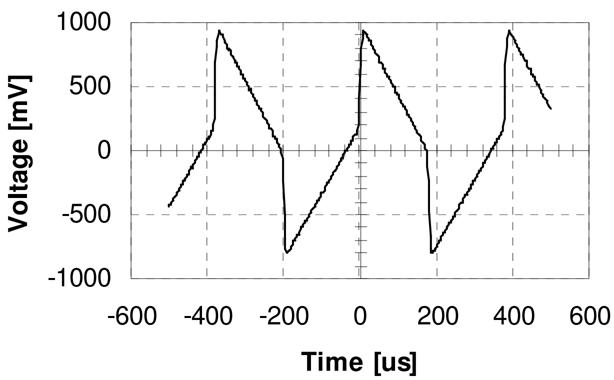

Fig. 6-14 Measured output signal of the integrator

The periods T_0, T_1 and T_2 are measured successively by a microcontroller, which results to the (digital) numbers M_0, M_1 and M_2 following

$$M_i = nT_i\,, \tag{6-31}$$

where n is the number of counts of the counter in the microcontroller per second.
By applying the 3-signal approach on the measured periods M_i we obtain

$$\frac{C_x}{C_{ref}} = \frac{M_1 - M_0}{M_2 - M_0}\,, \tag{6-32}$$

where all additive and multiplicative errors have been eliminated and only non-linearity and random errors remain.
Initially the non-linearity was proved to be less than 1000 ppm over a 50 fF range. In later measurements a non-linearity of 2000 ppm has been found over a 2 pF range.
The resolution of 20 aF has been found for a total measurement time of 100 ms.

The circuit in Fig. 6-13 is very simple and can be built at low costs, even by using discrete components. However, it can not be used to measure multi-terminal capacitors like the sum of two cross-capacitors. In a structure with two cross-capacitances there are also two trans-capacitances (apart from the parasitic capacitances) that need to be grounded during the measurement of the cross-capacitances. With the circuit in Fig. 6-13 this is impossible because the capacitances are only multiplexed on one side. However, when multiplexing at both sides (i.e. using the NAND gates to select which capacitance to drive and using switches at the input of the integrator to select which charge to measure) the parasitic capacitances of the cables will also be switched, causing a different parasitic capacitance at the input during the respective measurements.
To prevent this, a new circuit (Fig. 6-15) was proposed by Toth et. al. [77]. In this circuit the trans-capacitances are modeled by $C_{xt,1}$ and $C_{xt,2}$ and the cross-capacitance by $C_{xc,1}$ and $C_{xc,2}$. Switches (S_{w1} and S_{w2}) were added to the inputs, except for the reference capacitor. These switches are set to the appropriate capacitor and remain in this position during the whole measurement sequence during which the offset, reference and unknown capacitances are selected with the NAND gates (N_1 to N_3). Then the switches at the input are set to the next unknown capacitor and the procedure is repeated.
For instance, to measure $C_{xc,1}$ first S_{w1} is closed and S_{w2} is opened. While the switches remain in this position M_0 is measured with all NAND gates disabled. Then M_2 is measured by enabling only N_3 and M_1 is measured by enabling N_2. Applying Eq. (6-32) results to the ratio of $C_{xc,1}$ and C_{ref}.

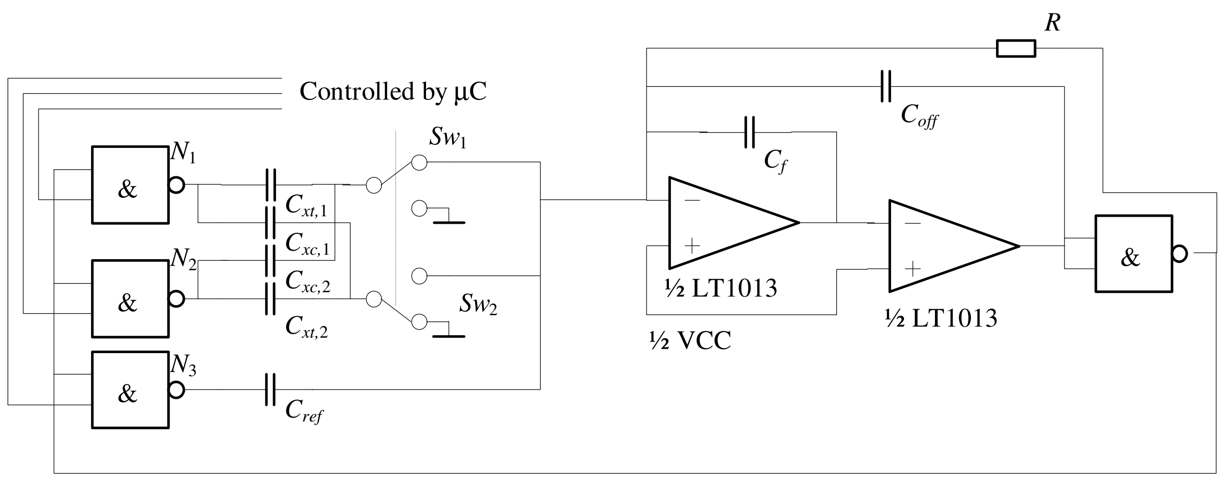

Fig. 6-15 Martin oscillator with double-sided multiplexing

Also the sources of the non-linearity were investigated, including the output resistance of the NAND gates, the bandwidth of the integrator and the slew-rate of the integrator op amp. The remaining non-linearity appears to be caused by the frequency dependent delay of the comparator. By choosing another type of op amp (LT1013) the non-linearity was reduced to 100 ppm over a 2 pF range.

A disadvantage with respect to the circuit in Fig. 6-13 is that the measurement sequence will take nearly three times longer, when measuring many capacitors, since in the former circuit C_{ref} and C_{off} are only measured once. In Fig. 6-16 the relative standard deviation is shown as a function of the measurement time. It is clear that the resolution of the measurement can easily be improved by increasing the measurement time. Below 300 ms, the standard deviation is inversely proportional to the measurement time, while above this value it is inversely proportional to the square root of the measurement time. At even longer measurement times (above 10 s), the standard deviation does not decrease any further due to 1/*f* noise. However, successive measurement results from Eq. (6-32) can be averaged, to obtain a further reduction of the standard deviation, which is inversely proportional to the square root of the total measurement time.

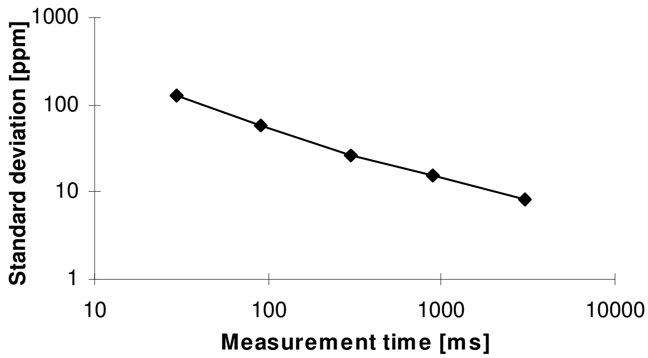

Fig. 6-16 Measured jitter as a function of the measurement time

An advantage is that the parasitic capacitances of the unknown capacitors are split, reducing the total parasitic capacitance during a measurement sequence, thereby reducing the noise in the circuit and improving the resolution.

6.5.3 Multiple-sensor modulator

Van der Goes presented a new type of modulator, called the multiple-sensor modulator [79]. The circuit is suitable for the measurement of a large range of sensing elements, including resistive and capacitive types and bridges. The type of measurement can be selected by choosing a mode using 4 pins of the integrated circuit.

For capacitance measurements [108] the circuit basically consists of a charge amplifier of which the output voltage is converted to a period, using the charge-discharge method (Section 6.4.3). The periodic output signal is used to drive the capacitances, thus forming a capacitance controlled oscillator. The circuit has the advantage, that a sort of synchronous detection combined with discrete time filtering is applied, to achieve excellent LF interference suppression. Also, dithering techniques have been used (Section 6.3.2) to reduce locking to HF interference, resulting in excellent EMC properties.

The measurement sequence may be controlled by the circuit the itself using an internal multiplexer and sequencer, or by an external multiplexer controlled by a microcontroller.

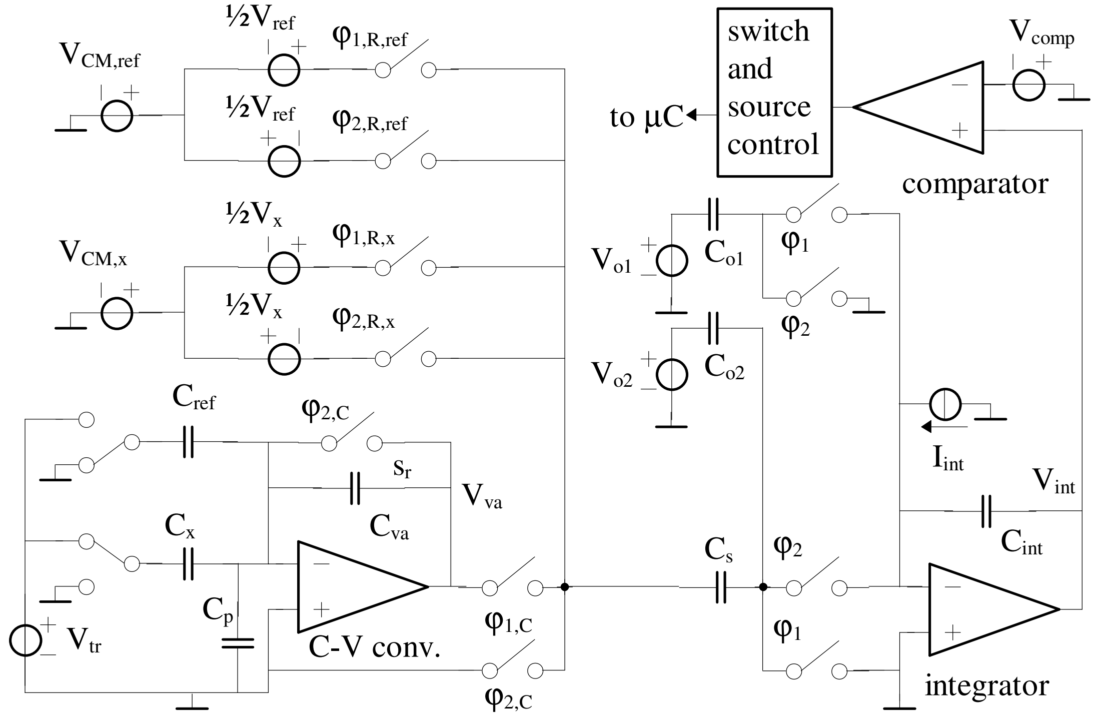

Fig. 6-17 Multiple-sensor modulator in capacitance measurement mode (reprinted from [79])

Because of the complexity of the circuit it is not suitable for a discrete implementation, however it has been incorporated into a commercially available device, the Universal Transducer Interface (UTI) by Smartec BV [109]. This modulator type is at present the most low-cost solution for medium- and low-speed precision capacitance measurements, especially since other sensing elements can be measured using the same device. Therefore, instead of going through the details of the measurement principles here, we will summarize the properties of the circuit only.

The circuit can measure either 3 or 5 capacitors using the internal multiplexer or a virtually infinite number using an external multiplexer. The range of the capacitors can be chosen to be 0 to 2 pF, 0 to 12 pF or up to 300 pF using a special mode.
Using the internal multiplexer and sequencer the measurement time per capacitance can be set to values of about 5 ms and 40 ms, resulting to resolutions of 50 to 200 aF, depending on the parasitic capacitance of the cables at the input (C_{p2} in most diagrams in this thesis), which is allowed to be up to 300 pF. The non-linearity of the modulator can be tested by choosing the appropriate mode and is less then 250 ppm of full scale, while the remaining offset is less then 15 fF.

When using an external multiplexer (that is controlled by a microcontroller), C_{p2} is allowed to be up to 10 nF, but the non-linearity is less then 250 ppm when C_{p2} < 300 pF. In this case, the remaining offset is less the 20 aF and depends only on the shielding. The microcontroller needs to measure the period of the output signal of the modulator, that can be set to either (approximately) 6 kHz or to 50 Hz.
The multiplexer (MUX) passes the UTI signal B to the selected capacitor. It can be constructed using NAND gates that are controlled directly by the microcontroller, or indirectly by a combination of (3 to 8) decoders or shift registers. The resulting block diagram is shown in Fig. 6-18.

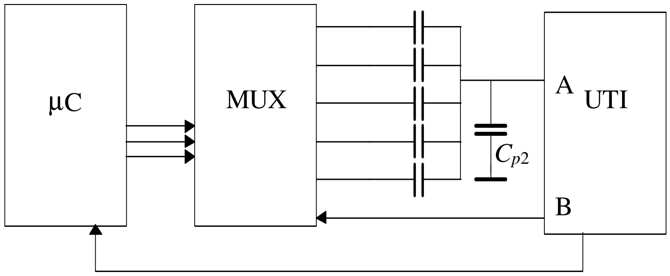

Fig. 6-18 Block diagram of the system using the UTI from Smartec

Naturally the 3-signal auto-calibration method is applied to eliminate the effects of additive and multiplicative errors, so one of the capacitors is the reference capacitor C_{ref}.

6.5.4 Smart charge redistribution

The modulators in the preceding sections are all optimized for a combination of linearity, resolution and measurement time at minimum costs. However, in some cases a minimal measurement time is required, while maintaining stability and resolution. This is the case when a capacitive sensor is incorporated into a control system. When the capacitive sensor is used to control for instance a (mechanical) position the bandwidth of the control loop is often required to be larger then 400 Hz, requiring a measurement time of less then 1 ms.

The relatively large measurement time in the presented oscillator circuits results from the fact that the capacitance of the sensing element is connected in parallel to an internal capacitance in the oscillator. This is necessary to prevent the oscillation frequency to become higher than the bandwidth of the electronic circuits when the capacitance is small. The oscillation frequency is limited by the bandwidth of the charge integrator, caused by the limited bandwidth of the op amp, which is effectively further reduced by the voltage divider formed by the feedback capacitance in combination with the total input capacitance.

> Example:
> Lets assume the op amp in the charge amplifier has a f_T of 2 MHz, the feedback capacitor has a value of 10 pF and the maximum parasitic capacitance at the input is 100 pF, the effective bandwidth of the charge amplifier will be only 180 kHz, resulting to a time constant of 0.9 μs. The minimum half period of the oscillator must be 10 times larger to obtain a linearity better then 50 ppm. With a half period of 9 μs, the resulting maximum frequency of the oscillator is about 50 kHz. With the discrete version of the modified Martin oscillator with a resistor of 10 MΩ this leads to a value for C_{off} of 0.5 pF. In the case of integrated oscillator circuits where a switched current source is used, similar values for C_{off} are obtained. When we want to measure capacitances smaller then 0.1 pF this can lead to a significant increase in measurement time.

Note that such an additional parallel capacitor is not required when applying a capacitive bridge.

An additional increase in measurement time results from the application of the 3-signal auto-calibration method, which requires additional measurements to eliminate the influence of unstable parameters that cause additive and multiplicative errors.

Even when the measurement time for these reference measurements is reduced (since the unstable parameters change slowly, they do not need to be measured continuously), the calculation that needs to be performed by the microcontroller causes some delay time. For instance, using an 12 MHz INTEL 8051FA, the calculation time for a 32 bit subtraction (to eliminate the offset) takes up to 100 µs, while a 24 bit floating point division can take up to 1 ms.

Although it is possible to increase the bandwidth of the op amps, to allow a higher oscillation frequency and thus a lower parallel capacitance, this increases the complexity of the circuit substantially, since high bandwidth op amps generally require a symmetric 15 V power supply, which is not compatible with the microcontroller power supply. Also additional circuitry is required for the necessary level shifts.

Since a capacitive bridge does not require an offset capacitor, it is in principle more suited for high speed measurements. A fast electronic way to balance the bridge is then required, preferably without requiring (high cost) transformers.
The circuit presented by Kung (see Fig. 6-11) provides such a method, as has been discussed in Section 6.4.3. However this circuit does not eliminate the charging voltage V_{src} nor the feedback capacitance C_f, as can be seen in Eq. (6-21). In Kung's circuit C_x and C_{ref} are switched simultaneously, resulting to a digital output proportional to their difference after eliminating the output offset voltage V_{oo}.
These drawbacks can be reduced by changing the switching scheme slightly. When C_x and C_{ref} would be measured separately, resulting to

$$V_x = V_{src} \frac{C_x}{C_f} + V_{oo} \tag{6-33}$$

and

$$V_{ref} = V_{src} \frac{C_{ref}}{C_f} + V_{oo} \tag{6-34}$$

the 3-signal auto-calibration method can again be applied to eliminate V_{oo}, C_f and V_{src}.

The resulting circuit is shown in Fig. 6-19. The switch SW_1 is required to set the (floating) input of the charge amplifier to an acceptable value (1/2 V_{cc}) but serves also to reduce the influence of LF interference, as discussed in Section 6.3.1. Still its effect can be increased by performing another measurement of V_{oo} after C_x (or C_{ref}) has been measured and by keeping the intervals between measurement equidistant. By averaging both values of V_{oo} we then have a more accurate estimate of the interference charge during the measurement of C_x.

Another problem in Kung's circuit is that some negative feedback results from the parasitic capacitance between the comparator's input and output (C_{comp}). To eliminate the influence of C_{comp}, we must exchange the comparator's inputs so that positive feedback occurs. Now, the comparator's output voltage is required to have the same value at the end of the A/D conversion as at the beginning. This means that the result of the A/D conversion is always rounded down. This does not influence the accuracy of the A/D conversion significantly and requires only a slight adaptation of the successive approximation algorithm, which can be efficiently programmed into the microcontroller. The resulting circuit is shown in Fig. 6-19.

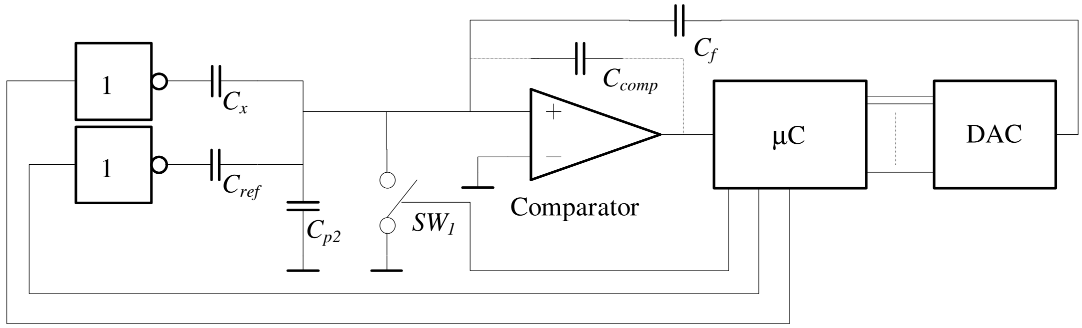

Fig. 6-19 Smart charge redistribution

To reduce the calculation time of the microcontroller a faster type then the 12 MHz INTEL 8051FA can be selected, for instance the new series INTEL 80251, which calculates up to 15 times faster, or the compatible 16 bit version from Philips. Naturally other 16 bit microcontrollers or digital signal processors (DSP) can also be used, but are generally in a price range from \$20 to \$100, which can not really be considered low-cost. Such high performance processors might be an economic choice when the whole control system is implemented into the same processor.

The resulting system has a similar behavior as the ones in preceding sections, and can also be made suitable for multi-electrode structures comparable to the modified Martin oscillator. The expected measurement time is less then 1 ms, based on the 20 μs conversion time achieved by Kung.
The advantages of the circuit appear when very small capacitances (< 100 fF) need to be measured at high speed. This does come at the expense of a faster microcontroller and a DAC with sufficiently high accuracy and resolution. For instance assuming a range for C_x of 0 to 100 fF, C_{ref} and C_f can best be chosen 100 fF. With a 12 bit D/A converter we could achieve 24 aF accuracy. Of course the comparator needs to be able to detect a 24 aF capacitance change, so when the parasitic input capacitance is 100 pF, the comparator's gain must be larger then $4 \cdot 10^6$.

6.6 Object model of modifiers for capacitive sensors

In Fig. 6-20 we show the class diagram for the class of capacitance modifiers. This scheme shows where the various types of modifiers fit in. Also it is hoped for that this classification will make it easier to derive a new type of modifier for applications that demand properties that neither of the presented modifiers can supply.

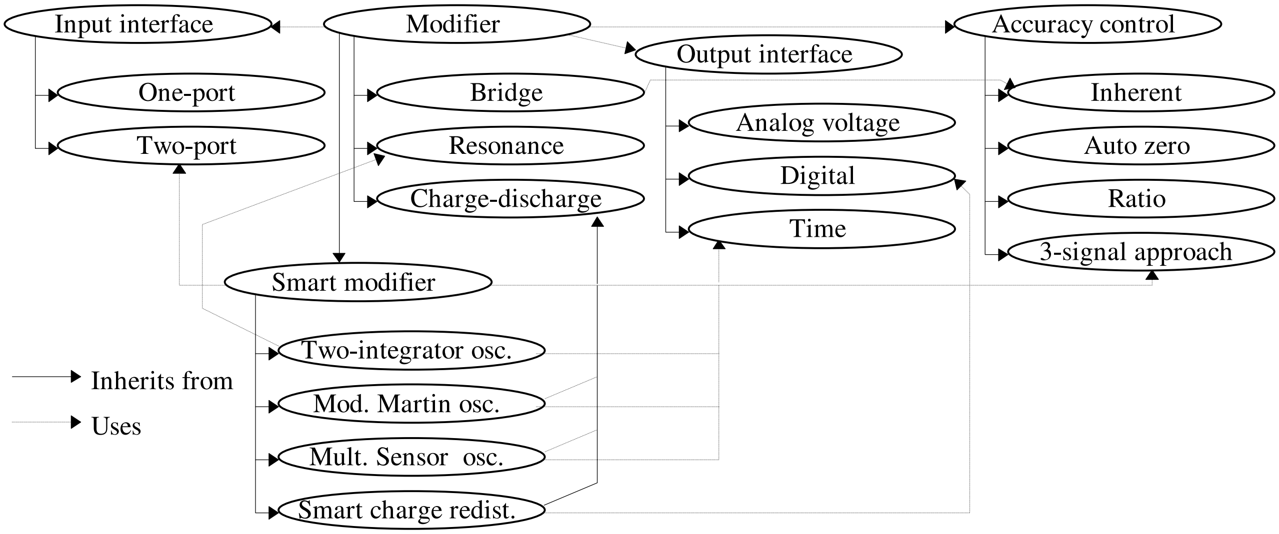

Fig. 6-20 Class diagram for smart modifiers

We have shown that the most accurate method for capacitance measurement is the capacitive bridge. The use of transformers to balance the bridge make it (nearly) inherently accurate but also unsuitable for capacitive sensors.

The class of smart modifiers makes use of a two-port measurement at the input interface to eliminate the effect of parasitic capacitances and of the 3-signal approach to achieve an accurate ratio of the measurand with respect to a reference capacitor. To reduce the costs of interfacing (and ensure interchangeability), the output interface of this class is microcontroller compatible, the digital and time-modulated output interfaces being preferred over the analog voltage types.

Four new classes have been derived from the parent class of smart modifiers. The classes of two-integrator oscillators, modified Martin oscillators and the Multiple Sensor oscillator have a period output while the Smart charge redistribution modifier has a digital output.

The two-integrator oscillator has a good stability (being a second order oscillator), but is rather difficult to implement. The modified Martin oscillator is very easy to build out of discrete components, but less suitable for integration.

The Multiple Sensor oscillator is very suited for integration and incorporates advanced LF and HF interference suppression. It can have single wire connection to the microcontroller or can be expanded by an external multiplexer. Moreover, it can be used with other types of sensing elements as thermistors and resistive bridges. Because it is available commercially, it is the preferred modifier for low-cost, medium speed capacitive measurements.

The Smart charge redistribution modifier is most suited for capacitive sensing elements with small capacitances (< 100 fF) that need to be measured at high speeds (< 1 ms). This can be achieved by applying a D/A converter and a high speed microcontroller, resulting to significantly higher costs. This modifier is most suitable for application in precision actuators where the sensor is used in the feedback loop and a high speed controller or a DSP is already available.

6.7 Conclusion

By now we have looked at different input and output interfaces, conversion principles and ways to control the conversion accuracy for capacitance modifiers. Clearly, the number of possible combinations are virtually infinite, and no schematic or text can cover them all. Instead we have tried to focus on the modifiers that on one hand are to a large extent compatible and on the other easily adaptable. In other words, they can replace each other without having a large influence on the system design and can be re-dimensioned to fit a specific purpose. We pointed out in an earlier stage that the class of modifiers that is most likely to fulfill these demands is the class of smart modifiers, of which we have shown a few variations.

For low-cost, medium speed applications the Multiple Sensor oscillator is most suited, being commercially available under the name Universal Transducer Interface (UTI). A second choice would be the modified Martin oscillator which can be built from discrete components.

For high speed measurement of small capacitances the Smart charge redistribution modifier is best suited, however the costs will be significantly higher.

---

72 Huang, S.M., M.S. Beck, R.G. Green and A.L. Stott, *"Electronic transducers for industrial measurement of low value capacitances"*, J. Phys. E: Sci. Instrum., 21 (1988) 242 - 250

73 Marioli, D., E. Sardini and A. Taroni, *"High-accuracy measurement techniques for capacitance transducers"*, Meas. Sci. Technol., vol. 4, no. 3, pp. 337 - 343, March 1993

74 Drecht, J. van, P.C. de Jong and G.C.M. Meijer, *"Concepts for the design of smart sensors and smart signal processors and their application to PSD displacement transducers"*, Transducers. '91, June 91

75 Meijer, G.C.M., J. van Drecht, P.C. de Jong and H. Neuteboom, *"New concepts for smart signal processors and their application to PSD displacement transducers"*, Sensors and Actuators A, 35 (1992) 23-30

76 Toth, F.N. and G.C.M. Meijer, *"A low-cost, smart capacitive position sensor"*, IEEE Trans. Instrum. Meas., vol. 41, no. 6, pp. 1041-1044, Dec. 1992

77 Toth, F.N., H.M.M. Kerkvliet and G.C.M. Meijer, *"Ultra-linear, low-cost measurement system for multi-electrode pF-range capacitors"*, IMTC'95, pp. 412 - 413, April 24 - 25, 1995

78 Mulder, J., *"Noise and accuracy of the Smart Signal Processor"*, Master's thesis, Delft university of Technology, Delft, Then Netherlands, March 1994

79 Goes, F.M.L van der, *"Lost-cost smart sensor interfacing"*, Ph.D. Thesis, Delft University of Technology, Apr. 1996

80 Trowbridge, A., *"On the differential transformer"*, Phys. Rev., vol. 20, pp. 65 - 76, 1905

81 Thompson, A.M., *"A bridge for the measurement of permittivity"*, Proc. IEE, Vol. 103, Pt. B., pp. 704 - 707, Nov. 1956

82 Thompson, A.M., *"The precise measurement of small capacitances"*, IRE transactions on instrumentation, vol. I-7, pp. 243-253, 1958

83 McGregor, M.C., R.D. Cutkowsky, F.K. Harris, J.F. Hersch and F.R. Kotter, *"New apparatus at the national bureau of standards for absolute capacitance measurement"*, IRE transactions on instrumentation, vol. I-7, pp. 253-261, 1958

84 Bachmair, H., T. Funck, R. Hanke and H. Lang, *"Realization and maintenance of the unit of capacitance with the PTB cross capacitor during the last ten years"*, IEEE Trans. Instrum. Meas., vol. 44, no. 2, pp. 440 - 442, 1995

85 Bertone, G.A., N.L. Carroll and Z.H. Meiksin, *"Investigation of a capacitance-based displacement transducer"*, IEEE Trans. Instrum. Meas., Vol. 39, No. 2, Apr. 1990

86 Bonse, M.H.W., J.W. Spronck and F. Zhu, *"A new two-dimensional capacitive position transducer"*, Sensors and Actuators A, 41-42 (1994) 29-32

87 Yang, W.Q., M.S. Beck and M.R. Brant, *"A multi-interface level measurement system using a segmented capacitance sensor for oil separators"*, Meas. Sci. Technol., vol. 5, no. 9, pp. 1177 - 1180, Sep. 1994

88 Yang, W.Q., M.S. Beck and A.L. Stott, *"High frequency and high resolution capacitance measuring circuit for process tomography"*, Proc. IEE, -Circuits Devices Syst., vol. 141, no. 3, Jun. 1994

89 *"User Manual level gauging system for service stations"*, B.V. ENRAF-NONIUS DELFT, Holland, 1983

90 Peters, R.D., *"Symmetric differential capacitive pressure sensor"*, Rev. Sci. Instrum., 64 (8) Aug. 1993, pp. 2256-2261

91 Peters, R.D., *"Full-bridge capacitive extensometer"*, Rev. Sci. Instrum., 64 (8) Aug. 1993, pp. 2250-2255

92 Moore, T.D., C.C. Speake and M. Turner, *"A capacitance displacement transducer with large dynamic range, good linearity and frequency read-out"*, Meas. Sci. Technol., vol. 4, no. 12, pp.1519 - 1521, Dec. 1993

93 Tapson, J. and J.R. Greene, *"Improved capacitance measurement by means of resonance locking"*, Meas. Sci. Technol., 5 (1994) 20-26

94 Bonse, M.H.W., H.F. van Beek and F. Zhu, *"A long-range capacitive displacement sensor having micrometer resolution"*, Meas. Sci. Technol., 4 (1993) 801-807

95 Shi, T.M., M.S. Beck, S.M. Huang, R.A. Williams and C.G. Xie, *"Capacitance-based instrumentation for multi-interface level measurement"*, Meas. Sci. Technol., vol. 2, no. 10, pp. 923 - 933, Oct. 1991

96 Wouters, P., M. de Cooman and R. Puers, *"A multi-purpose CMOS sensor interface for low-power applications"*, IEEE J. Solid-State Circuits, vol. 29, no. 8, Aug. 1994

97 Endress and Hauser Ltd., *"On the capacitance comparator measuring circuit"*, Patent 84087

98 Jordan, J.R., D.W. Kent, K.W. Peter and D. Renshaw, *"A capacitive ratio to frequency converter using switched-capacitor techniques"*, Sensors and Actuators A, 29 (1991) 133-139

99 Jordan, J.R. and K.W. Peter, *"ASIC implementation of a capacitance ration to frequency ratio converter using switched capacitor techniques"*, Meas. Sci. Technol., 4 (1993) 1201-1207

100 Jong, G.W. de, *"Smart capacitive sensors"*, Ph.D. Thesis, Delft University of Technology, 1994

101 Kung, J.T., H-S. Lee and R.N. Mills, *"Digital cancellation of noise and offset for capacitive sensors"*, IEEE Trans. Instrum. Meas., vol. 42, no. 5, pp. 939-942, Oct.. 1993

102 Doorenbosch, F., *"An integrated wide-tunable sine oscillator"*, IEEE J. Solid-State Circuits, no.6, Jun. 1976

103 Toth, F.N., *"Application of a two-integrator oscillator in a capacitive displacement sensor"*, Masters thesis (in Dutch), Delft University of Technology, Delft, The Netherlands, Mar. 1990

104 Messchendorp, E., *"Research for an integrated second-order oscillator for capacitive smart-sensor applications"*, Masters thesis (in Dutch), Delft University of Technology, Delft, The Netherlands, Aug. 1993

105 Martin, K., *"A voltage-controlled switched-capacitor relaxation oscillator"*, IEEE J. Solid-State Circuits, vol. 16, no. 4, pp. 412-413, Aug. 1981

106 Drecht, J. van, "Oscillator??", Patent application

107 Jong, G.W. de, A.M.M. Aalsma, A.J.M. Bertels, K. van der Lingen, G.C.M. Meijer and J.W. Spronck, *"A smart capacitive absolute angular-position sensor"*, Sensors and Actuators A, 41-42 (1994) 212-216

108 Goes, F.M.L. van der and G.C.M. Meijer, *"A novel low-cost capacitive-sensor interface"*, IEEE Trans. Instrum. Meas., vol. 45, no. 2, pp. 536 - 540, April 1996

109 Data sheet, *"Smart products need smart solutions - Universal Transducer Interface - revolution in sensor interfacing"*, Preliminary V2.1, Smartec BV, The Netherlands, June 1995

7 DESIGN OF AN INTELLIGENT CAPACITIVE FORCE SENSOR

Force sensors are abundantly available on the market and are based on several well known principles:

- The applied force changes the resonance frequency of a string. The string is brought into resonance by an electromagnet which is part of an electronic oscillator. The frequency of the oscillator is measured. This type is known as a resonant force sensor.
- The applied force causes a spring to bend. The strain on the surface of the spring is measured using a resistive strain gauge. This type is also known as a load cell.
- The applied force causes a spring to bend, after which the displacement of the free end of the spring is measured, for instance using a Position Sensitive Detector (PSD), a Linear Variable Differential Transformer (LVDT) or a capacitive displacement sensor.

The resonant force sensor has several advantages:

- The force is measured directly (it is not converted to another physical quantity), but is directly related to the resonance frequency.
- The spring, electromagnet and electronic circuitry form a closed loop.
- The electronic circuitry performs an AC measurement, so electronic offsets and the transfer function of the electromagnet have little effect. Also mechanical offsets caused by the temperature expansion coefficient have no effect.
- The sensor may be well suited for dynamic force measurements when a double-ended tuning-fork (DETF) resonator is applied (Cheshmehdoost [110]). The DETF is a two-beam resonating structure that may be clamped at both ends.
- The output signal of the sensor is a frequency that can be directly measured by a microcontroller.

Although the accuracy of this type of sensor can be quite high (in the order of $\pm 0.02\%$), the costs are mostly concentrated in the mechanical part (temperature compensation). Also (similar to capacitance controlled oscillators) the sensor needs to be preloaded (a force offset), to prevent the oscillation frequency to become zero. This force offset causes, together with the temperature coefficient of the spring constant, a temperature dependent offset of the sensor, destroying one of the advantages of the sensor principle.

Another disadvantage can be the vulnerability of the spring to mechanical shocks that can easily destroy the sensor.

For low-cost force sensors the type based on resistive strain gauges is the most popular one. The temperature dependence of the resistances is often compensated by applying them in a full or half-bridge configuration. An advantage is that the strain gauges measure the stresses in the beam to which the force is applied (which is directly related to the applied force) instead of the displacement (which can also be caused by other parameters). However the sensitivity of the bridge is rather low ($\Delta R/R$ < 0.3%) and the problem of rigidly mounting the strain gauges to the beam needs to be solved. Sometimes, an attempt is made to compensate the creep that occurs in the beam by choosing an appropriate glue to fix the strain gauges (Bethe and Baumgarten [111]). This technique is often applied in for instance low-range aluminum load cells in which the load can be quickly applied or removed and the creep of the material is known to be relatively high. It will be clear that such a compensation is difficult to obtain over larger temperature ranges.

High-quality spring steels are available in the form of wire or sheet. The latter lends itself best to create a bending beam of which the displacement is measured when a force is applied. In this chapter we will examine the feasibility of a low-cost capacitive force sensor that is suitable to measure static forces over a large temperature range. The sensor is basically a capacitive position sensor in which the position sensing element is replaced by a capacitive force-sensing element.
In Section 7.1 we will define the specifications of the sensor in more detail. An object model as well as a data flow model will be derived for the force sensor and its components in Section 7.2. The basic design of a capacitive displacement sensor object is described in Section 7.3. The design of a suitable force sensing element is described in Section 7.4.
Finally the objects are assembled and some experimental results are given in Section 7.5.

7.1 Specifications and target cost of the sensor

For a certain application we needed a force sensor with the specifications shown in Table 7-2. We will show how far these specifications can be met and will use this table as a reference point to discuss further improvements.

Table 7-2 Basic specifications for the capacitive force sensor

Parameter	Specification
Range (static)	0 N to 2 N
Preload	0 N to 6 N
Temperature range	-25 ºC to +75 ºC
Accuracy	2 mN
Resolution (high)	1 mN
Resolution (low)	10 mN
Measurement time (high resolution)	2 s
Measurement time (low resolution)	0.1 s

Other specifications need further clarification. Force, being a vector quantity, has a direction as well as a magnitude. A force sensor can be designed to measure the

magnitude of the force or just one of the components in a certain direction. Also, in many cases exerting a force will simultaneously exert a moment to the sensor, to which the sensitivity may not be zero. Another consideration is, if the force is applied to a point on the sensor or to an area. These considerations can lead to completely different force sensing element designs. For the force sensor considered here, we assume that the force will be transferred to the sensor through a wire to a fixed point on the sensor and that the angle of the force remains constant.
Also the target cost needs to be specified. A similar sensor exists based on the principle of the resonant force sensor. The manufacturing costs of this sensor (including the costs of calibration) are in the order of \$200. Also commercially available load cells exist that nearly have the required accuracy when the temperature range is not considered. To apply such a load cell electronic circuitry needs to be added to measure the output of the resistive bridge and to measure the temperature of the sensor, so that temperature compensation can be applied. The costs of these load cells (excluding electronic circuitry) are in the order of \$60, so the total cost of manufacturing can be expected to be around \$100, when the temperature dependence of the load cell is not considered.
This leads to the additional requirements in Table 7-3.

Table 7-3 Additional requirements for the force sensor

Parameter	Specification
Force transfer	fixed point, constant angle
Output signal	RS232
Cost	< \$100

It can be expected that the above requirements can be satisfied by applying a capacitive displacement sensor in combination with a leaf spring.

7.2 Object and data flow models for the capacitive force sensor and it's components

A capacitive force sensor inherits its properties simultaneously from the classes of capacitive sensors and force sensors. This leads to a new class which has a force input and a capacitive force sensing element. Since capacitive sensing elements can not measure force directly, the capacitive force sensing element will consist of the objects electrode structure (for displacement measurement) and spring (for force to displacement conversion).
In some cases it may be possible to combine these objects into a single new object (multiple inheritance). For instance, capacitive pressure sensors often make use of a membrane that functions as an electrode and a spring simultaneously. Likewise a force may be exerted on the dielectric, that in turn causes the displacement of the electrodes. These special cases are not considered further here.

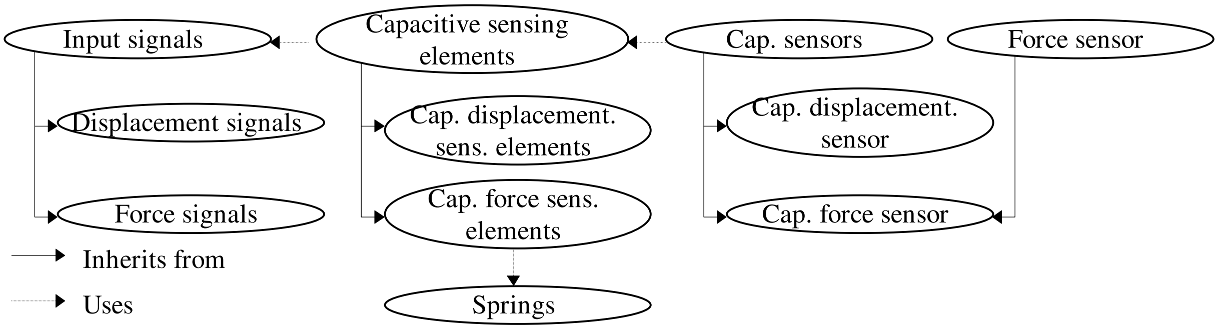

Fig. 7-21 Class diagram for capacitive displacement and force sensors and sensing elements

When the capacitive sensor is of the class of intelligent sensors, the process of designing the force sensor only consists of designing an intelligent capacitive displacement sensor (Fig. 7-22) and replacing the sensing element by a capacitive force sensing element.

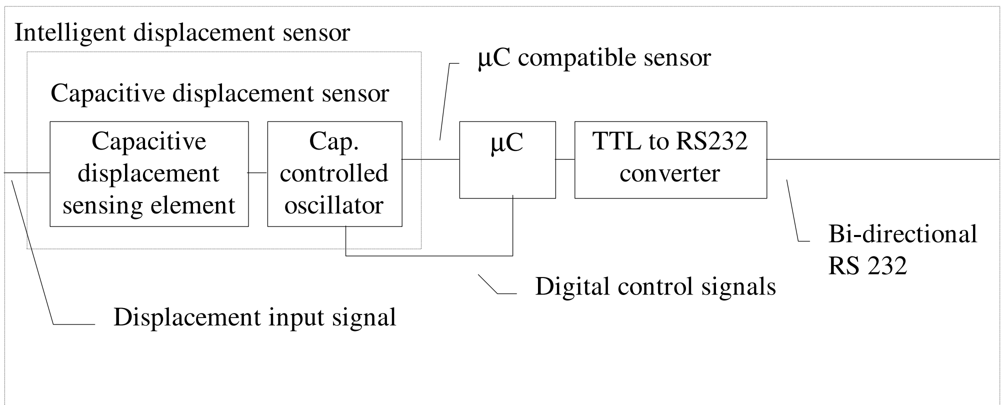

Fig. 7-22 Data flow diagram for an intelligent displacement sensor

This leads to the data flow diagram for the intelligent force sensor in Fig. 7-23. The design of the force sensing element is then reduced to cascading a spring and the electrode structure.

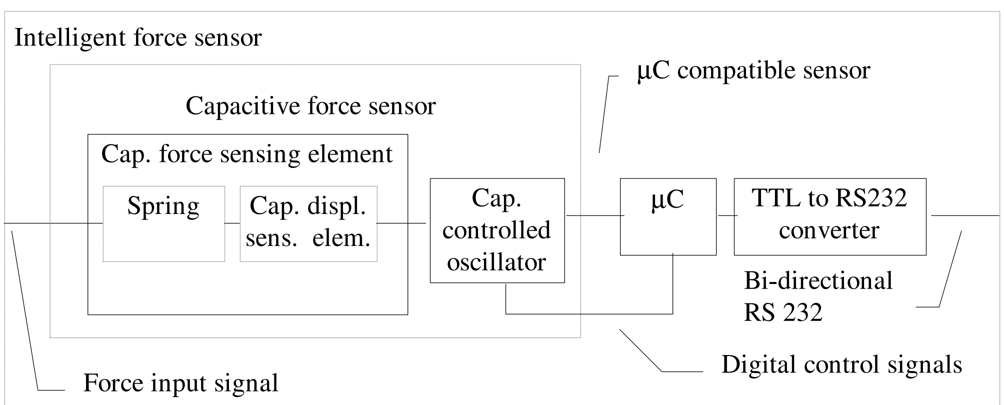

Fig. 7-23 Data flow diagram for an intelligent force sensor

The advantage of this approach is that the performance of the parts that are already available are well known and that the performance of the combination of the parts can easily be estimated.
The capacitive displacement sensor used here, is based on the intelligent capacitive sensor object, which consists of a capacitance controlled oscillator and a

microcontroller. From previous designs the performance can be estimated beforehand:

- The resolution of such a system will be in the order of 50 fF with a measurement time of 100 ms per capacitor.
- The accuracy will be in the order of 100 fF over a range of 1 pF.

The hardware costs can also easily be estimated when a specific implementation has been selected.

- Selecting a INTEL 83C51FA microcontroller costs approximately $6 in quantities of 1000's when the software is programmed in mask ROM at the factory.
- Selecting a discrete implementation of the modified Martin oscillator leads to a cost of the capacitance controlled oscillator of about $3, while selecting a Smartec UTI would cost about $1.5.
- The TTL to RS232 converter is also a standard component. For instance a MAX232 from Maxwell costs about $4.

Other parts like the electrode structure that is used as a capacitive displacement sensing element can be designed from the rules in Chapter 5. The cost will mainly depend on the costs of manufacturing and materials. For instance biplanar electrodes manufactured from printed circuit board will cost approximately $1, while selecting an alumina substrate will raise the cost to about $6 (depending on the size of the electrodes).

The design of the capacitive force sensor clearly demonstrates the flexibility of the proposed design method. For instance:

- At the time of the design, a UTI was not available. Instead a modified Martin oscillator was used, which can easily be replaced by a UTI with minor changes to the electronic circuitry and the software.
- At the time of the design, it was not clear if the electrodes could be manufactured from printed circuit board with an acceptable temperature stability. Alumina substrates can then be selected without affecting other parts of the design.
- At the time of the design, it is assumed that the temperature stability of the spring can be achieved by selecting an appropriate spring steel (a form of mechanical temperature compensation). However, when the costs of such a material would prove to be extremely high, ordinary spring steel can be used and the temperature dependence can be compensated by adding a smart temperature sensor (for instance a Smartec SMT130 which costs $2) and by calibrating the temperature dependence of the spring steel (either per batch or each sensor individually). This also requires only minor changes in the design since the smart temperature sensor can be directly connected to the microcontroller. The calibration constants require a programmable memory, for which a small serial (I^2C) FLASH EPROM can be used. This form of temperature compensation will add about $10 to $20 to the cost of the sensor.

7.3 The capacitive displacement sensor

In Section 5.2.2 we calculated the relative sensitivity S_d of the biplanar electrode structure for distance changes and found that it was approximately equal to -1. Remembering that the range of the force sensor is 2 N with a relative accuracy of

1000 ppm over the full temperature range and also assuming the relative sensitivity of the spring to be approximately 1, this means that a relative electrode distance change of 0.1% results in a relative capacitance change of -0.1%.
Considering the accuracy of an intelligent capacitive sensor system based on a modified Martin oscillator (100 aF), a displacement over the full range should cause a capacitance change of at least 100 fF.
The design of a capacitive displacement sensor is now reduced to the design of the sensing element and the design of a stable reference capacitor (which is required by the capacitance measurement system).

7.3.1 The capacitive sensing element

Since the displacement range is relatively small, a biplanar electrode structure of which one of the electrodes is surrounded by a guard ring is best selected (see Section 5.2). This electrode structure has the advantage that it is insensitive to lateral displacements and rotations and a relatively small (second order) sensitivity to obliqueness. This capacitance has an initial electrode distance d_0 and an area A.
When choosing a low cost material like printed circuit board, we have to keep in mind that the thermal expansion coefficients of the material are different in the lateral directions (20 ppm / ºC) and perpendicular direction (60 ppm / ºC) and that electrode bending can occur due to the components of the substrate (glass fiber and epoxy).
Electrode bending effectively causes a temperature dependence for d_0, which is undesirable. To prevent bending, it is advantageous to keep the radius of the sensing element as small as possible and also to glue the electrode to a rigid material, like steel. Furthermore it is necessary to prevent angular changes from being translated to displacements (the so-called Abbe error), so a symmetrical design is required and the electrode should be fixed at a single point in the center of the structure.

There are four important geometrical parameters to choose:
- The initial distance between the electrodes d_0
- The displacement over the full range Δd
- The electrode area A
- The guard electrode width w_g

Assuming that we want to minimize the electrode area (which determines in part the size of the sensor), we also need to minimize the initial distance since the initial capacitance is fixed at a minimum of 100 fF (assuming an infinite value for Δd). The minimum initial distance is, however, limited by the minimum electrode gap width, which is 0.2 mm for ordinary printed circuit board. According to Fig. 5-20 in Section 5.3.3 the electrode distance should be at least 6 times larger then the gap width for a relative error that is smaller then 0.1% (for thick electrodes). When we choose an initial distance of 2 mm, the relative error amounts about to 0.03%, which is acceptable.
The absolute sensitivity of the electrode structure decreases with the electrode distance, so it is necessary to limit the full-range displacement Δd to a value that is smaller then d_0. A range of 1 mm and an accuracy of 1 µm seems a good starting point.
From this the minimum electrode area can be calculated:

$$\Delta C = \varepsilon_0\, \varepsilon_r\, A\left(\frac{1}{d_0} - \frac{1}{d_0 + \Delta d}\right). \tag{80}$$

With the above values and $\varepsilon_r = 1$, this leads to a minimum area of about 68 mm^2.
To calculate the guard electrode width, Heerens rule of thumb for guards is applicable (Section 5.3.1). Assuming equal electrode and guard widths and using Eq. 5-31 it can easily be calculated that for a relative error of 0.01% the guard width must be larger then 5 mm.

To prevent the so-called Abbe error a symmetrical design is required, preferably circular. The proposed electrode structure is shown in Fig. 7-24.

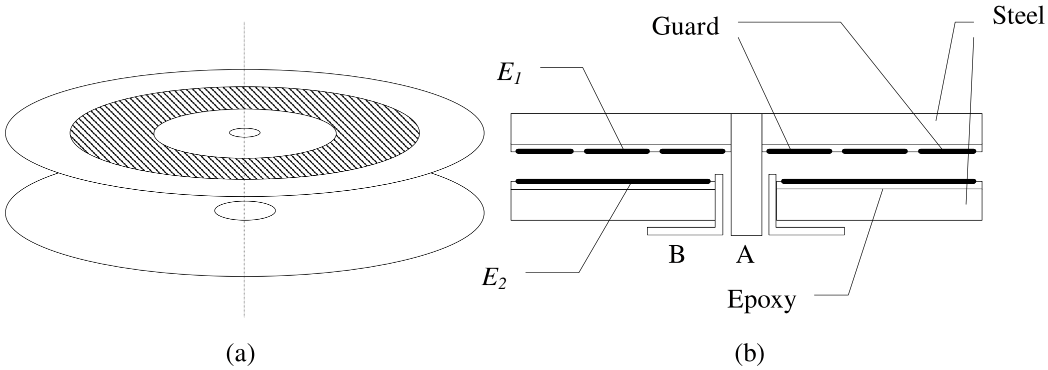

Fig. 7-24 The proposed capacitive sensing element (a) perspective (b) cross section

The ring shaped electrode E_1 is made out of a circular piece of PCB and has an inner radius of 11 mm and an outer radius of 14 mm. It is surrounded by an outer guard ring with a width of 8 mm and an inner guard ring with a width of 9.5 mm. The diameter of the structure is then 44 mm. This is glued onto a steel carrier after which a hole with a diameter of 3 mm is drilled in the middle. In this hole a steel bar (A) is placed which is glued to the PCB which is eventually used to connect the displacement sensor to the spring.
The opposite electrode E_2 has an outer diameter of 44 mm and is also glued to a steel carrier. It has a larger hole in the middle with a diameter of 6 mm so that a steel tube (B) can be used to connect it to the spring.
The area of the small electrode is now about 236 mm^2 resulting in a capacitance of 1 pF at a distance of 2 mm and 0.7 pF at 3 mm respectively.
When the capacitance is accurately measured at d_0 (C_0) and at $d_0 + x$ (C_1) the displacement of the electrode can be calculated from

$$\Delta x = \frac{\frac{1}{C_x} - \frac{1}{C_0}}{\frac{1}{C_1} - \frac{1}{C_0}} \cdot x \tag{81}$$

with Δx the displacement, x the displacement range and C_x the capacitance of the displaced electrode. However, when the displacement sensor is used as a force sensor an overall system calibration will be required only at zero and full scale force.

The steel carrier serves to prevent electrode bending when the temperature changes. This is likely to happen when PCB is used as the substrate. Also a ceramic substrate can be used, in which case the steel carrier is not required. However this choice hardly influences the design of the electrodes themselves. The final choice will need to be based on the actual costs of ceramic substrates versus the additional costs of mounting the steel carrier.

Other temperature effects arise from the thermal expansion coefficients of the substrate (which affects the electrode area) and of the bar (A) and tube (B), which affect the electrode distance. When steel is used for all parts, which has an expansion coefficient of 14 ppm/ºC, the relative change over the temperature range in the electrode area will be 0.14% (since the electrodes are solidly glued to the steel carrier), while the change in d_0 will be 0.07%. As a result of the partial compensation the capacitance will change 0.07% or 0.7 fF at a distance of 2 mm. Such a change in capacitance will result in an offset of ±2.3 µm at the extremes of the temperature range.
This means we will have to relax our requirement for the temperature range, use materials with smaller temperature coefficients or apply some form of temperature compensation. Since the temperature dependence appears to be small, we assume that we need only add a (smart) temperature sensor and determine the temperature calibration values per batch. This way we can achieve the original specifications at marginally increased costs.

7.3.2 The reference capacitor

When using a linear capacitance controlled oscillator as a modifier for capacitance measurements an accurate reference capacitor is required to eliminate the unknown gain factor in the transfer function. The unknown offset term also needs to be eliminated, which can be done by an offset measurement. Since these unknown terms are determined by parameters of the electronic circuit (like the voltage of the power supply), they can not assumed to be constant but need to be calibrated several times per second to achieve good results with this method. This technique is known as continuous autocalibration or as the three-signal approach and has been extensively described in Chapter 6.
Fortunately, using a capacitance controlled oscillator and electronic switches that are controlled by a microcontroller this can easily be achieved. Some smart capacitance modifiers that are suitable for this purpose have been described in Section 6.5.2. As a result, the ratio of the capacitance of the sensing element and of the reference capacitor is accurately measured several times per second.
When this capacitance ratio is used in a position or force sensor a one time system calibration will be performed, so therefore the reference capacitors value need not be accurately known. Only the long-term stability of the reference capacitor is important.

Such a reference capacitance can of course be constructed in a way similar to the sensing element. However the difference between the sensing element and the reference capacitor is that the sensing element should be sensitive to electrode distance changes while the reference capacitor should be constant. Constructing another sensing element but with a fixed electrode distance does not necessarily lead to the optimal solution. One reason for this is that the sensing element presented in the previous section requires a steel carrier to prevent electrode bending. A capacitor which is inherently insensitive to the electrode distance would not require such measures.

In [112] and [113] Toth *et. al.* presented a stable reference capacitor based on a circular cross-capacitor. The principle of cross-capacitance has been discussed extensively in Section 5.2.1. A distinction has been made between linear and circular

cross-capacitors. The structure is based on a biplanar capacitor in which the overlap of both (guarded) electrodes is exactly zero.
The main difference between the linear and the circular version is that a linear cross-capacitor has a value which depends only on the length of the structure (and not on the area of the electrodes or the distance between them) while in a circular cross-capacitor a small dependence on the electrode distance remains. However, a circular cross-capacitor has a larger symmetry so that positioning errors (since the overlap must be zero) have a smaller influence.
The circular cross-capacitor was implemented using low-cost printed circuit board material and a ceramic spacer (Fig. 7-25). The cross-capacitances between electrode E_1 and E_4 and E_2 and E_3 are measured respectively and averaged. The resulting capacitance displays a stability of 0.1% over a temperature range from -25°C to +75°C (18 ppm/ºC) and humidities ranging from 0% to 100% (non-condensing). The small temperature dependence results from the effect of the thermal expansion coefficient on the circumference of the circular electrodes. It is interesting to note that since we will measure the ratio of capacitance of the sensing element and the reference capacitor, the effect of non-condensing humidity will be compensated and also the temperature dependence of the capacitance ratio will be reduced to 4 ppm/ºC (the difference between the temperature sensitivity of the capacitance of the sensing element and the reference capacitor). From this value we can easily estimate the final position error to be about 0.7 μm at the extremes of the temperature range, which is just below our original requirement of 1 μm.

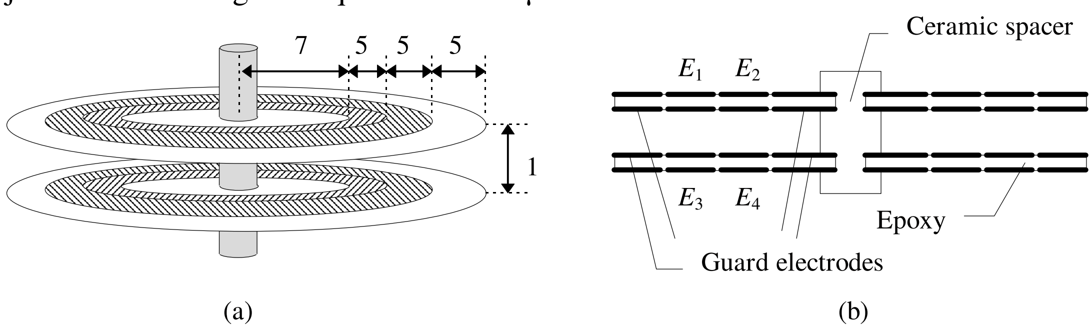

Fig. 7-25 Proposed circular cross-capacitor (a) perspective (b) cross-section

7.4 The force sensing element

As we have shown in Fig. 7-23, the capacitive force sensing element consists of a cascade of a spring and a capacitive displacement sensing element. The requirements for the spring can therefore partly be derived from those for the displacement sensor. The spring must change the distance between the electrodes by 1 mm when the applied force is increased by 2 N with an accuracy of 1 μm.
The most important effects that degrade the accuracy of the spring will now be discussed. These effects are caused by variations in the load transfer to the spring, the non-linearity of the spring, the thermal expansion coefficients of the materials, temperature coefficient of the spring constant and creep.

- Variations in the load transfer to the spring

In general a force and a moment are applied simultaneously to the spring, which also causes a deflection. But since we assumed a force with a constant angle that is exerted on a fixed point on the spring, this effect will be proportional to the effect of the force and thus may be incorporated into the spring constant C:

$$x = \frac{F}{C} + x_0 , \tag{82}$$

with F the exerted force and x the position.
The spring constant can be calculated by first calculating the stress σ at each point in the spring that is caused by the applied load. According to Hooke's law the strain ε at each point can then be calculated:

$$\sigma = \varepsilon E \ , \tag{83}$$

with E Young's modulus of elasticity of the spring material. From this the displacement can be calculated

- The non-linearity of the spring

This is a well known effect in spring design, that occurs in the region of the stress-strain curve where the elastic deformation of the spring material changes to a plastic deformation. This point is known for each spring material. When the spring is dimensioned in such a way that the stresses in each point of the spring remain a certain factor (often 10) below the maximum stress, the non-linearity is usually neglected. Sometimes this is not possible, because the resulting spring will become too large. In that case a calibration of the non-linearity becomes necessary.

- The thermal expansion coefficients of the materials

The thermal expansion coefficients of the material of the spring, but also of the materials used to fix the electrodes to the spring (as discussed in Section 7.3) can also have a large effect. In general is it beneficial to choose the materials in such a way that their expansion coefficients are as equal as possible.
When the length of the spring increases, the position where the load is applied changes so the moment acting on the spring also changes. Since up to now we assumed a fixed point, constant angle connection, this effect must be taken into account. The relative change in the moment will be equal to the thermal expansion coefficient of the spring steel.

- The temperature coefficient of the spring constant

The spring constant has a temperature coefficient κ so Eq. (82) (including the preload force F_p) must be modified to

$$x = \frac{F + F_p}{C(1 + \kappa \Delta T)} + x_0 , \tag{84}$$

with ΔT the temperature change. The displacement Δx of the sensor is now

$$\Delta x \approx \frac{F}{C}(1 - \kappa \Delta T) - \frac{F_p \kappa \Delta T}{C} . \tag{85}$$

So we can see that κ not only causes a temperature dependent error on the spring constant (a scale error) but also a temperature dependent offset. Both errors should lead to a displacement that is smaller then 1 µm. With the sum of F and F_p having a maximum of 8 N and C a value of 2 N/mm the maximum allowable value for κ is 5 ppm/ºC. This means that we can not use ordinary spring steel but have to turn to low temperature coefficient spring steel like Durinval [114] or Thermelast [115], of which the latter has a value of κ of 5 or 10 ppm/°C, depending of the specific type. By applying the appropriate heat treatment the value for κ can be reduced to within ±2 ppm/ºC, according to the specifications of the material.

• Creep

Another important parameter in spring design is the occurrence of creep. Creep is described as the relative change in the strain at constant load measured directly after loading and after a suitably chosen waiting time, and is therefore also known as the "elastic after effect". The effect is that for fast changing loads the spring constant is different then for loads that change slowly. This can easily be perceived as an hysteresis effect, when the measurement of the strain (or equivalently the deflection) takes place before system reaches steady state. The effect can be modeled by a series connection of two ideal springs of which one has a damper connected in parallel (Fig. 7-26a).

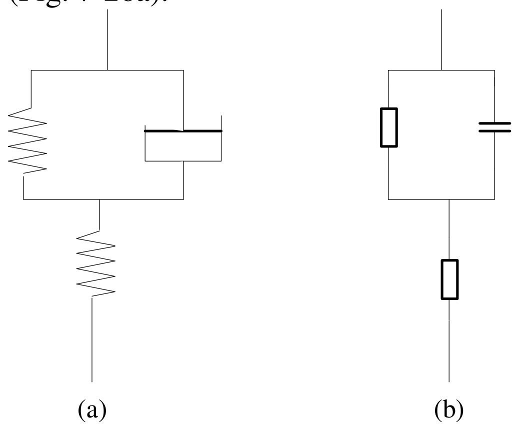

Fig. 7-26 Mechanical (a) and equivalent electrical model (b) for time-dependent anelastic deformation

An equivalent electrical model is shown in Fig. 7-26b, where the ideal springs are represented by resistors and the damper is represented by a capacitor. In this case the applied stress is modeled by the current flowing into the circuit, while the strain is represented by the voltage.

Bethe *et al* [116] show that creep is caused by two different effects:

1. The anelastic effect, which is caused by a redistribution of atoms in a deformed lattice. During the first loadings of the spring this leads to a permanent (plastic) deformation of the spring. Since the sensor will be calibrated after an initial loading cycle, this permanent deformation will not be considered here. After the initial loading cycle, only a reversible anelastic effect remains.

The anelastic effect is a diffusion dominated process that depends on the stress gradient in the spring, which increases as the thickness of the spring is decreased. It can be expected that a monocrystalline crystal structure (for instance silicon) will suffer less from this effect than a polycrystalline lattice (like aluminum). Also the effect of a heat treatment (which is often prescribed for spring steel to remove local stresses in the material) can be expected to have a large influence on the creep.

Example:

The creep in aluminum in a certain setup can reach 20% (Baumgarten, [117]) while Silicon has a value of 0.1‰ (Bethe *et al* [116]).

$CuBe_2$ (beryllium-copper) has a value of 0.6‰ while after the prescribed optimum heat treatment this value is reduced to 0.08‰.

2. The thermoelastic effect, which is caused by the change of an adiabatically deformed body leading to a temperature gradient in the spring, which in turn causes a dimensional change. The magnitude of this effect will depend in large on the linear expansion coefficient of the material, while the time constant will depend on the design of the spring. With a thin beam the time required to reach a thermal equilibrium in the spring will be much smaller then in a thick beam and so the time constant will be less.

Bethe and Baumgarten show that the optimal beam thickness for many materials is in the order of 1 mm. They modeled the relative creep as a sum of two exponential functions with different time constants τ_1 and τ_2 and weight factors a_1 and a_2 (= 1 - a_1)

$$\frac{\varepsilon(t)}{\varepsilon_0} = \Delta\left[a_1\, e^{-\frac{t}{\tau_1}} + a_2\, e^{-\frac{t}{\tau_2}}\right] \tag{86}$$

where Δ is the total after effect amplitude.

In the case of a 1 mm Thermelast beam, a value of 0.33‰ for Δ has been obtained. The dominant time constant has a value of 9.2 s, with a weight factor a_1 of 0.74. The second time constant has a value of 770 s.
The result is that a Thermelast spring will reach a “steady state” (within 85 ppm) after about 10 s, while the second time constant will cause an error smaller then 75 ppm.

Thermelast appears to be a suitable material for the spring presented here both for its low value of κ, as well as for its low creep value. Moreover, it can be worked on without special precautions to prevent health hazards (compared to for instance beryllium-copper), which reduces costs.
For force sensors where even lower creep values are required, beryllium-copper, silicon or germanium are to be preferred, although a temperature compensation for the spring constant is then required. Another disadvantage of silicon (and germanium) is the high cost of the material, which limits its use to applications where very small springs can be applied, like precision measurements of micro-mechanical forces [118].
Aluminum has the advantage that it can be worked on at very low costs. However, it does not seems to be suitable for use in precision force sensors with a large temperature range.

The proposed spring is shown in Fig. 7-27. The spring is made from a 1.5 mm thick Thermelast strip. The thick lines in the figure are cut using spark erosion.

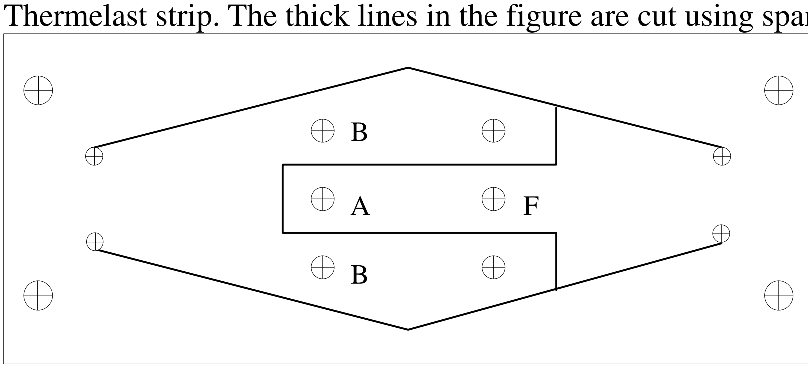

Fig. 7-27 Proposed leaf spring

The spring is clamped at one side while both electrodes are mounted onto the spring itself. The moving electrode is fixed at point A, while the other is fixed to the points marked B. The force is then applied at F. This design has several advantages:

- It can be manufactured at low costs.
- The behavior of the clamp does not influence the electrode distance.
- When the load is applied at the appropriate point the electrodes are displaced with minimal tilting (Fig. 7-28).

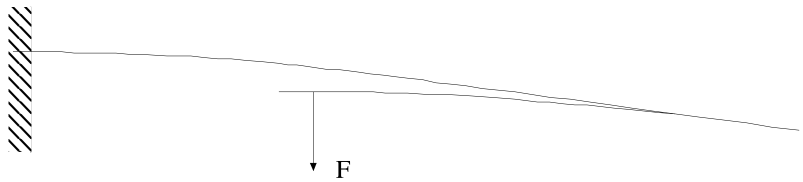

Fig. 7-28 Cross-section of the leaf spring under load

7.5 Experimental results

Although the development phase of the force sensor is at the time of writing not yet completed, several parts of the sensor have already been tested. On other parts, numerous experiments have been performed, some with disappointing results, others leading to the design in the previous sections.

7.5.1 The capacitive displacement sensor

The first system that has been tested is the capacitive displacement sensor described in Section 7.3. The results of these measurement have been previously published by Toth and Meijer [119].

The electrodes were made of low cost printed circuit board material with an effective electrode area of 12 mm x 12 mm. The smaller of the electrodes was surrounded by a 15 mm wide guard electrode while the initial electrode distance was 5 mm. When the distance of the electrode is varied over a 1 mm range the capacitance changes from 0.25 pF to 0.30 pF.

For the capacitance measuring system a modified Martin oscillator was used running at approximately 10 kHz, with a TLC272 dual opamp for the integrator and the comparator and controlled by a μC from Intel (87C51FA). It was found that the resolution of the capacitance measuring system was 20 aF in a total measurement time of 100 ms.

The electrodes were fixed to an electrical XY table. To achieve the required accuracy of 1 μm the XY table was auto-zeroed every minute. In this way the accuracy and repeatability of the displacement sensor have been found to be better then 1 μm over a 1 mm range.

This corresponds to an accuracy of the capacitance measurement system of at least 50 aF over a 50 fF range.

In a later publication [120] several characteristics of the capacitance measurement circuit have been improved:

- the measurement range was increased to 2 pF with 100 ppm linearity (200 aF)
- offset capacitance was determined at -40 aF (which can be reduced even further with improved shielding)
- double-sided multiplexing makes the circuit suitable for the measurement of cross-capacitors

This measurement circuit has been tested over a temperature range of -25 ºC to +75 ºC in a temperature controlled oven, with the capacitance under test and the reference capacitor at a constant temperature outside the oven. No measurable temperature effect has been observed.

Then the temperature dependence of the electrode structure presented in [119] was tested in the oven and found to be much too large. After this a circular electrode structure was designed similar to the one in Section 7.3.2. With this structure the cross-capacitance can be tested simultaneously with the trans-capacitance (the ordinary biplanar capacitance surrounded by a guard capacitor). With this structure it was found for the cross-capacitance that:

- The sum of the two cross-capacitances was 0.15 pF.
- The temperature coefficient was about 18 ppm/ºC. In Fig. 7-29 the result of a temperature cycle from room temperature to 80ºC, down to -25ºC and back to room temperature is shown.
- The dependence of the capacitance on non-condensing humidity was less then 1000 ppm. Condensing humidity occurred in these experiments at 90% RH at 20ºC and 60% RH at 80ºC.

The temperature coefficient of the cross-capacitance can be explained by the linear expansion coefficient of the printed circuit board material.

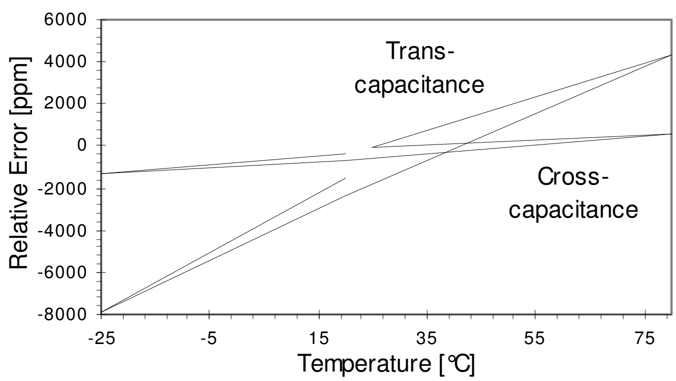

Fig. 7-29 Temperature effects on the circular cross-capacitor and the circular trans-capacitor

For the trans-capacitance (using the same electrode structure but connected differently) it was found that:

- The value of the sum of the two trans-capacitances was 2.5 pF.
- The temperature coefficient was 115 ppm/ºC (Fig. 7-29).
- The dependence of the capacitance on non-condensing humidity was also less then 1000 ppm. Condensing humidity occurred in these experiments at 95% RH at 20ºC and 70% RH at 80ºC.

Since the electrodes are the same ones as used for the cross-capacitance measurement, the high temperature coefficient can not be explained by the change in electrode area. Nor can it be explained by the expansion coefficient of the ceramic spacer (15 ppm/ºC). Therefore it must result from electrode bending, actually causing a displacement of the electrode distance.

The temperature coefficient of this structure is six times too high for our application. However, it can be expected that glueing the electrodes to a rigid substrate made from steel, (as has been suggested in Fig. 7-24 in Section 7.3.1) electrode bending can be prevented and the temperature coefficient sufficiently reduced.

7.5.2 The capacitive force sensing element

A Thermelast spring has been fabricated according to Fig. 7-27 and partially tested. The whole sensor was calibrated at zero force and full scale force (2 N). The linearity of the spring was within the specified range (0.1%). The time constant due to creep was measured to be in the order of 10 s.
However the long term stability and the temperature dependence could not be tested at the time, due to the temperature dependence of the electrode structure.
It can be expected though, that the spring will behave as specified since its behavior depends mostly on well specified material properties.

7.6 Conclusion

A low cost capacitive force sensor has been designed and has been partially realized and tested. The experiments have proven the feasibility of the concept. Expected features of the force sensor are:

- Measuring range of 2 N (static force) with 0.1% accuracy
- Can be operated with a pre-load up to 6 N
- Large temperature range from -25 ºC to +75 ºC
- Manufacturing costs approximately $50
- Robust
- 2 point factory calibration
- Temperature compensation probably not required

Using existing parts like the intelligent capacitive sensor, and the capacitive sensing elements presented in earlier chapters, the performance and cost of the complete system could reasonably well be estimated beforehand. The design of the sensor was then reduced to developing the parts that were new, like the spring.
Similary, for the spring also existing parts were used as a design template. Still the design of precision mechanical parts for a large temperature range remains to be a challenge for the (mechatronics) engineer, while the testing of these parts requires a lot of time.

As has been stated before, at the time of the design an IC for the measurement of capacitance was not available, so the modified Martin oscillator circuit was used. At present, an IC like the Universal Transducer Interface (UTI) can easily replace the discrete oscillator circuit, without the need for a complete redesign, since both circuits belong to the same family (class) of intelligent capacitance measuring circuits. This way costs can be reduced even further.

Another way to reduce costs is to change the specifications for the sensor. If the temperature range would have been smaller (like in consumer electronics) or the requirement for the accuracy would have been relaxed to for instance 1%, the design of the presented sensor can be much simplified and materials with lower costs (like plastics and aluminum) can be used. In fact, such a capacitive (kitchen) weighing scale is brought on the market by Soehnle already, for the price of $40 including batteries and LED display (range 2 kg, resolution 2 g, accuracy not specified).

---

110 Cheshmehdoost, A., B.E. Jones, B. O'Connor, S. Stroumboulis, *"Dynamic characteristics of a resonating force transducer"*, Sensors and Actuators A, 41-42 (1994) 74-77

111 Bethe, K., D. Baumgarten, *"Creep of low-range scales"*, Proceedings of XIth Int. conference on measurement of force and mass, pp. 323-329, May 86

112 Toth, F.N., A.J.M. Bertels and G.C.M. Meijer, *"A low-cost, highly stable reference capacitor for capacitive sensor systems"*, IMTC'95, pp. 412 - 413, April 24 - 25, 1995

113 Toth, F.N., A.J.M. Bertels, G.C.M. Meijer, *"A low-cost, stable reference capacitor for capacitive sensor systems"*, IEEE Trans. Instrum. Meas., vol. 45, no. 2, pp. 526 - 530, April 1996

114 Data sheet, *"Nickel alloys"*, Métalimphy

115 Data sheet, "Thermelast 4002, 5409, 4290", Vacuumschmelze GMBH, February 1972

116 Bethe, K., D. Baumgarten, J. Frank, *"Creep of sensor's elastic elements: metals versus non-metals"*, Sensors and Actuators A, A21-A23 (1990) 844-849

117 Baumgarten, D., "Bestimmung der elastischen nachwirkung von metallischen und nichtmetallischen federwerkstoffen im kriechversuch", Ph.D. Thesis, Technischen Universitaet Carolo-Wilhelmina zu Braunschweig, 1989

118 Wolffenbuttel, M.R., P.P.L. Regtien, *"The accurate measurement of a micro-mechanical force using force-sensitive capacitances"*, IEEE Trans. Instrum. Meas., vol. 44, no. 2, pp. 188 - 191, 1995

119 Toth, F.N., G.C.M. Meijer, *"A low-cost, smart capacitive position sensor"*, IEEE Trans. Instrum. Meas., vol. 41, no. 6, pp. 1041-1044, Dec. 1992

120 Toth, F.N., H.M.M. Kerkvliet, G.C.M. Meijer, *"A very accurate measurement system for multi-electrode capacitive sensors"*, IEEE Trans. Instrum. Meas., vol. 45, no. 2, pp. 531 - 535, April 1996

8

DESIGN OF A CAPACITIVE LIQUID LEVEL GAUGE

Many different types of liquid-level sensors are used throughout the industry. In some cases these sensors are merely used to set an alarm when the level in a storage tank is above or below a specified level. In other cases the measured level is used to accurately calculate the volume or even the mass of the liquid that is present in the tank. A level sensor can even be used to detect a leak in the tank that causes an undesired flow of liquid into or out of the tank.
As a result, numerous types of liquid level sensors and detectors are available on the market, based on every conceivable physical effect. Examples include:

- Differential pressure sensors. The difference of the pressure at the bottom and the top of the tank is related to the liquid level and its specific mass density.
- Float type level sensors. The position of the float in its turn can be measured by measuring the length of the wire from which it hangs, or by using it as a mirror in combination with a laser interferometer, etc.
- Radar or sonar sensors. The position of the interface relative to a position at the top of the tank can be measured by measuring the delay time of a pulse or another waveform reflected by the liquid's surface.
- Capacitive sensors. The permittivity of the liquid causes a change in the capacitance, from which the position of the interface (which must lie between the electrodes) can be calculated.

Often combinations are made to form a sensor system that is suitable to automatically measure level, specific mass density, volume and mass, for instance by combining a float type gauge with a pressure sensor.

The sensor presented here is suitable for use in underground storage tanks at petrol stations. These tanks usually contain non-conductive liquids like leaded or unleaded gasoline or diesel.
Sometimes also the level of conductive liquids like water need to be measured, for instance when the fuel is floating on top of a layer of water. The sensor should be able to set an alarm when the water level exceeds a certain limit, while for calculating the net fuel volume the difference of the fuel and water level is required.

Another reason is that in order to calculate the volume from the measured level, a conversion table is required. This table is often obtained by calibrating the sensor by filling the tank with known volumes of water.

Liquid-level gauges are used at petrol stations for several purposes:
- To warn when a new supply of fuel is required.
- To inform the driver of the tank truck of the actual contents of the storage tank, to prevent overflows when filling the tank.
- To check the amount delivered by the tank truck.
- To detect unauthorized withdrawals from the storage tank (like overnight theft).

Also government regulations can lead to a demand for a level gauge:
- The gauges in the fuel pumps need to be regularly calibrated (for tax purposes). A level gauge can be used to check the calibration of the gauges in the pumps.
- Liquid-level gauges can be used to detect leakages in the tank. For this a high resolution is required.

In this chapter a high resolution capacitive sensor is presented, that uses a new low-cost electrode structure. The sensor is able to simultaneously measure the level of both conducting and non-conducting liquids with an equal accuracy.

8.1 Specifications and target costs of the level gauge

An important advantage of a capacitive level gauge is that it is in principle a solid state device that is virtually maintenance free. This is an important aspect for an electronic level sensor since the alternative, manual measurement of the level using a so called 'dip stick', requires periodically opening the tank. The life time of the sensor should in general be relatively long, i.e. longer then 10 years.
The size of the storage tanks can be up to 4 m in diameter and can contain up to 120 m^3 fuel. For a fairly common size, an accuracy of 1 mm translates to a worst case volume accuracy of 20 l, which is acceptable for calibration purposes. Such an accuracy can currently only be obtained by the high end gauges on the market.
For the detection of leaks, generally the tank station is periodically shut down so undesired changes in the liquid levels can be monitored. For instance the EPA (US Environmental Protection Agency) requires a periodic measurement that can detect leak rates of 0.4 l/h with a 95% confidence. This corresponds to a level change of 0.02 mm/h in a 10 m^3 tank. Since shutting down the pumps results to a loss of sales for the owner of the petrol station, the detection of leaks should require as little time as possible. This requires a resolution in the micrometer range as well as a high resolution measurement of the temperature change during the measurement.
For very high resolution measurements care must be taken for standing waves in the tank which often have a frequency around 1 Hz. When the measurement time is around 1 s aliasing effects can occurs that cause the frequency of the standing wave to appear much smaller. As a result the wave can easily be mistaken as a leak. To prevent this the measurement time should be much smaller then 1 s, so the waves will be sufficiently oversampled. When this is not possible, random sampling must be applied. This means increasing the sample time by a value that is randomly chosen between zero and the period of a wave, which can lead to a severe increase of the time required for leak detection.

Specific requirements for all electronic circuits that operate inside fuel tanks (or in the presence of explosive gasses and liquids) have been laid down in safety regulations like *Ex* II. Basically these regulations limit the maximum surface temperature of the device by limiting the total amount of energy stored in it. This leads to requirements for the total maximum capacitance and inductance as well as the maximum supply voltage and current. In our case this leads to a maximum power consumption of 300 mW.
The requirement for the costs of the sensor can again be estimated from the costs of similar sensors that are available on the market. The list prices appear to range from $500 to $2000 per tank depending on the specific features of the sensor. Since the sensor presented here covers the most important features and can therefore be considered to be targeted at the high end of the market, a target list price of $1000 to $1500 seems reasonable. Obviously, the cost of manufacturing must be much lower.
The above requirements are summarized in Table 7-2.

Table 8-1 Target specifications for the capacitive liquid level sensor

Parameter	Specification
Measurement range	4 m
Level accuracy	1 mm
Resolution	0.1 mm
Measurement time	0.2 s
Volume	with appropriate conversion table
Leak detection time	20 min.
Detectable leak rate	0.02 mm/h
Operating temperature	-40 ºC to +60 ºC
Temperature accuracy	1 ºC
Temperature resolution	0.01 ºC
Power consumption	< 300 mW
Liquids	All car fuels as well as water and methanol M85
Diameter	< 50 mm
MTBF	> 10 years
List price	<< $1500

8.2 Concept of the system

The system is again based on the intelligent capacitive sensor object model and the resulting data flow diagram discussed in Section 4.3. The resulting data flow diagram is shown in Fig. 8-1.

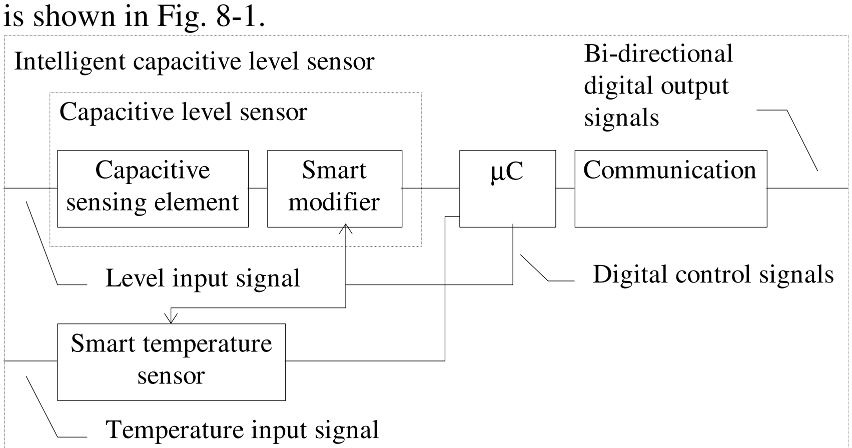

Fig. 8-1 Data flow diagram for the intelligent capacitive level sensor system

The design of the sensor is now simplified to finding a suitable physical effect of the liquid level interface on capacitance. Then a suitable capacitive sensing element can be selected or derived from the types discussed in Chapter 3 as well as a suitable Smart Capacitance Modifier from Section 6.5.

A biplanar capacitor surrounded by a guard ring (Fig. 8-2a), that is partially filled with two substances that are separated by an interface (Fig. 8-2b), has a capacitance that is equal to the capacitance in vacuum times the weighted dielectric constants of the substances

$$C = \varepsilon_o \left(\frac{\varepsilon_{r1}\, x\, l\, w}{d} + \frac{\varepsilon_{r2} (1-x)\, l\, w}{d} \right) = \varepsilon_0 \frac{l\, w}{d} \left(x\, \varepsilon_{r1} + (1-x)\, \varepsilon_{r2} \right) \tag{8-87}$$

with x the relative position of the interface. This physical effect will be used as a basis for the sensing element.

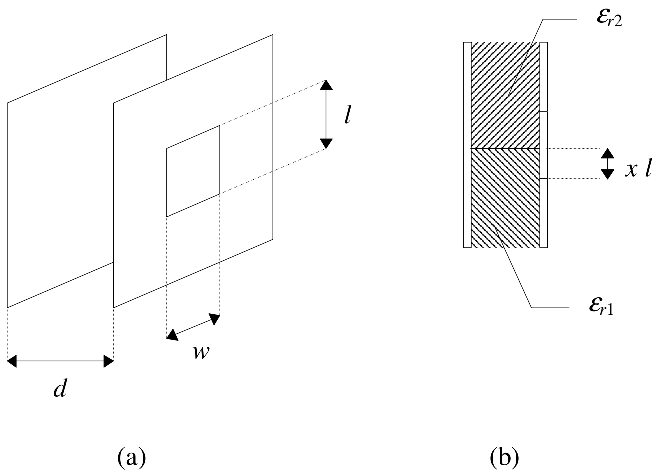

Fig. 8-2 Biplanar capacitor filled with two substances (a) perspective (b) cross-section

It can easily be shown that Eq. (8-87) not only holds for the biplanar capacitor with guard ring, but for every electrode structure where the capacitance is proportional to the segment length l.

8.3 Design of the electrode structure

To calculate the relative position x of the interface, the capacitance in vacuum as well as both dielectric constants must be known. Alternatively a multi-electrode structure can be used.

8.3.1 Biplanar multi-electrode structure

The multi-electrode structure in Fig. 8-3 consists of a long electrode (E_0) and one that is divided into insulated segments (E_1 to E_n). The relative position of the segmented electrodes is fixed by the mechanical construction, while the absolute position requires a one-time calibration (for the offset).

The capacitances C_{i-1} to C_{i+1} between electrodes E_{i-1} to E_{i+1} and E_0 can be measured sequentially (with respect to a reference capacitor C_{ref}), while the other electrodes are used as guard electrode and are connected to ground. As a results all electrodes are connected to a low impedance at all times.

When we assume that the capacitances in vacuum are equal, with value C, a calibration for the electrode area and distances is not required. But in practice it might prove to be difficult to realize the electrode structure in such a way that the offset capacitance for all the capacitances is equal. This offset capacitance might be caused by imperfect shielding on the "back-side" of the electrodes. It that case the relative capacitance values can be calibrated using values that are determined in the factory.

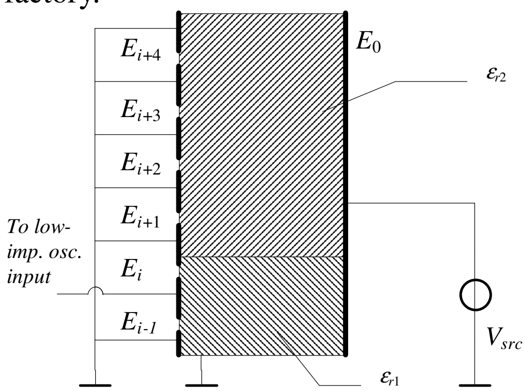

Fig. 8-3 Multi-electrode structure where C_i is measured

In Fig. 8-3, C_{i-1} has a value of ε_{r1} C and C_{i+1} has a value of ε_{r2} C. The interface level can be calculated by finding the interface segment i, which has a value between C_{i-1} and C_{i+1}. Then the capacitance of the interface segment C_i can be interpolated to find the interface position p accurately:

$$p = l \cdot \left(\frac{\frac{C_i}{C_{ref}} - \frac{C_{i+1}}{C_{ref}}}{\frac{C_{i-1}}{C_{ref}} - \frac{C_{i+1}}{C_{ref}}} + i \right) = l \cdot \left(\frac{C_i - C_{i+1}}{C_{i-1} - C_{i+1}} + i \right) \tag{8-88}$$

Using this algorithm means that the minimum layer thickness that can be measured is also l. The minimum layer thickness determines the minimum and maximum level that can be measured, since when the tank is nearly empty or nearly full C_{i-1} or C_{i+1} respectively, does not exist. It is also important when multiple interfaces are present, for instance in the case of fuel floating on top of water, since with layers that are thinner then l, the value of the reference measurements C_{i-1} or C_{i+1} will be influenced by the position of the interface. A small value of l is therefore advantageous.
Another reason to choose a small value for l is that the required relative accuracy of the capacitance measurement will also be smaller, as will be the influence of electrode contaminations on the measurement result.
However, the smaller the value of l, the more electrode segments are required, as well as switches to select them, and thus the higher the costs. For instance, with a length of the electrode structure of 4 m and a value of 2 mm for l, the number of segments will amount to 800.

8.3.2 Interface between a conductive liquid and a non-conductive liquid or gas

Up to now, an interface between two non-conductive substances was assumed. An example of such an interface is that between diesel and air (which is possibly saturated with diesel vapor). The sensor should also be able to measure interfaces between a conductive liquid and a non-conductive liquid or gas, for instance a water-air or water-diesel interface. Also methanol can be assumed to be conductive because it is highly hygroscopic and can easily absorb up to 5% water from the air in the storage tank.

To measure conductive liquids like water, the electrodes need to be covered with an isolator. This material also protects the electrodes against the possibly aggressive liquids (as is the case with methanol). However, the presence of this coating will also cause some electric field bending around the interface, both when conducting and non-conducting liquids are measured.

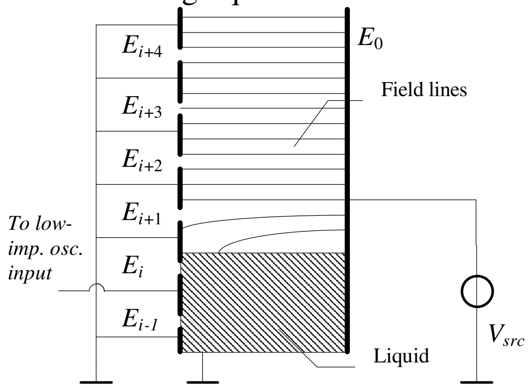

Fig. 8-4 Conductive liquid connected to ground

This can be explained by assuming a parallel plate electrode structure, covered with an infinitely thin isolator. In this case the conductive liquid can be regarded as a shield (Fig. 8-4) that is connected to ground. The capacitance between a single electrode segment E_i and the opposite electrode E_0 can be calculated as a function of the interface level. The non-linearity in the characteristic is caused by field-bending effects.
In the case of non-conductive liquids a similar effect occurs but in this case the non-linearity is symmetrical around the center of the interface segment.

It is important to note that this non-linearity only occurs when the interface is near the edge of the interface segment. This means that by connecting a suitable number of segments around the interface in parallel (so the interface is always near the middle of the thus formed larger segment) this effect can be eliminated for non-conductive liquids (due to the symmetry), while for conductive liquids only a constant offset will remain.

8.3.3 Uniplanar multi-electrode structure

The parallel plate electrode structure has the advantage of a simple physical structure. However, the costs of constructing such a structure with a constant electrode distance over a length up to 4 m are considerable.
To reduce costs, the transmitting electrode segments and the receiving electrode can be integrated on the same substrate. Shi *et. al.* [121] presented a structure where electrode E_0 is removed and the capacitances are measured between the successive electrodes E_i and E_{i+1}. This method leads to a rather complex model to retrieve the level from the measured capacitances. An alternative approach is to integrate electrode E_0 also on the same substrate. Such a structure has been suggested previously by Heerens *et. al.* [122]. The prototype presented there was a circular version with the electrodes on the outside of a glass tube, which is also not very suitable for low-cost manufacturing. By projecting this circular structure on a plane, a planar electrode structure has been obtained (Fig. 8-5).

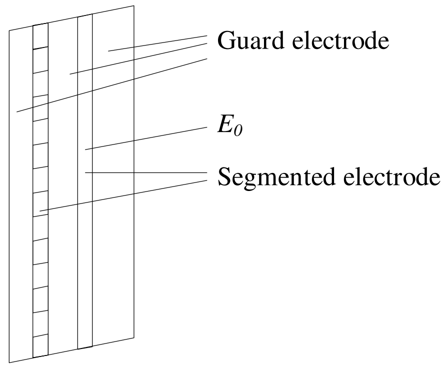

Fig. 8-5 Novel planar electrode structure

To reduce the effect of non-idealities near the electrode surface (like water droplets), a thin guard has been placed between the segmented electrodes and the common electrode. The resulting capacitance in air is only 2 fF/mm. To optimize the use of the available area (and to obtain a more evenly distributed sensitivity), the whole structure is duplicated which results to 3 capacitances that are connected in parallel. The resulting segmented electrode structure has a capacitance of about 6 fF/mm in air and 12 fF/mm in unleaded fuel.
Note that the electrode structure is a descendent of the uniplanar square-strip electrode structure in Section 5.2.3 and therefore the capacitance between each electrode square and each strip can easily be calculated by applying Eq. (5-23).

8.4 Smart capacitance modifier

To achieve the required measurement time of 0.2 s an intelligent measurement algorithm is required. Not all capacitance contain relevant information about the liquid level. As a result only the capacitances around the interface need to be measured.
The most important tasks for the capacitance measurement system are to select the correct capacitance, to eliminate the effect of the large parasitic capacitances caused by the long wires and to convert the capacitance to a form that is compatible with a microcontroller input.

The intelligent capacitance measurement object meets these requirements again. A capacitance controlled oscillator may be used to convert the selected capacitance value to a periodic signal. A microcontroller is used to measure the period and convert the value to a relative capacitance value using the 3-signal approach. If necessary the (relative) capacitance values are then calibrated using factory determined values that are stored in EPROM. The microcontroller can also determine which capacitances to measure. It will start by searching for the interface capacitor by sequentially measuring all capacitances. But once the interface capacitor has been found only the three capacitors around the interface need to be measured to track the interface position.
The microcontroller can then use the value for the interface position to calculate the volume or the leak rate.

At the time of the experiments the multiple-sensor modulator was not yet available, so the modified Martin oscillator (Fig. 8-6) was used. The modified Martin oscillator had the advantage that it could be built using discrete components. However with the commercial availability of the multiple-sensor modulator even better results can be expected at even lower costs.

The operation of the modified Martin oscillator has been explained in detail in Section 6.5.2. but will be briefly repeated here:

> The circuit is based on a switched-capacitor oscillator presented by Martin [123] with the switched capacitor replaced by a resistor. The period of the oscillator has a linear relationship between the capacitance and the period. Using a multiplexer that is controlled by a microcontroller, as has been suggested by Toth and Meijer [124], [125], the capacitances C_{off}, $C_{off} + C_{x,1}$ and $C_{off} + C_{x,2}$ can be selected independently. This results to the periods T_{off}, $T_{x,1}$ and $T_{x,2}$, respectively. The microcontroller measures the period of the oscillator and calculates the capacitances. By applying the three-signal autocalibration technique,
>
> $$\frac{C_{x,1}}{C_{x,2}} = \frac{T_{x,1} - T_{offset}}{T_{x,2} - T_{offset}} \tag{8-89}$$
>
> all additive and multiplicative errors are eliminated.

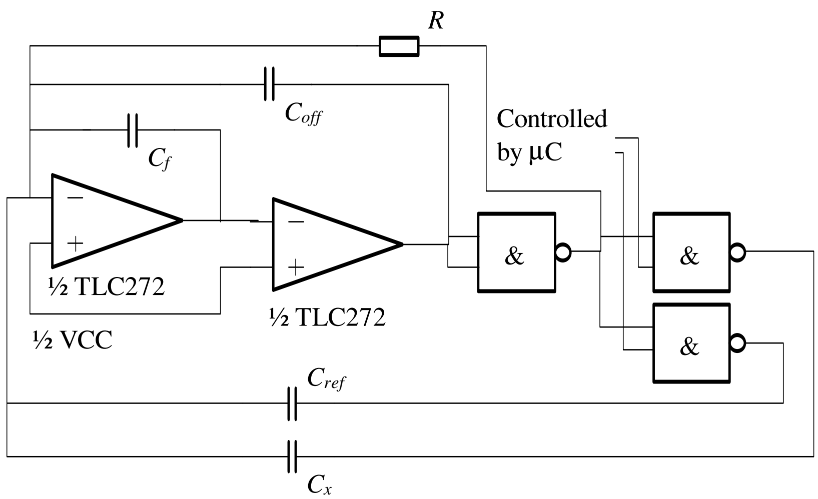

Fig. 8-6 The modified Martin oscillator

> This system measures capacitances of 100 fF with an accuracy of 50 aF with respect to the reference capacitor. The influence of grounded parasitic capacitances up to 800 pF is reduced to an insignificant level.

The multiplexer consists of the NAND gates, that require a wire per gate to select them. For the selection of large number of electrodes, as is the case here the number of wires to the microcontroller must be reduced.
The microcontroller has been programmed to select the appropriate capacitances, to calculate Eq. (8-89), to search for and track the interface segment i and calculate the interface position x. A PC is used to query the calculated position and store it to disk.

8.5 Capacitance multiplexer

All the smart capacitance modifiers incorporate a part that that has not been discussed in detail up to now: a multiplexer. This component is required to be able to perform the 3-signal approach. This means that the modifier must be able to

sequentially select the capacitance under test, the reference capacitor or neither, in such a way that the linear relation between the capacitance and the output signal of the modifier does not change. The selection of the capacitance that is measured can be controlled externally by the (digital) control signals of the microcontroller.
Typically the multiplexer consists of electronic switches, which can be simplified to digital gates (for instance a NAND gate) when the voltages applied to the capacitances are limited to TTL levels. This is the case for the modified Martin oscillator, the multiple sensor modulator and the smart charge redistribution modifier. To reduce the number of wires to the electrode structure the switches will need to be placed near the segmented electrodes, while a serial signal is preferred to turn on the desired switch. This can be realized by using an addressable switch, for instance by using a bus protocol like I^2C or IS^2. The advantage of this approach is that the switches can be accessed at random. However, the address recognition logic will then be duplicated in each switch. Given the large number of switches, the cost of randomly accessible switches is too high for this sensor.
Sequential accessibility can be achieved at much lower costs, by applying a shift register (Fig. 8-7). A certain electrode can be selected by shifting a “1” to the respective NAND gate. This also has the advantage that the number of electrodes can easily be extended by adding additional shift registers. Given the small propagation delay of CMOS shift registers, the time required to randomly select a certain capacitor will be determined by the speed at which the microcontroller can generated the shift pulses, which is several μs when an INTEL 8051 series microcontroller is used. As a result, the selection time for (pseudo) random access will be in the order of several milliseconds, which is acceptable compared to the measurement time per capacitor (tens of milliseconds).

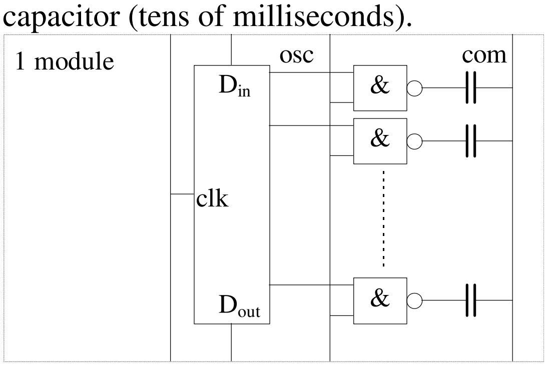

Fig. 8-7 Multiplexer circuit for capacitances

In this way a modular electrode structure may be created from printed circuit board, with a fixed length and a fixed number of electrodes. Depending on the desired length of the sensor, the appropriate number of electrode modules can be cascaded to form the final electrode structure.
Since the diameter of the sensor is limited to 50 mm, the number of connections that can be made from module to module is limited to a maximum of about 10. Using the proposed multiplexer, 2 wires are required for the selection of the electrodes (D_{in} and clk), 2 for the power supply, 1 for the oscillator (osc) and 1 for the common electrode (com).

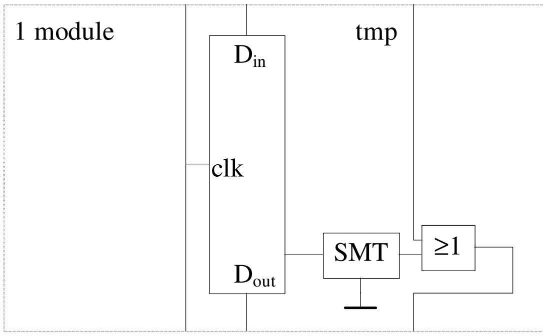

Fig. 8-8 Multiplexer circuits for Smartec temperature sensors

Finally, the same shift register can be used to select the temperature sensors (Fig. 8-8). When smart temperature sensors (SMS) are used (with a TTL duty-cycle modulated output) no extra circuitry is required except an OR gate to tie the outputs of several temperature sensors together. This way only 1 additional wire is required for the temperature measurements resulting to a total number of wires of 7.

8.6 Temperature measurement

The measurement of temperature can be realized in several ways to obtain an accuracy of 1 ºC. However, the temperature in a large storage tank with a diameter of 4 m is not likely to be equal at all points. To be able to measure the temperature distribution above and below the interface, temperature sensors will need to be placed at several points on the electrode structure.
Given the intelligent sensor concept, the choice for a temperature sensor with a microcontroller compatible output seems evident. At this moment only one device exists that has a microcontroller compatible output (duty-cycle modulation) and the required accuracy and resolution at minimal costs: the SMT130 from Smartec. The absolute accuracy of this device is specified at ±0.7 ºC while resolutions of 0.01 ºC can easily be obtained.

8.7 Experimental results

The concept has been tested in an experimental setup, with 2 electrode modules of 48 capacitors each fabricated from multi-layer printed circuit board (PCB). The length of each of the capacitors was about 8 mm. The PCB's are glued to a glass filled plastic carrier to accurately fix the position of the electrodes. The switches that are required to select the appropriate capacitors are mounted on the back side of the PCB's. One of the layers is connected to ground, shielding the electrodes from the switches.
The resulting capacitance in air was about 45 fF and in unleaded fuel about 95 F. The PCB tolerances resulted to tolerances in the capacitances of about ±1 fF, except for the capacitors at the end of each module, that appeared to have an offset capacitance of about 10 fF due to an unfortunate placement of via's on the PCB. For this reason, the offset values were determined using a one-time calibration and stored in the microcontroller's memory.

Then the effect of field bending was measured for conductive (Fig. 8-9) and non-conductive liquids (Fig. 8-10).

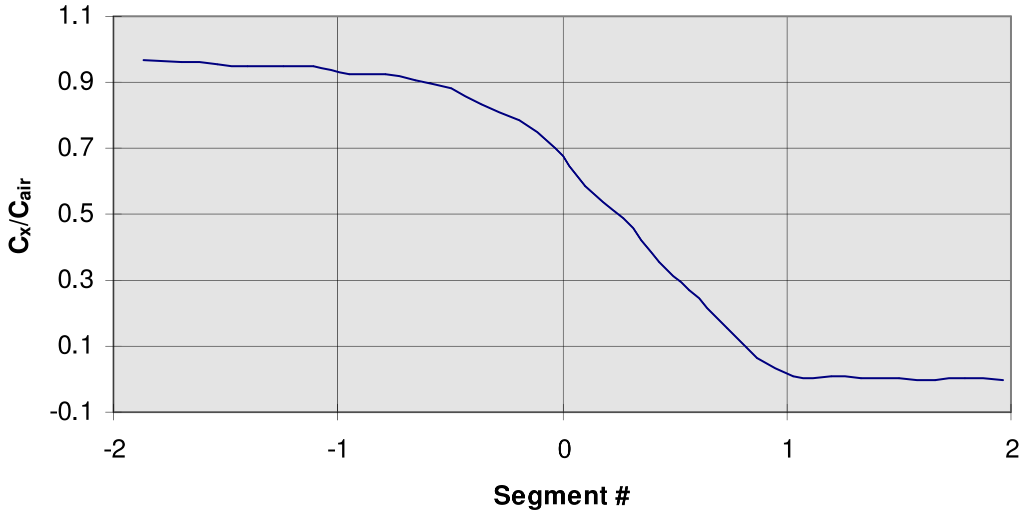

Fig. 8-9 Measured capacitance ratio versus interface level for conductive liquids

For conductive liquids (tap water) we can see that when the electrode is completely covered with liquid (Level below Segment 0) that the capacitance is very near to zero. When the capacitance is completely uncovered (Level above Segment 1) the relative capacitance approaches 1 (the capacitance of air) the further the interface is away. In between the curve is S-shaped, with a linear region in the middle. It can be shown that by switching more segments in parallel (effectively creating a segment with a larger length) the linear region is extended to a region larger than one segment length. This way the interface segments can always be chosen in such a way that the interface is in the linear region. As a result, the non-linearity will be reduced to an insignificant level. The asymmetry of the curve in Fig. 8-9 merely causes an offset that can be calibrated in the factory.

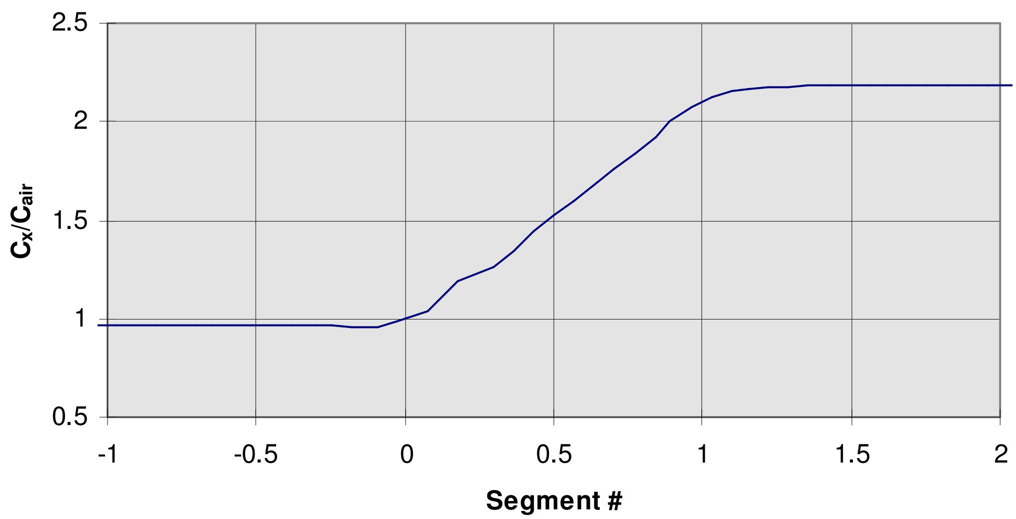

Fig. 8-10 Measured capacitance ratio versus interface level for non-conductive liquids

For non-conductive liquids a similar curve has been obtained. In Fig. 8-10 the results are shown for unleaded car fuel (Euro super). The non-linearity can be reduced in a similar way as for conductive liquids. In this case however, no offset arises due to the symmetry of the curve.

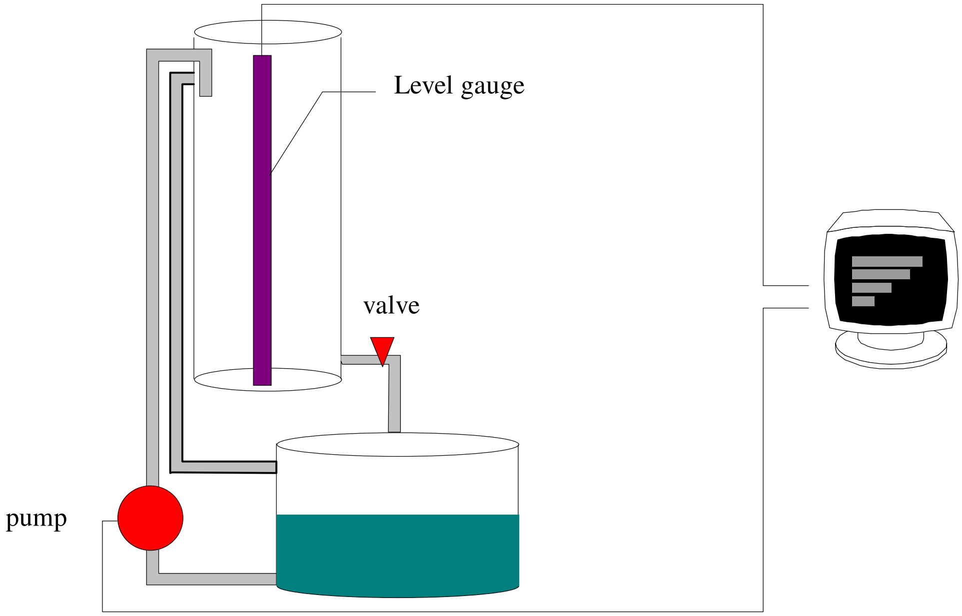

Fig. 8-11 Experimental setup

A fully automated measurement setup has been constructed (Fig. 8-11), to test several different types of car fuels like unleaded super, diesel and tap water. The setup consists of a vertical tank with a height of 1.2 m containing 0.01 m^3 liquid. At the bottom of the tank, is a valve that is connected to the reservoir. A computer controlled pump, pumps the liquid back from the reservoir to the tank.

When the valve is opened slightly, the liquid level decreases from about 500 mm to 160 mm in about 2 hours, following a parabolic curve as a function of time. The PC is used to store the measured level every 2 seconds.

By fitting a second order polynomial, the error can be determined as a function of the level (Fig. 8-12).

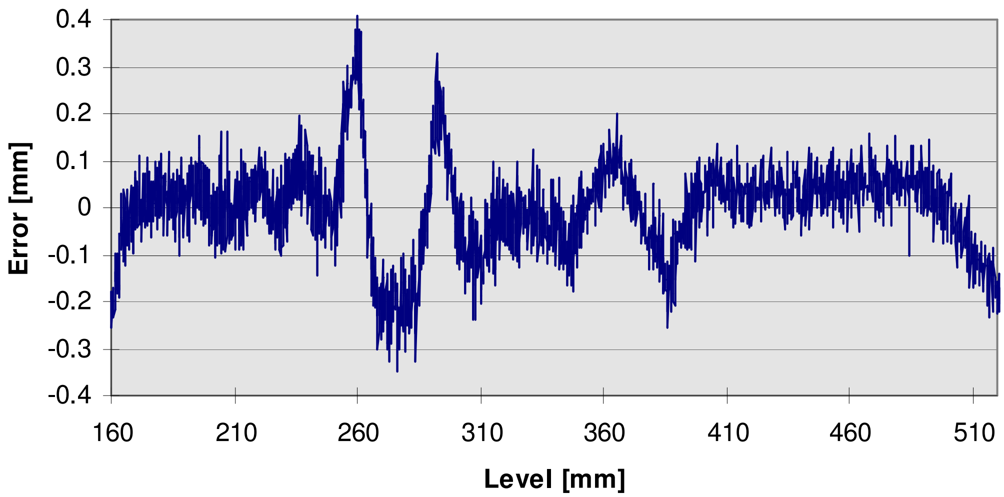

Fig. 8-12 The total error for Euro Super over a measurement range of 300 mm

The errors that occur when the level is around 280 mm where reproduced in subsequent measurements and could be traced back to the calibration values of each of the capacitances. Apparently some change in the capacitance has occurred after

calibration, for instance by the presence of tiny water droplets on the electrode structure.
Due to the fitting process, the calculated error excludes the absolute position offset (which is determined by a factory calibration), the scale error (which is determined by the lithographic process used for the PCB and by the thermal expansion coefficient) and the second order term (which can be assumed to be negligible).
With Euro Super, the remaining error is less than ±0.4 mm, while the resolution (σ) is about 0.03 mm with a 0.2 s total measuring time. With tap water and diesel similar results have been obtained.
It can easily be calculated that when this system is used for leak detection in a 10 m^3 tank, a 0.02 mm/h level change (caused by leak) can be detected in only 18 min. For a 10 m^3 tank this corresponds to a worst case leak rate of 0.4 l/h (as is required by the EPA).

The measurements clearly demonstrate the feasibility of the proposed sensor. Using the design presented here as a starting point, the requirements presented in Table 7-2 for the accuracy, resolution, measurement time and leak detection should be easily obtainable. Also it can be expected that the required list price should be obtainable using the proposed low-cost electrode structure and electronic circuitry. Also the cost of the development of the embedded software should not increase the costs dramatically, as long as the functionality is restricted to the requirements specified in Table 7-2.

Requirements in Table 7-2 that have not been tested include the Mean Time Between Failure (MTBF), the actual time required to detect leaks and the effects of other than regular car fuels or tap water (like methanol M85).
Although the requirements for the power consumption were met, the present design did not include a (FLASH) EPROM, which is necessary to store the software, calibration constants and volume conversion table. At the time of writing, FLASH EPROMS that operate on 5 V only are known to consume 500 mW during an erasure cycle, which is more then the whole sensor is allowed to consume. As a result part of the circuitry will need to be designed for either 3 V (for which FLASH EPROMS are available that consume less then 150 mW). An alternative is to allow the sensor to be removed from the tank during programming (which is probably unacceptable).

8.8 Conclusion

A low-cost capacitive liquid level sensor has been designed and an experimental version has been realized and tested. The experiments have proven the feasibility of the concept. Measurement results show:

- Accuracy of 0.4 mm over a 720 mm range (excluding factory offset calibration)
- Resolution 0.1 mm with a measurement time of 0.1 s per interface
- Suitable to measure conductive and non-conductive liquid levels simultaneously

The sensor has been tested with Euro super, diesel and tap water over a temperature range from 5 ºC to 25 ºC. A one-time factory calibration of the capacitances in water and air was performed to eliminate offset capacitances on the “back-side” of the electrode structure.

Using existing parts like the intelligent capacitive sensor, and a capacitive sensing element based on the uniplanar square-strip capacitor presented in earlier chapters,

the performance and costs of the complete system could be reasonably well be estimated beforehand. The design of the sensor was then reduced to developing the parts that were new, like the mechanical construction and the software algorithms.
Of course for the software algorithms also existing parts were used as much as possible, for instance the software routines for communication and period measurement remain basically unchanged from those used in other capacitive sensor designs. On the other hand much time was required to actually realize the sensor and the experimental setup. For a large part this is caused by the large effort required to produce a single device (as compared to series production) and the effort required to create an intrinsically safe experimental setup.

As has been stated before, at the time of the design an IC for the measurement of capacitance was not available, so the modified Martin oscillator circuit was used. At the present time, an IC like the Universal Transducer Interface (UTI) can easily replace the discrete oscillator circuit, without the need for a complete redesign, since both circuits belong to the same family (class) of intelligent capacitance measuring circuits. This way costs can be reduced even further.

The largest reduction in costs can be obtained by optimizing the construction even further for series production, since the costs of materials and electronic components in the present design are substantially lower then the costs of assembling them.

---

121 Shi, T.M., M.S. Beck, S.M. Huang, R.A. Williams and C.G. Xie, *"Capacitance-based instrumentation for multi-interface level measurement"*, Meas. Sci. Technol., vol. 2, no. 10, pp. 923 - 933, Oct. 1991

122 Heerens, W. Chr., G. Keizer and F.W. Wedman, *"Theory and practice of multi-terminal capacitor bar and tube sensors for chemical and physical process applications"*, Proc. Sensor'83, vol. 5, pp. 27 - 40, Basel, 17 - 19 May 1983

123 Martin, K., *"A voltage-controlled switched-capacitor relaxation oscillator"*, IEEE J. Solid-State Circuits, vol. 16, no. 4, pp. 412-413, Aug. 1981

124 Toth, F.N. and G.C.M. Meijer, *"A low-cost, smart capacitive position sensor"*, IEEE Trans. Instrum. Meas., vol. 41, no. 6, pp. 1041 - 1044, Dec. 1992

125 Toth, F.N., H.M.M. Kerkvliet and G.C.M. Meijer, *"A very accurate measurement system for multi-electrode pF-range capacitors"*, IEEE Trans. Instrum. Meas., vol. 45, no. 2, pp. 531 - 535, Apr. 1996

9 DESIGN OF A CAPACITIVE PERSONS DETECTOR

Entrance counters are used in many public places. Often a double light switch is used, which enables the detection of the direction of the passing persons. However, these light switches can easily be destroyed by vandalism. Other well known principles are:

- Infrared movement detectors
- Sonar and microwave detectors
- Television cameras
- Mechanical switches

The cost of most of these systems (except the mechanical switch type) is in general rather high, while the reliability is not very impressive.
To improve the reliability, the more advanced systems utilize more types of sensors, which increases the cost even further [126].

In this chapter the design of a low-cost capacitive persons detector is discussed. The detector is less sensitive to contamination as compared to optical detectors [127]. Furthermore, the construction can be made more robust. Although the sensor is optimized for human adults, is can easily be adapted to suit the detection of for instance children or animals.

We start by defining possible specifications for such an entrance detector in Section 7.1. Then the system concept is described in Section 9.2. In this section a model describing the capacitance changes for various types of persons is derived. The calculated capacitances are compared to measurement results. It will be shown that even though the capacitance changes are in the order of only 0.1 pF, it is possible to realize a reliable system at low costs using a first-order relaxation oscillator that is connected to a microcontroller.
In Section 9.3 the non-idealities that are specific to capacitive person detectors are analyzed. These non-idealities would limit the application of a capacitive person detectors to just detection, although position information is present in the sensing elements output signal.
In Section 9.4 the possibility to estimate the persons position using fuzzy logic is discussed.

To demonstrate the feasibility of the concept, two experimental person detectors have been realized. The first sensor that has been designed utilizes three transmitter and one receiver electrodes. This system is capable of estimating the position of up to three persons and could therefore find use in safeguarding automatically working machines [128]. Fuzzy logic is used to minimize the number of floating point operations and thereby to speed up the signal processing [129]. In this way, even with low-cost microcontrollers, a fast position estimation can be achieved. The reliability of the method will be discussed.
The same electronic circuit and microcontroller are used in a simplified design using only two transmitter and one receiver electrodes. Since this sensor is capable of measuring both the presence of a person and the direction of movement, it is very suitable as an entrance detector or counter.

9.1 Specifications and target cost of the sensor

The required reliability of person detectors depend very much on the cooperation of the subjects. This can easily be seen from the following examples:

- In the case of burglary alarms not every person needs to be detected, but the person that definitely must be detected (the burglar) will take every possible action to prevent detection. The cooperation of the subject in this case is very low.
- In the case of a pedestrian-crossing light the person wants to be detected so the light will change to green. The person will therefore be inclined to press the button (a mechanical switch). In this case the cooperation is very high.
- In the case of persons detectors that are used for safeguarding in industry (for instance switching of robots in the presence of a person) cooperation of the subject depends on the sensitivity of the detector. Operators are known to switch off devices that are installed for their safety and which they perceive as overly sensitive.

The first sensor presented in this chapter, might find use to safeguard robots. When an operator comes to close in the proximity of the robot it may be switched off or return to a safe position. The chance of a false alarm in such a sensor should be as small as possible to ensure the operators confidence and cooperation. For the purpose of demonstrating the principle we will assume a cost in the order of $100
The second sensor, a capacitive entrance detector that could be used for instance in subway stations, does not require a very high accuracy. Apparently an accuracy higher then 80% would be acceptable. Also the cooperation of most persons can be assumed to be relatively high. On the other hand, the possibilities for vandalism should be small. As a result, the costs of installing these sensors might dominate the total costs when the costs of the sensor itself will be less then $50.

9.2 Concept of the system

The principle is based on the fact that the human body consists of a large percentage of water. This can be used to cause a change in the dielectric of a capacitive sensing element that can be detected (ε-type capacitive sensor).

9.2.1 Physical aspects

We will assume that we can model a person passing the detector to behave (electrically) as a conductor that moves through the electrode structure. The persons shoes are assumed to isolate his body from the ground plate, although this is not a requirement. A simplified model is shown in Fig. 9-1.

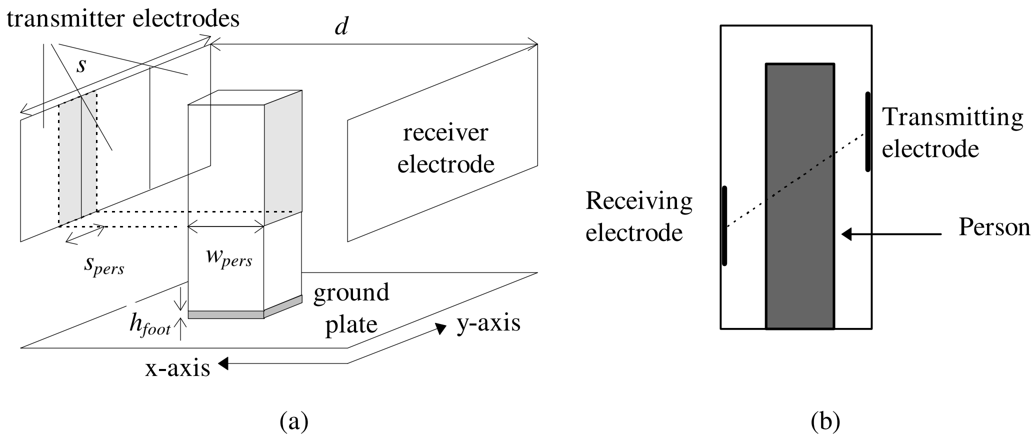

Fig. 9-1 Simplified model of the electrode structure, (a) perspective of the position sensor (b) cross-section of the entrance detector

For the entrance detector, a minimum of two transmitting electrodes is required to determine the direction of the passing person. It has been assumed that the entrance detector will be incorporated into a gate, through which the person walks. The distance between the transmitting electrodes and the receiving electrode is chosen wide enough for one person to pass through (Fig. 9-1b). To optimize the change in capacitance when a person passes the detector, the transmitting electrode has been placed higher then the receiving electrode.

For the position sensor, the distance between the receiving and transmitting electrodes is wider, so that a person can move freely around between them. This decreases the position accuracy of the sensor. To improve the accuracy, three transmitting electrodes are used, as is shown in Fig. 9-1a. In this case, placing the electrodes at different heights does not improve the sensor response significantly.

9.2.2 Capacitance model

To reduce the effect of parasitic capacitances $C_{par,1}$ and $C_{par,2}$ in the connecting cables (Fig. 9-2) the electrodes must all be connected to either a low-impedant voltage source V_{src}, a low-impedant input of the measurement system or to ground (a 2-port measurement). We can also assume the conductivity of a persons body to be high enough so that it can be considered an electrode at a constant potential. Now we can derive an electrical model of the system.

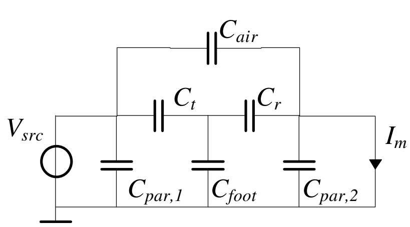

Fig. 9-2 Simple electric model of the structure

In Fig. 9-2, C_t is the capacitance from one of the 'transmitting' electrodes to the person, C_r from the 'receiving' electrode to the person, C_{foot} the capacitance from the persons feet to the ground plate and C_{air} the parasitic capacitance from the transmitting electrode to the receiving electrode. Note that C_{air} has a different value when there is no person present between the electrodes.

The capacitances can be estimated from Fig. 9-1 by

$$C = \frac{\varepsilon_0 \varepsilon_r A}{d} \tag{9-90}$$

with A the effective area and d the distance. The measured capacitance is then

$$C_m = C_{air} + \frac{C_r C_t}{C_r + C_t + C_{foot}} \tag{9-1}$$

9.2.3 Capacitance measurement and the intelligent sensor concept

The sensor is again based on the intelligent capacitive sensor object model and the resulting data flow diagram discussed in Section 4.3. From this the data flow diagram is shown in Fig. 8-1 is derived.

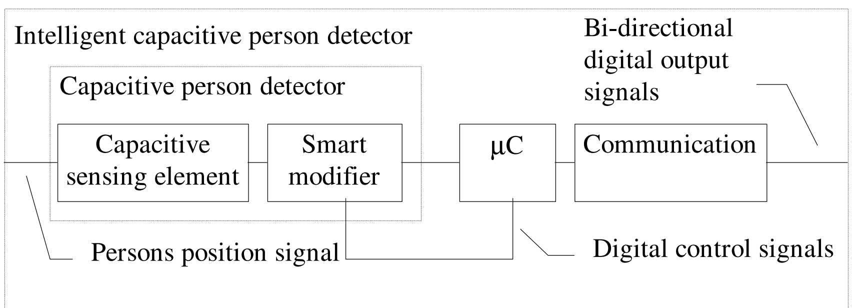

Fig. 9-3 Data flow diagram for the intelligent capacitive person detector

The capacitive sensing element is connected to the smart modifier, a first-order capacitance dependent oscillator presented by van der Goes [130, 131] and commercially available under the name Universal Tranducer Interface (UTI from Smartec [132]). This one-chip solution has a built-in multiplexer, so that up to 3 capacitances can be measured with respect to a (external) reference capacitor. The period of the oscillator signal can easily be measured by a microcontroller (µC). The µC can at the same time calculate the ratio of the selected capacitances with respect to the reference capacitor C_{ref}, while eliminating the internal offset capacitance, by using the 3-signal autocalibration method

$$\frac{C_x}{C_{ref}} = \frac{T_x - T_{off}}{T_{ref} - T_{off}}\,. \tag{9-2}$$

In the case of the entrance detector, the µC continuously determines the nominal value of the two electrode capacitances and detects changes from these values. The direction can be determined from the capacitance that changed first.

The more advanced position sensor tries to calculate the persons position from the three capacitance values. This also gives the possibility to detect up to three persons between the detector. Fuzzy logic has been applied to reduce the μC's calculation time by eliminating floating point operations.

9.3 Non-idealities

Several non-idealities result from the measurement system such as sample-rate effects, quantization and thermal noise and electromagnetic interference. Other non-idealities result from incomplete modeling or unknown properties of the detected person.

- Sample-rate effects

Sample-rate effects are caused by the finite measurement, calculation and communication time and the speed of the person. The minimum required sample rate follows from the maximum speed of the person and the size of the detector. By multi-tasking the operations in the μC, the sample rate can be increased (although the total measurement remains the same). The sample rate is then determined by the largest of the three. When floating point calculations are required, the calculation time can easily be larger than 10 ms using a low-cost Intel 8051FA processor.

- Quantization and thermal noise.

Several capacitance measurements have to be performed for each sample. The limited measurement time results to both quantization and thermal noise, of which the former is dominant when using a measurement time shorter than 40 ms (using the built-in timers of a 8051FA μC).

- Electromagnetic interference

Since the electrode sizes need to be quite large the capacitance between them and an electromagnetic interference (EMI) source can be expected to be quite large. This capacitance can not easily be reduced by shielding, since a person should be able to pass between the sensors electrodes. It seems reasonable to assume a capacitance between the EMI source and the receiving electrode that has the same order of magnitude as the capacitance between a transmitting and the receiving electrode.
Fortunately the UTI, which is used for the capacitance measurement has built-in LF interference suppression that is capable of sufficiently suppressing 220 V, 50 to 60 Hz interference.

- Contamination and condensation

Contamination and condensation do not have a large influence on this system since the electrodes and the distances between them are large.

- Incomplete modeling and unknown parameters.

In the model of Fig. 9-1 it is assumed that the electric field is uniform and the person is shaped as a cube. In reality neither of these assumptions are true. Also, the actual size of the person is unknown. Calculations show that the parameters A_{foot}, h_{foot} and w_{pers} influence C_m only slightly. The influence of the persons position on the x-axis on the ratio C_m/C'_m (the capacitance with and without a person between the electrodes) has also been determined (Fig. 9-4). Calculations show that at certain positions this ratio is near to one, meaning that the sensitivity of the sensor can be zero. However, according to measurements, this effect occurs only when the person walks very near to the electrodes, which can easily be avoided by adapting the construction to prevent persons walking to near to the electrodes.

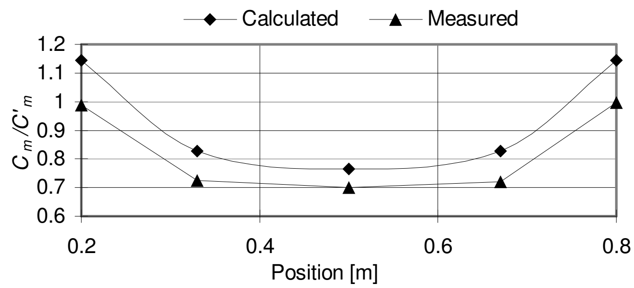

Fig. 9-4 Relative capacitance as function of the position on the x-axis of the person

9.4 Fuzzy logic

To improve the reliability of the position sensor, three electrodes are applied. To efficiently combine these values, while avoiding floating point operations, fuzzy logic has been used.

To this end, each of the measured capacitances C_i (i = 1, 2, 3) are first normalized to their average (empty) values and stored as a one byte value η_i. Then these values are fuzzified, which results to the fuzzy variables M_i with fuzzy groups F(ull), H(alf-full) and E(mpty) (Fig. 9-5).

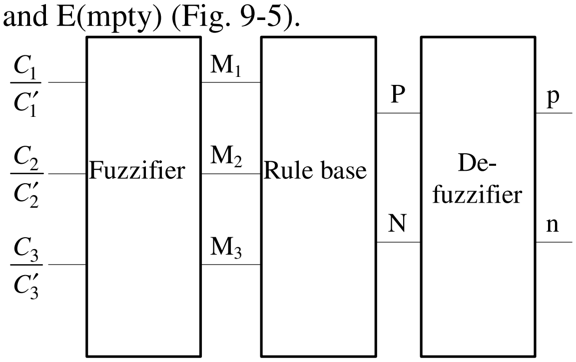

Fig. 9-5 Fuzzy logic data flow

Each fuzzy variable consists of a set of membership values μ_i^F, μ_i^H and μ_i^E, that represent the degree of association according to the memberships function (Fig. 9-6), so M_i = $(\mu_i^F, \mu_i^H, \mu_i^E)$. This membership function has been determined experimentally for our setup.

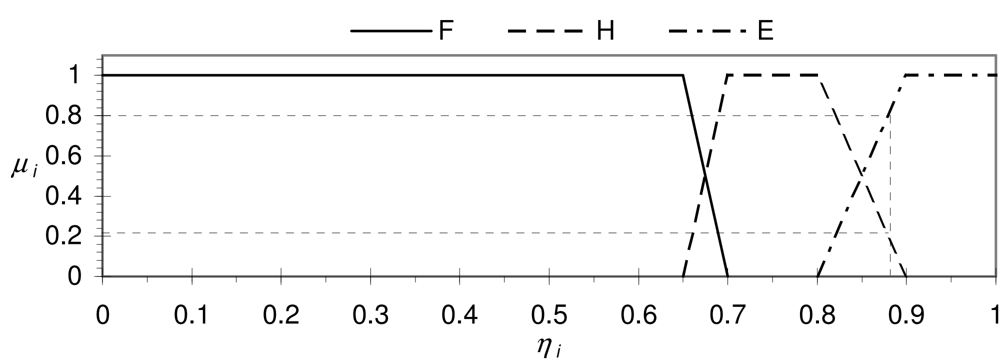

Fig. 9-6 Memberships function of the groups F, H and E

Example:

Lets assume that a person is standing between the electrodes at a position so that the normalized value η_1 of C_1 is 0.88, η_2 of C_2 is 0.87 and η_3 of C_3 is 0.68. In human language this could mean that capacitance 3 decreased significantly compared to its value without a person between the electrodes, while capacitance 1 and 2 decreased only slightly. From Fig. 9-6 we can see that μ_1^F is 0, μ_1^H is 0.2 and μ_1^E is 0.8. This means that the fuzzy variable M_1 has a value of (0, 0.2, 0.8). Likewise, we have M_2 = (0, 0.3, 0.7) and M_3 = (0.4, 0.6, 0), respectively. These values are summarized in Table 9-1.

Table 9-1 Sample values for the normalized capacitances and the resulting fuzzy variables

i	Normalized capacitance η_i	Fuzzy groups		
		F(ull)	H(alf)	E(mpty)
1	0.88	0	0.2	0.8
2	0.87	0	0.3	0.7
3	0.68	0.4	0.6	0

These membership values are fed to the fuzzy system, so the inference process can take place. The inference is based on a table of 27 rules (Table 9-2). One of the advantages of fuzzy logic is that the modeling of the problem can be done using human language.

Example:
When we look at rule 6, we can see that there is an E in column M_1, an H in column M_2 and an F in column M_3. E, H and F again stand for the fuzzy groups Empty, Half-full and Full. The relationship between these column should be read as "and", while the relationship between the various rules (the rows) should be read as "or".
Since M_1 is the fuzzy variable representing C_1 and so on, rule 6 should be read as: "IF M_1 IS E AND M_2 IS H AND M_3 IS F THEN N BECOMES 1 AND P BECOMES 5". In human language this may be read as: "if capacitance one is empty and capacitance two is half full and capacitance three is full then the number of persons between the detector is one and the position is five".

The words in capital letters are fuzzy operators with a similar function as their logical counterparts. With the logical operator, the statement "capacitance one IS Empty" would be either TRUE or FALSE. However, in the case of the fuzzy operator, the result may also be (in human language) "partly", "very" etc. This is achieved by taking the appropriate membership value as the result of the IS operation. In the case of the statement "M_1 IS E" the result would be μ_1^E.

The logical operator AND yields the result TRUE when both its parameters are TRUE. With fuzzy logic, the parameters are allowed to be more or less true. Consequently the result of the fuzzy AND is also more or less true. Often the minimum or the product of the both parameters is taken to calculate the result of the fuzzy AND operation. In our case we have chosen to take the minimum, because it is computationally much more efficient.

The number of persons is represented by the fuzzy variable *N* with fuzzy groups 0 to 3, so $N = (\mu_N^0, \mu_N^1, \mu_N^2, \mu_N^3)$. The position is represented by *P* with fuzzy groups 1 to 5 and - (not relevant). The case "-" is specific to our problem and merely indicates that the value for P is not calculated in this case. As a result $P = (\mu_P^1, \mu_P^2, \mu_P^3, \mu_P^4, \mu_P^5)$.

Each rule assigns a value to *N* and *P* using the BECOMES operator. However the statement "the position if five" is probably only true in part. The truth of the statement is the truth of the premises (which in our case was the minimum of the result of the IS operators). This value is assigned to the membership value of the appropriate group.

> Example:
> For instance, for rule 6 it follows that $\mu_N^1 = \mu_P^5 = \min(\mu_1^E, \mu_2^H, \mu_3^F)$. Using the values from Table 9-1, min(0.8, 0.3, 0.4) = 0.3 will be assigned to μ_N^1 and μ_P^5 .

Each rule is applied simultaneously. As has been said before, the relation between them is the fuzzy OR. The fuzzy OR operator is most often (and also in our case) implemented by taking the maximum of the parameters. So, when other rules also yield values for μ_N^1 (for instance rule 3, 5 and 7) or μ_P^5 (for instance rule 3, 5 and 12), the maximum of these values is taken, as is shown at the bottom of Table 9-2.

Table 9-2 The rule base and values for *N* and *P* using the sample values from Table 9-1

Rule no.	M_1	M_2	M_3	*N*	*P*	*N* $(\mu_N^0, \mu_N^1, \mu_N^2, \mu_N^3)$	*P* $(\mu_P^1, \mu_P^2, \mu_P^3, \mu_P^4, \mu_P^5)$
1	E	E	E	0	-	(0 0 0 0)	
2	E	E	H	0	-	(0.6 0 0 0)	
3	E	E	F	1	5	(0 0.4 0 0)	(0 0 0 0 0.4)
4	E	H	E	0	-	(0 0 0 0)	
5	E	H	H	1	5	(0 0.3 0 0)	(0 0 0 0 0.3)
6	E	H	F	1	5	(0 0.3 0 0)	(0 0 0 0 0.3)
7	E	F	E	1	3	(0 0 0 0)	(0 0 0 0 0)
8	E	F	H	1	4	(0 0 0 0)	(0 0 0 0 0)
9	E	F	F	1	4	(0 0 0 0)	(0 0 0 0 0)
10	H	E	E	0	-	(0 0 0 0)	
11	H	E	H	0	-	(0.2 0 0 0)	
12	H	E	F	1	5	(0 0.2 0 0)	(0 0 0 0 0.2)
13	H	H	E	1	1	(0 0 0 0)	(0 0 0 0 0)
14	H	H	H	1	3	(0 0.2 0 0)	(0 0 0.2 0 0)
15	H	H	F	1	5	(0 0.2 0 0)	(0 0 0 0 0.2)
16	H	F	E	1	3	(0 0 0 0)	(0 0 0 0 0)
17	H	F	H	1	3	(0 0 0 0)	(0 0 0 0 0)
18	H	F	F	2	4	(0 0 0 0)	(0 0 0 0 0)
19	F	E	E	1	1	(0 0 0 0)	(0 0 0 0 0)
20	F	E	H	1	1	(0 0 0 0)	(0 0 0 0 0)
21	F	E	F	2	3	(0 0 0 0)	(0 0 0 0 0)
22	F	H	E	1	1	(0 0 0 0)	(0 0 0 0 0)
23	F	H	H	1	2	(0 0 0 0)	(0 0 0 0 0)
24	F	H	F	2	3	(0 0 0 0)	(0 0 0 0 0)
25	F	F	E	1	2	(0 0 0 0)	(0 0 0 0 0)
26	F	F	H	2	2	(0 0 0 0)	(0 0 0 0 0)
27	F	F	F	3	-	(0 0 0 0)	
Final values (maximum)						(0.6 0.4 0 0)	(0 0 0.2 0 0.4)

It can be seen that only a few rules influence the final result. In the case of the sample values displayed in Table 9-2, rules 2 and 3 lead to the value of *N* = (0.6, 0.4, 0, 0). Likewise, rules 3 and 14 lead to the value of *P* = (0, 0, 0.2, 0, 0.4). The algorithm may be further optimized by eliminating unnecessary rules.

These value values for *N* and *P* are fed to the defuzzifier algorithm. Often this is done by determining the center of gravity (COG), shown in Fig. 9-7.

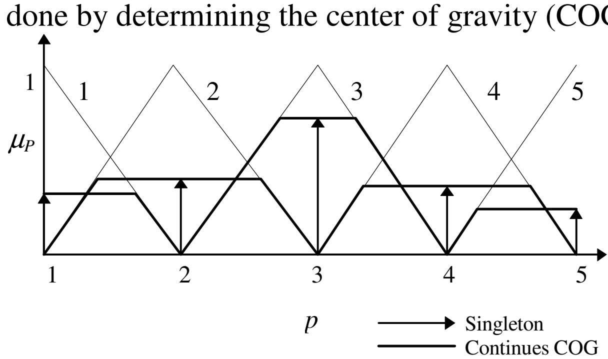

Fig. 9-7 Defuzification using singletons

However, to save calculation time for the defuzzification process singletons have been used, so the calculation of p is simplified to:

$$p = \frac{\sum_j j\,\mu_P^j}{\sum_j \mu_P^j}\text{, (j = 1 to 5)} \tag{9-3}$$

with p the calculated position. A similar equation is used to calculate the number of persons n. In the case the number of persons is two we choose the two positions around the calculated one, while when three persons are detected their position becomes irrelevant since the sensor is full. These values are communicated to a PC that displays the position of the person(s) between the sensor.

In our example, the number of detected persons n is 0.4 and the position p is 4.3. This means half a person is detected at one end of the sensor. In our case the value for n is rounded down to zero, so no person will be displayed on the PC screen and the value of p is irrelevant.

To improve the reliability of the sensor further, additional fuzzy variables may be used, for instance the change of the individual capacitances (positive, no change, negative) or the last calculated position.

9.5 Experimental results

The position sensor consists of 3 electrodes of 0.5 m high and 0.4 wide on one side and a 1.2 m wide electrode on the opposite side. A grounded electrode has been placed on the floor between them. The electrodes are made of a double sided material of which the backside is grounded, so that it functions as a guard electrode and shield. The electrodes are placed 1 m above the ground, while the distance between them is 1.1 m. The resulting capacitances are about 2 pF.

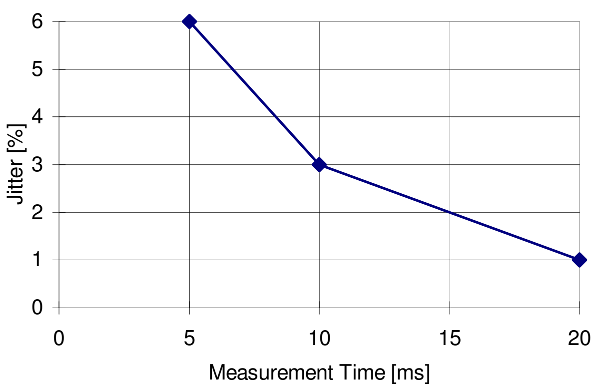

Fig. 9-8 Jitter of the measurement system versus measurement time

The capacitances are connected to a UTI that consists of a capacitance controlled oscillator and a built-in multiplexer. The interface also contains circuitry to suppress electromagnetic interference. The UTI is connected to an INTEL 87C51FB microcontroller that measures the period with a 0.33 µs resolution. The resulting jitter is shown in Fig. 9-8 as a function of the measurement time.
The total measurement time amounts to 50 ms while the evaluation of the fuzzy rules takes 35 ms. The result is communicated to a PC and displayed which takes several milliseconds.

The displayed results appear to be fairly reliable. In the case of a single person, the system is quite capable of detecting his presence and in most cases gives an acceptable estimation of the position. When more persons are detected the estimation of their position is detected less accurately.

The simplified persons detector consists of only two transmitting electrodes (0.5 m high and 0.1 m wide) and one receiving electrode (0.5 m high and 0.2 m wide) facing each other at a distance of 0.6 m. The receiving electrode is placed lower then the transmitting electrode to increase the capacitance change when a person passes the gate. In this case the capacitance nearly doubles. Because the electrode width is much smaller then in the case of the advanced position sensor, the capacitance measuring time has been set to only 5 ms per capacitance. When we choose the measurement sequence to be: C_{offset}, C_1, C_2, C_{ref}, C_1, C_2 and so on, the average sample time amounts to 15 ms, provided the calculation time can be neglected. In this time a person walking at 6 km/h moves only 2.5 cm. The algorithm in the μC needs only to detect which of the two capacitances changes first to detect the passing of a person and the direction.

9.6 Conclusion

Two low-cost capacitive personal detectors have been developed. One is able to estimate the position and could find use in safeguarding automatically working machines while the other measures the presence and direction of a passing person and is most suitable as an entrance detector or counter. The use of an electrode structure makes the system very rugged. The capacitances are measured with a readily available low-cost Universal Transducer Interface connected to a microcontroller, that processes the capacitance values to find the presence of a person.

The use of fuzzy logic has been found to be a very flexible and fast technique to calculate the position from the different capacitances, while achieving an acceptable reliability.

---

126 Jamshidi, M., T.J. Ross, N. Vadiee, eds., *"Fuzzy logic and control - software and hardware applications"*, Englewood Cliffs, NJ: Prentice Hall, 1993, Chap. 10, pp. 217 - 231

127 Toth, F.N., G.C.M. Meijer, J.A. Zapico, *"A low-cost capacitive personnel detector with fuzzy logic position estimation"*, Proc. IMTC'96 and IMEKO TC-7, Brussels, pp. 1270 - 1274, June 4 - 6, 1996

128 Karlsson, N., *"Theory and application of a capacitive sensor for safeguarding in industry"*, IMTC '94, May 10-12, Hamamatsu, pp. 479 - 482

129 Thomas, D.E., B. Armstrong-Hélouvry, *"Fuzzy logic control - a taxonomy of demonstrated benefits"*, Proceedings of the IEEE, vol. 83, no. 3, mar. 1995

130 Goes, F.M.L. van der, G.C.M. Meijer, *"A novel low-cost capacitive-sensor interface"*, IEEE Trans. Instrum. Meas., vol. 45, no. 2, pp. 536 - 540, April 1996

131 Goes, F.M.L., *"Low-cost sensor interfacing"*, Ph.D. thesis, Delft University of Technology, April 1996

132 Data sheet, *"Universal transducer interface - revolution in sensor interfacing"*, v2.1, June 1995, SMARTEC BV, The Netherlands

10 CONCLUDING REMARKS

In Chapters 7, 8 and 9 examples of intelligent capacitive sensors have been presented. These sensors have very advantageous properties by themselves or compared to other sensors for the same purpose. However now the time has come to evaluate the design method and to draw conclusions about the advantages and drawbacks of the intelligent capacitive sensor model itself.
In Section 10.1 we look back at the research problem and the main objectives presented in Section 1.2 and in Section 10.2 we will draw conclusions. Finally, in Section 10.3 we elaborate further on possibilities for future work.

10.1 Evaluation of the research objectives

The main question that is dealt with in this thesis is: "Can the development time and the cost of sensors in general and capacitive sensors in particular be reduced and the performance increased by adding intelligence to the sensor?".

To investigate this the following four objectives have been researched:
1. Finding a design strategy for capacitive sensors that reuses existing knowledge, parts *and* designs as much as possible, to simultaneously reduce manufacturing and development costs.
2. Finding flexible basic capacitive sensor designs that lend themselves for reusability
3. Implementing and evaluating capacitive sensor designs to demonstrate the feasibility of the approach.
4. Explore the area where capacitive sensors may be successfully applied.

A design strategy for reusable components
The complexity of designing systems in general and the multidisciplinary character of designing sensors and sensor systems in particular requires a hierarchical, structured approach. Usually an iterative procedure is followed based on the general systems theory, consisting of repetitive top-down decomposition and bottom-up composition. However, it does not provide a general method for finding a reusable design.
In software design similar problems have lead to a new design strategy called object-oriented analysis and design, which is also based on the general systems theory but considers an additional aspect of the elements that make up a system - inheritance.

Applying an object-oriented approach to sensor design leads to a decomposition of the systems elements (objects) that are more self-contained and more modular. As a result of this, for instance parasitic capacitances are thought to be part of the sensing element (and not of the sensor), while calibration of the sensors values is thought to be a property of the sensor and not of the system it is part of.

Basic reusable capacitive sensor designs

The object-oriented design approach leads to the concept of the intelligent sensor and from there to the intelligent capacitive sensor. This class of capacitive sensors should be flexible enough to be reused in general.

Of course, every other design forms its own class of sensors, from which new designs can be derived. When a design works satisfactorily, so will designs that are derived from it, when they are applied for similar purposes. However, sensors derived from the class of intelligent capacitive sensors cover a very wide area, since literally every part can be replaced by other parts to form a completely different sensor.

The intelligent capacitive sensor consists of a capacitive sensing element, a smart modifier, a microcontroller and a digital interface. The capacitive sensing element in turn consists of an electrode structure (including parasitic capacitances, shielding, guard electrodes etc.) and parts to interface with the physical signal like a spring to measure force. The smart modifier has a microcontroller-compatible output and may consist of a capacitance-controlled oscillator and includes selection switches for selecting several capacitances in the same way.

Using the above concept, we can step-by-step reduce the effects of the most important error sources to an insignificant level:

1. Guarding reduces the effect of fringing fields, resulting in a predictable relation between the measurand and the capacitance
2. Shielding reduces the effect of interference and of the parasitic capacitor parallel to the sensing capacitance
3. Applying a two-port measurement reduces the effect of the remaining parasitic capacitances (connected to ground)
4. Applying the three-signal auto-calibration eliminates unknown offset and gain errors in the modifier.

When these measures are taken, a simple capacitive sensor based on this concepts can easily be constructed with 0.1% accuracy, 100 ppm resolution and a measurement time between 10 ms and 1 s at a cost for the electrodes and electronic circuitry below $10.

In most cases only the sensing element needs to be changed to obtain a new sensor from one based on this design, but also the modifier can be replaced with one that suites a specific application better (for instance one with a higher speed, lower cost or built from specific discrete components). Also the microcontroller can be selected without changing the basic design much (high speed, low cost or low power etc.).

It might be thought that any one of the proposed measures is optional and can be left out, to reduce costs further. In general this is not the case. Leaving out the microcontroller, generally has the consequence of not applying the three-signal calibration which results to a serious degradation of the accuracy of the capacitance measurement. Replacing the two-port measurement by the (in many cases) simpler one-port measurement, means the effect of many parasitic capacitances can not be eliminated or only at considerable extra effort.

Implementation and evaluation of capacitive sensor designs

The proposed intelligent capacitive sensor object has been used as a template for the capacitive sensor designs in the last three chapters, the capacitive force sensor, the capacitive liquid level gauge and the capacitive persons detector. In this way, three completely new sensors have been designed with only slight variations of the basic design, but with completely different functionality.

All three sensor designs have been realized and extensively tested and exhibit very competitive specifications and costs compared to existing sensors for the same market.

Of course a few design examples are not sufficient enough to prove the design method; a design method must prove itself over time. But since this method seamlessly resembles the way experienced designers work when a short development time is required to minimize overall costs (by using existing components or by modifying older design etc.), it can be expected that the object-oriented approach is the most suited method in cases where (production) quantities are generally small, such as in the case of sensors.

Application field for capacitive sensors

Capacitive sensors appear to have a very high resolution. Also, no power is dissipated in the sensing element itself. This makes capacitive sensors very suitable in control applications where a high sensitivity is required or for measurements at very low temperatures.

We have shown that the capacitance of the sensing element can be measured accurately and at relatively low costs. Since the capacitance of the sensing element does not *directly* depend on temperature, humidity, pressure etc. it can be expected that capacitive sensors can obtain a high accuracy in industrial applications. However, since the dimensions of the electrodes and the permittivity of the dielectric does depend on these physical quantities, care must be taken that these influences have a negligible effect on the final measurement result. This can in many cases be ensured by performing relative measurements, with respect to a reference capacitance. Also care must be taken that the permittivity of the dielectric is not negatively influenced by contamination of the electrodes.

As a result the field where capacitive sensor can be successfully applied can be summarized as: the industrial sensor market for the measurement of physical quantities that can be related to the electrodes area or distance or to the permittivity of the dielectric, as well as sensors for the consumer market, where the incorporation of a microcontroller is not considered too expensive or where one is already available.

Although the number of design possibilities is reduced by the above considerations, the number of possible sensors is still infinitely large. And so we can confirm the main question of this thesis: By adding intelligence to a sensor, the accuracy can be improved, since the three-signal auto-calibration technique can be applied At the same time many other functionality can be implemented at virtually no extra cost, like adaptability (power-down function, adjustable data acquisition rate), interchangeability (internal calibration tables), identification (addressing, status information), data reduction and standardized bi-directional communication. At the same time, design time can be reduced and parts of the sensor can be reused (resulting to larger production series of the components) resulting to lower costs.

10.2 Conclusions

The following conclusions can be drawn:

1. Since the market for sensors is generally small, total costs (including design, production and support) need to be considered.
2. An object-oriented approach can help to create reusable components and designs and thus to reduce total costs.
3. The proposed intelligent capacitive sensor object, provides a reusable design that can reduce the development time and the cost while increasing the performance of capacitive sensors.
4. Although the concept of capacitance is accurately described by fundamental physical laws, to reduce design time only a few electrode structures are suitable as low-cost capacitive sensing elements. Among these, are the sensing elements based on biplanar or uniplanar electrode structures.
5. Guard electrodes are required to reduce the influence of fringing fields, so that the relation between the capacitance and the measurand can easily be predicted.
6. The effect of all parasitic capacitances can be reduced to an insignificant level by applying proper shielding and a two-port measurement.
7. The three-signal auto-calibration reduces the effect of unknown conversion constants (gain and offset) of the modifier to an insignificant level. For this reason the intelligent capacitive sensor object requires a microcontroller and a modifier with a microcontroller compatible output.
8. Suitable modifiers are the modified Martin oscillator, the multiple-sensor modulator, the two-integrator oscillator and the smart charge-redistribution modifier.
9. Starting from the proposed intelligent capacitive sensor object, an intelligent capacitive force sensor, a capacitive liquid level gauge and a capacitive persons detector could easily be derived.

10.3 Recommendation for future work

With the recent results of the work of four Ph.D. students cooperating in a team on the subject of capacitive sensors and on the subject of (capacitive) modifiers, it would seem that there is little else to know on the subject. That is however not the case.

Apart from all the possible sensors that can now be built using state-of-the-art knowledge, two other classes of capacitive sensors deserve our attention. These are the classes of high-speed capacitive sensors and of high-frequency capacitive sensors.

Generally high speed measurements are needed in mechanical control of which the bandwidth can be up to 1 kHz. This requires position measurements at a rate of 0.1 ms to ensure stability of the control system. For this reason it might even be necessary to incorporate the control software in the processor of the sensor. This is probably a formidable task that requires a digital signal processor (DSP) and a high integration between sensor and control software to optimally exploit features like adaptability and data reduction of the intelligent capacitive sensor.

Although these sensors (or control systems) do not belong to the class of low-cost sensors in an absolute way, they can still be considered low-cost according to the definition used in this work. It can be expected that such a positioning system can easily compete with those based on laser interferometers (like wafer steppers etc.) but at much lower costs.

The field of high-frequency capacitive sensors might also give interesting research options. Up to now we have concerned ourselves with low-frequency capacitance measurements. However, when a sweep could be performed over a range from 0 Hz to 1 GHz or so, frequency-analysis sensors can be built, for instance for the analysis of dielectric constants of materials, or for the determination of mixtures.

It took a century for science to accurately model the physical effect that was observed in the 'Leyden Jar'. And it has taken nearly another century before this effect could be put into a use other then the electrical component known as the capacitor.
I hope this work contributes to a quick adoption of low-cost, capacitive sensors to make everyday life easier or to provide us with better information about our environment.

SUMMARY

With the recent growth of the capabilities of automatic information processing systems, there is a demand for more information, at higher speeds and from more different sources, at much lower costs then ever before. It is this growing demand for information that presently drives the development of low-cost, high-performance sensors. And it is believed by many that sensors based on the use of capacitive sensing elements can play an important role in this development.

However, the time required to develop a new sensor is in general very long, typically more than 5 years. This explains the relatively slow development in sensor technology and also the relatively high costs of sensors.
The main question that is dealt with in this thesis is: “Can the development time and the cost of sensors in general and capacitive sensors in particular be reduced and the performance increased by adding intelligence to the sensor?”. To find the answer, the following objectives have been formulated and researched:

1. Finding a design strategy for capacitive sensors that reuses existing knowledge, parts *and* designs as much as possible, to simultaneously reduce manufacturing and development costs.
2. Finding flexible basic capacitive sensor designs that lend themselves for reusability
3. Implementing and evaluating capacitive sensor designs to demonstrate the feasibility of the approach.
4. Explore the area where capacitive sensors may be successfully applied.

The sensors and sensor systems that will be considered in this thesis are targeted at a cost-driven, medium-volume, industrial market or the high-end consumer market. Unfortunately, traditional top-down and bottom-up design approaches appear to have serious limitations for these types of sensors and sensor systems, due to the interdisciplinary and relatively open character of the (sub-)systems. Often many iterations are required, resulting in long design times and relatively inflexible designs.
To help overcome these limitations, a new systematic design approach that originates from software engineering is introduced, called object-oriented analysis and design. This approach focuses on the reuse of components, designs and specifications as much as possible, using the concept of inheritance. When these objects have standardized interfaces they can be truly reusable in new designs or in variations of older designs.

To facilitate the reuse of components and of designs, it appears that standardization of interfaces and signal types is required. To increase the flexibility, the addition of intelligence to low-level components is also necessary, to achieve adaptability, reliability, interchangeability, identification, data reduction and standardized bi-directional communication. The lowest level to which this intelligence can be added completely, is the sensor object. This leads to a generic design for an intelligent sensor, that consists of a sensing element, a modifier with a microcontroller compatible output (also known as smart sensor interface) and a microcontroller.
Considering the relatively low cost of microcontrollers, it can be expected that the total costs of the category of sensors and sensor systems described in this thesis can be decreased by following the presented approach.

In this thesis a sensing element is defined as "the smallest part in the sensor that interacts with the physical world and outputs an electrical signal". As a result, intelligence can not be added to the sensing element directly. The only way to achieve reusability in sensing elements is by deriving them from the same class object. In other words, they must all behave in the same standardized way to the interfacing objects. Fortunately, this does not limit the freedom of a capacitive sensor designer too much, since many capacitive sensing elements can, under certain conditions, be modeled in the same way, i.e. as a so-called multi-electrode (or multi-terminal) capacitor. These conditions are:

1. the quasi-static approach is valid, which means that the wavelength of the signals in the circuit is much larger then the physical dimensions,
2. the isolation resistance between the electrodes is high enough.

The multi-electrode capacitor can be considered the abstract parent object of the capacitive sensing elements considered in this thesis. To make it suitable as a capacitive sensing element, two properties have been added: guarding and shielding. By applying a grounded guard electrode, the electrical field is much better defined, so the output of the sensing element is not influenced by the presence of other objects that may or may not be in its vicinity. At the same time its transfer function may be much easier to calculate and understand.
By applying grounded shielding, the parasitic capacitance that can be found in parallel to the sensing capacitor will be practically eliminated.
From the general multi-terminal capacitor, several types with advantageous properties can be derived:

- Thompson and Lampard cross-capacitors, which are very suitable as reference capacitors
- Biplanar electrodes, of which the parallel-plate capacitor is very suitable to measure electrode small distance changes, while the differential-plate and the multi-electrode biplanar structure are very suitable to measure lateral displacements over large ranges.
- Uniplanar electrodes, which have a lower cost and higher accuracy and may be very suited to measure liquid levels or other dielectric interface displacements.

Of these classes of capacitors, the influence of finite guard ring widths and finite inter-electrode gap-widths have been calculated, as well as the influence of humidity and pressure (for air capacitors).

Because guarding and shielding increase the remaining parasitic capacitors to ground, the multi-electrode capacitive sensing element places a strict requirement on

the interfacing circuitry (the modifier): it must perform a two-port measurement. By performing a two-port measurement, the remaining parasitic capacitors are effectively short-circuited by a low-impedance voltage source at one terminal and a low-impedance current or charge amplifier at the other.
The modifier has an unknown, inaccurate transfer function of itself, of which the influence must be eliminated. This can be achieved by applying a 3-signal autocalibration, which is effectively a combination of a zero and a reference measurement. For this, a stable reference capacitor is required.
As a result, a class of modifiers is defined, that combines a two-port measurement with the 3-signal approach and is suitable to directly interface with a microcontroller, using digital or time-modulated signals. This class is called the class of Smart modifiers. Members of this class include the two-integrator oscillator, the modified Martin oscillator, the multiple sensor modulator and the smart charge redistribution circuit.

The class of Smart modifiers can interface the result of the 3 or more separate measurements, required by the 3-signal autocalibration, to the microcontroller. The microcontroller then can perform the required calculations, to obtain the measurement result: a capacitance ratio. In some cases, the communication is bi-directional and the measurement sequence of the Smart modifier is controlled by the microcontroller, in others, the Smart modifier controls the measurement sequence itself.

The design approach has been applied for three very useful cases:

- A capacitive force sensor. This sensor uses a leaf spring and a capacitive displacement sensor to achieve a high accuracy and large temperature range at relatively low costs.
- A capacitive liquid level gauge. This sensor uses a uniplanar electrode structure to measure the level of two non-conducting liquids or between one conducting and one non-conducting liquid over a large range with a very high accuracy.
- A capacitive persons detector. This sensor utilizes a large electrode structure that may be used as a vandal-proof entrance detector. Using fuzzy logic the sensor could estimate the position of a person which may be useful to safeguard automatically working machines.

These examples show that the same basic design can be reused at the level of sensing element, modifier, sensor and sensor system, which greatly reduced design time as well as costs.
By adding intelligence at every possible level, starting with the Smart Modifier and followed by the microcontroller and possibly a Smart Sensor bus, all kinds of variations of the multi-electrode capacitive sensing element can be used, without making drastic changes to the basic design. It appears that a large number of capacitive sensing elements can be considered a multi-electrode structure, so that the basic sensor design can be applied to a large number of different sensors. Moreover, is appears to be possible to classify the multi electrode structures in such a way that also the design time of this part can be limited to the minimum.

SAMENVATTING

De recente toename van de mogelijkheden van informatieverwerkende systemen heeft geleid to een groei van de vraag naar informatie. Het gaat hierbij niet alleen om meer informatie, maar ook om snellere informatie en informatie afkomstig van meerdere bronnen. De kosten van de systemen die deze informatie moeten leveren dienen lager te zijn dan ooit tevoren. Het is deze groeiende vraag naar betere en goedkopere informatie, die de ontwikkeling van sensoren met een hoge prijs/prestatieverhouding stuurt. Velen geloven dat capacitieve sensoren een belangrijke rol in deze ontwikkeling kunnen spelen.

Echter, in het algemeen is er veel tijd nodig om een nieuwe sensor te ontwikkelen; vaak meer dan vijf jaar. Dit verklaart de relatief trage ontwikkeling van de sensortechnologie en ook de relatief hoge kosten van sensoren.
In dit proefschrift staat de volgende vraag centraal: “Kunnen de ontwikkeltrajecten van sensoren in het algemeen en van capacitieve sensoren in het bijzonder worden verkort, de kosten verlaagd en tegelijkertijd de prestaties verhoogd door het toevoegen van intelligentie aan de sensor?”. Om deze vraag te beantwoorden is onderzoek verricht op de volgende hoofdonderdelen:

1. Het vinden van een ontwerp-strategie voor capacitieve sensoren die bestaande kennis, onderdelen en ontwerpen zoveel mogelijk hergebruikt, en tegelijkertijd fabricage en ontwikkelingskosten te reduceert.
2. Het vinden van flexibele basisontwerpen van capacitieve sensoren, die geschikt zijn voor hergebruik.
3. Het implementeren en evalueren van capacitieve sensorontwerpen.
4. Het in kaart brengen van de terreinen waarop capacitieve sensoren met succes toegepast zouden kunnen worden.

De sensoren en sensorsystemen die in dit proefschrift worden onderzocht zijn gericht op een prijsgestuurde, middelgrote industriële markt. Helaas blijken de gebruikelijke top-down en bottom-up ontwerpbenaderingen ernstige beperkingen te vertonen voor deze sensoren en sensorsystemen als gevolg van het interdisciplinaire en relatief open karakter van de (sub)systemen. Vaak zijn vele iteraties noodzakelijk, hetgeen resulteert in lange ontwikkeltrajecten en relatief starre ontwerpen.
Om deze beperkingen te overwinnen wordt een nieuwe systematische ontwerp-methode, afkomstig uit de informatietechnologie, geïntroduceerd: object-georiënteerde analyse en ontwerp. Deze ontwerpmethode concentreert zich op het zoveel mogelijk hergebruiken van componenten, ontwerpen en specificaties, met

behulp van het concept overerving. Als deze objecten voorzien zijn van gestandaardiseerde interfaces zijn ze werkelijk te hergebruiken in nieuwe ontwerpen of in variaties op een ouder ontwerp.
Het blijkt dat deze standaardisatie van de interfaces en signaaltypen noodzakelijk is voor het hergebruik van componenten en ontwerpen. Om de veelzijdigheid te vergroten blijkt het bovendien noodzakelijk om intelligentie aan componenten op lagere niveaus toe te voegen. Dit om aanpassingsvermogen, betrouwbaarheid, inwisselbaarheid, identificatie, datareductie en een gestandaardiseerde tweerichtingscommunicatie te verkrijgen.
Het laagste object waar intelligentie aan toegevoegd kan worden, is het sensorobject. Dit leidt tot een generiek ontwerp voor een intelligente sensor dat bestaat uit een ‘sensingelement’, een microcontroller en een ‘modifier’ met een uitgang die daarmee compatibel is. Een dergelijke modifier wordt ook wel ‘smart sensor interface’ genoemd.
Als we de relatief lage kosten van een microcontroller in beschouwing nemen dan kunnen we verwachten, dat de totale kosten van de in dit proefschrift beschouwde sensoren en sensorsystemen verlaagd kunnen worden met de voorgestelde aanpak.

In dit proefschrift wordt een sensingelement gedefinieerd als “het kleinste deel in de sensor die een interactie heeft met de fysische wereld en een electrisch signaal voortbrengt”. Als gevolg hiervan, is het niet mogelijk intelligentie direct aan het sensingelement toe te voegen. De enige manier om herbruikbaarheid bij sensingelementen te bereiken is door ze af te leiden van hetzelfde klasseobject. Met andere woorden: vanuit het oogpunt van de objecten waar interactie mee is, zullen varianten van het sensingelement er hetzelfde uit moeten zien.
Gelukkig wordt de vrijheid van de ontwerper hier niet al te zeer door beperkt, aangezien veel capacitieve sensingelementen, onder bepaalde voorwaarden, op dezelfde manier gemodelleerd kunnen worden, namelijk als een zogenaamde multi-elektrodecondensator. Deze voorwaarden zijn:

1. De quasi-statische benadering moet geldig zijn, wat concreet betekent dat de golflengte van de signalen in het electrische circuit groter moeten zijn dan de fysieke maten.
2. De isolatieweerstand tussen de elektroden moet groot genoeg zijn.

De multi-elektrodecondensator kan worden beschouwd als het abstracte moederobject van alle capacitieve sensingelementen in dit proefschrift. Om het geschikt te maken als capacitief sensingelement zijn er twee eigenschappen aan toegevoegd: ‘guarding’ en afscherming. Door het toevoegen van een geaarde guardelektrode wordt het elektrische veld veel beter gedefinieerd, zodat het uitgangssignaal van de sensingelement niet wordt beïnvloed door de aanwezigheid van andere objecten in de omgeving. Tegelijkertijd is de relatie tussen in- en uitgangssignaal veel beter te berekenen en te begrijpen.
Door het toepassen van geaarde afscherming wordt de parasitaire capaciteit die wordt aangetroffen parallel aan de meetcapaciteit, praktisch geëlimineerd.
Van de generieke multi-elektrodecondensator kunnen enkele typen met bijzonder gunstige eigenschappen worden afgeleid:

- De zogenaamde Thompson and Lampard cross-capacitors die bijzonder geschikt zijn als referentiecapaciteiten.

- Biplanaire elektroden, van welke de parallelle-plaatcondensator en de biplanaire multi-elektrodestructuur het meest geschikt zijn om laterale verplaatsingen over grote afstanden te meten.
- Uniplanaire elektroden, die een lage kostprijs en hoge nauwkeurigheid hebben en zeer geschikt zijn om vloeistofniveaus en verplaatsingen van interfaces tussen verschillende diëlectrica te meten.

Van elk van deze klassen van condensatoren is de invloed van de eindige breedte van guardringen en spleetbreedte tussen de elektroden bepaald, alsmede de invloed van luchtvochtigheid en druk (voor luchtcondensatoren).

Aangezien het aanbrengen van guardringen en afscherming de resterende parasitaire capaciteiten naar aarde vergroot, legt het multi-elektrodesensingelement een strikte voorwaarde op aan het circuit waar het interactie mee heeft (de modifier): die moet een tweepoortmeting uitvoeren. Door het uitvoeren van een tweepoortsmeting worden de resterende parasitaire capaciteiten als het ware kortgesloten naar aarde door een laagimpedante spanningsbron aan de ene aansluiting en een laagimpedante stroom- of ladingsversterker aan de andere.
De modifier heeft zelf een onbekende, onnauwkeurige overdrachtsfunctie waarvan de invloed moet worden beperkt. Dit kan worden bereikt door het uitvoeren van een 3-signaal autokalibratie. Dit komt neer op het tegelijkertijd uitvoeren van een nulpuntsmeting en een referentiemeting. Hiervoor is de beschikbaarheid van een stabiele referentiecondensator noodzakelijk.
Dit resulteert in het definiëren van een klasse van modifiers die in staat zijn een tweepoortmeting te combineren met een 3-signaal autokalibratie en bovendien direkt kunnen communiceren met een microcontroller, door middel van een digitaal- of tijdgemoduleerd signaal. Deze klasse heet de klasse van Smart modifiers. Tot deze klasse behoren onder anders de twee-integratoroscillator, de aangepaste Martin-oscillator, de Multiple Sensor modulator en het Smart Charge Redistribution circuit.

De klasse van Smart modifiers kan het resultaat van de drie (of meerdere) metingen die nodig zijn voor de 3-signaal autokalibratie doorgeven aan de microcontroller. De microcontroller kan dan de benodigde berekeningen doen om het uiteindelijke meetresultaat te verkrijgen: een capaciteitsverhouding. In sommige gevallen is er tweerichtingscommunicatie en wordt de meetvolgorde van de Smart modifier bepaald door de microcontroller. In andere gevallen bepaalt de Smart modifier dit zelf.

De ontwerpmethode is gebruikt en beproefd bij het ontwerp van een drietal sensoren:

- Een capacitieve krachtsensor. Deze sensor maakt gebruik van een bladveer en een capacitieve verplaatsingssensor om een zeer hoge nauwkeurigheid en groot temperatuurbereik te behalen tegen relatief lage kosten.
- Een capacitieve vloeistofniveaumeter. Deze sensor gebruikt een uniplanaire elektrodestructuur om het niveau van de interface tussen twee niet-geleidende vloeistoffen te meten, met een zeer groot meetbereik. Het is met deze sensor ook mogelijk het niveau van de interface tussen een geleidende en een niet-geleidende vloeistof nauwkeurig te meten.
- Een capacitieve personendetector. Deze sensor gebruikt een grote elektrodestructuur en is geschikt als vandaalbestendige toegangsdetector. Door het toevoegen van Fuzzy Logic is de sensor zelfs in staat van een persoon tussen de

elektroden de positie te bepalen. Een dergelijke functie zou toepassing kunnen vinden bij het beveiligen van automatisch werkende machines en robots.

Deze voorbeelden laten zien dat het mogelijk is hetzelfde basisontwerp te hergebruiken op de niveaus van sensingelement, modifier, sensor en sensorsysteem, hetgeen het ontwerptraject drastisch verkort.
Door het toevoegen van intelligentie op alle niveaus waar dat mogelijk is, te beginnen bij de Smart modifier, gevolgd door de microcontroller en eventuele smart-sensorbus, kunnen allerlei variaties op deze bouwstenen worden gemaakt zonder dat hun ontwerp wezenlijk verandert.
Een zeer groot deel van de capacitieve sensingelementen blijkt te beschouwen als een multi-elektrodestructuur, zodat dit model voor een groot aantal capacitieve sensoren bruikbaar is. Bovendien blijkt het mogelijk de diverse multi-elektrodestructuren zodanig te classificeren dat ook het ontwerptraject van dit onderdeel beperkt blijft.

ACKNOWLEGDEMENTS

Although carrying out a Ph.D. project is more or less a solitary task, that does not mean that one can do it all by oneself. In fact, I found it both necessary and pleasant to rely on the scientific, technical and emotional support of many colleagues and friends. I would like to take this opportunity to thank all of them for their help and cooperation.
There are however a few people who I would like to thank in particular. First of all, I would like especially thank my tutor and supervisor Dr. Gerard Meijer, not only for teaching me research, technical writing and interesting me for instrumentation and sensor technology, but also for having determined my professional carrier to such a large extent.
I would also like to thank Prof. Jan Davidse, for initially accepting me as a member of the Electronics Research Laboratory and Prof. Arthur van Roermund for being my ‘promotor’.

Further I would like to thank:
My roommates Frank van der Goes and Jeroen Kuenen for their pleasant company.
My colleagues Frank van der Goes, Paul de Jong, Wouter Serdijn, Gerben de Jong, Stoyan Nihtianov and Li Xiujun, for the scientific battles we have fought.

Harry Kerkvliet, for building various test setups. Loek van Schie and Jan Nusteling, for keeping all the computers running at full speed, and Rob Janse, for administering the software packages and maintaining backups, just in case.

The people at the Laboratory for Micro Engineering, especially Marcus Bonse, Dorus Bertels, Jo Spronck and Gert-Jan Nijsse, for their essential input on the mechanical aspects of capacitive sensors.

The people at Enraf BV, especially Thijs van der Lee, for providing clear research goals, a critical eye and the financial support that made this project possible, and Jan Vos, for his extraordinary help building the prototype level gauge as well as a complete test site on the companies premises.

My friends Willem-Jan de Hoog and Martin Heijne, for their support and for proofreading the manuscript, and Andreas Nyland, for designing the cover of the manuscript.

And last but not least, my partner in life, Marja Elsinga, who urged me to start (and finish!) the Ph.D. project and, finishing her own Ph.D. project on ‘Home ownership on a low budget’ a year before me, showed me how it’s really done by receiving her degree ‘cum laude’.

BIOGRAPHY

Ferry N. Toth was born in Sydney, Australia, on August 4, 1966. He received the ingenieurs (M.S.) and Ph.D. degrees in electrical engineering from the Delft University of Technology, Delft, The Netherlands, in 1990 and 1997, respectively.
From 1990 to 1991, he was employed by Delft Instruments Tang Gauging BV, formerly known as Enraf Nonius, where he was engaged in the development of a capacitive level gauge. After this he was employed by the Delft University of Technology, where he was involved in scientific research on intelligent capacitive sensors. He is currently employed by ENRAF BV, which is part of the Delft Instruments Group, Delft, and is involved in the development of a new generation of intelligent capacitive level gauges.